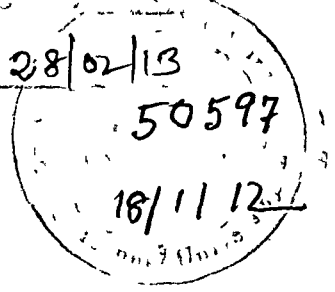


T 192

50597

| | |
|--------|----------|
| CP | T 192 |
| TE | |
| ACCESS | T 192 |
| Date | 28/02/13 |
| | 50597 |
| | 18/11/12 |



**MOLECULAR AND BIOCHEMICAL CHARACTERIZATION OF FOUR
ARACEAE SPECIES**

**A THESIS
SUBMITTED IN PARTIAL FULFILLMENT OF THE REQUIREMENTS
FOR THE DEGREE OF
Doctor of Philosophy**

BY
Jyoti Prasad Saikia, M Sc (Biotech)
Registration No. 009 of 2010



**School of Science and Technology
Department of Molecular Biology and Biotechnology
Tezpur University, Napaam-784028
Tezpur, Dist Sonitpur, Assam
March, 2011**

**I WOULD LIKE TO DEDICATE THE THESIS OF MY
Ph.D. WORK TO MY PARENTS:
SREEJUT SATYA PRASAD SAIKIA
SHREEJUTA AKASHI SAIKIA**

Abstract

Araceae remains to be one of the most inadequately known families of plants to science. There are 104 genera and about 3,700 species. Aroids are mostly tropical and include members from terrestrial, aquatic and epiphytic habitats. They are not uniformly distributed in the world, being much more copious in tropical and subtropical areas. There are two foremost species diversity centers, tropical Asia with 44 indigenous genera Croat (1992)¹. Edible aroids consist of taro (*Colocasia esculenta*; Assamese: *panchmukhia kochu*), tannia (*Xanthosoma sagittifolium*; Ass: koladohi kochu and *Xanthosoma caracu*; Ass: bogadohi kochu) and elephant foot yam (*Amorphophallus paeoniifolius*; Ass: *Ool kochu*) which contribute to food for almost 200 million people in the tropics and subtropics. This tuberous crop grows widely in North East India including Assam. These four species were selected for their morphological, nutritional, chromosomal and genomic study as well as biochemical analyses. Morphological characterization was done with respect to corm diameter, petiole length, leaf blade color, length, breadth, surface area and primary lateral vein number using standard methods. The corm of *A. paeoniifolius* and the leaf of *C. esculenta* were recorded to be the biggest among the aroids studied. Biochemical characterization was done with respect to moisture, ash, crude lipid, crude protein and crude fiber using the standard protocols. *C. esculenta* was found to be rich in nutritious components. Chromosomal study was done on root tips using the standard method of acetocarmine staining. *A. paeoniifolius* ($2n=2x=28$), *X. caracu* ($2n=2x=26$) and *X. sagittifolium* ($2n=2x=26$) were found to be diploid, whereas *C. esculenta* ($2n=4x=28$) tetraploid. Genome size of the aroid species was determined using the method described by Konwar et al. (2007)². Size of the genome was found to follow the order as *C. esculenta* (14.1 pg) > *X. caracu* (8.21 pg) > *X. sagittifolium* (8.04 pg) > *A. paeoniifolius* (5.04 pg). RAPD analysis of the aroid genomic DNA was done using six different primers [OPW-04 (5-CAGAAGCGGA-3), OPW-05 (5-GGCGGATAAG-3), OPW-08 (5-GACTGCCTCT-3), OPW-10 (5-TCGCATCCCT-3), OPW-15 (5-ACACCGGAAC-3) and OPW-16 (5-CAGCCTACCA-3)] already known for their high polymorphism in some of the aroid species. Data were analyzed using the NTSys PC software and the dendrogram generated showed 100% similarity between *X. caracu* and *X. sagittifolium* and 67% similarity of the

Xanthosoma cluster with that of *A. paeoniifolius*. *C. esculenta* possessed 11% similarity with the *Xanthosoma-Amorphophallus* cluster. Before the compound isolation, the corm extracts (water, methanol and 80% methanol in water) were characterized for bioactive compounds like polyphenols and flavonoids using the standard spectrophotometric methods. Polyphenol content was found to be in the order of *A. paeoniifolius* (0.303 ± 0.02 mg/100 g) > *C. esculenta* (0.21 ± 0.03 mg/100 g) > *X. caracu* (0.16 ± 0.06 mg/100 g) > *X. sagittifolium* (0.11 ± 0.02 mg/100 g) and flavonoid content in the order of *A. paeoniifolius* (178.71 ± 12.22 mg/100 g) > *C. esculenta* (142.39 ± 11.94 mg/100 g) > *X. caracu* (93.54 ± 7.85 mg/100 g) > *X. sagittifolium* (86.02 ± 5.55 mg/100 g). After confirming the presence of active compounds, the crude extracts were subjected to antioxidant, antimicrobial and blood coagulation activity. The antioxidant activity was in the order of *X. caracu* > *A. paeoniifolius* > *X. sagittifolium* > *C. esculenta*. With the exception of *C. esculenta* extract of 80% methanol, other corm extracts were found to enhance the blood clotting, whereas, water extract of aroid corms inhibited the clotting. On the basis of antimicrobial and antioxidant activity, polyphenol and flavonoid contents in 80% methanol extract were selected for the purification of major compounds using thin layer chromatography (TLC), column chromatography (CC) and HPLC. Out of 19 resolved fractions from the studied four aroid corms, 14 major ones were selected for structure elucidation and identification [using fourier transform infrared spectroscopy (FTIR), ^1H and ^{13}C Nuclear Magnetic Resonance (NMR)]. These 14 fragments were subjected to bioactivity assessment with respect to antibacterial activity (*Escherichia coli* and *Staphylococcus aureus*), antifungal activity (*Candida albicans* and *Fusarium oxysporum*), haemolysis and haemolysis prevention. These purified fractions were identified as protocatechuic acid, caffeic acid, coumaric acid, ferulic acid and syringic acid. The activity of protocatechuic acid [AC-I (1) and XC-I (1)] was found to be the highest against *E. coli*; and coumaric acid [BC-I (2), CC-I (4) and CC-II (4)] against *S. aureus*. Haemolysis prevention by caffeic acid [CC-I (2)] was found to be highest. High haemolysis was exhibited by coumaric acid [CC-II (4)] followed by protocatechuic acid [AC-I (1)]. The starch polymeric compound isolated from the aroid corms was characterized for their physicochemical properties with respect to moisture, amylose, ash, lipid, carbon, oxygen, phosphorus and starch granule size. The starch granules of *C.*

esculenta were the smallest having high amylose content ($22.4 \pm 4.5\%$), water binding capacity ($87.7 \pm 3.5\%$), acid hydrolysis (40%) and α -amylase hydrolysis (56.15 ± 1.9); but, the relative crystallinity of *C. esculenta* starch was low (35.77%).

The above feature, especially the small granule size promotes *C. esculenta* starch to be the most suitable for use in the preparation of composites. Polyaniline is known to be unique among the family of π -conjugated polymers. The compound was selected to prepare composite with aroid corm starch of *C. esculenta* due to its high antioxidant activity, ease of synthesis, good environmental stability and simple acid/base doping/dedoping chemistry. On the basis of the above information, three starch-polyaniline composite (S1, S2 and S3) were prepared. The composites were formed by using *in situ* polymerization and the formation was confirmed by scanning electron microscopy (SEM), X-ray diffraction study (XRD), differential scanning calorimetry (DSC), FTIR and UV-Vis spectroscopy. The antioxidant activity of the synthesized composites was characterized on the basis of DPPH scavenging and haemolysis prevention activity. Out of three, the composite S1 with the haemolysis prevention of 50 % was found to be the most biocompatible.

In the present investigation, the corm starch of *C. esculenta* was found to be potential in food processing owing to its nutritional parameters. The corm starch of *C. esculenta* could be used in baby food formulation because of its small granule size, high acid and enzyme hydrolysis. The starch-polyaniline composite could be used as the base material for making biosensors, wound dressing material and other biomedical devices and applications.

References

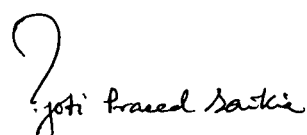
1. Croat, T. B. Species Diversity of Araceae in Colombia: A Preliminary Survey. *Annals of the Missouri Botanical Garden* **79**, 17-28 (1992).
2. Konwar, B.K.; Chowdhury, D.; Buragohain, J.; Kandali, R. A new less expensive method for genome size determination of plants. *Asian Journal of Plant Sciences* **6**, 565-567 (2007).

DECLARATION

I hereby declare that the thesis entitled 'MOLECULAR AND BIOCHEMICAL CHARACTERIZATION OF FOUR *ARACEAE* SPECIES' being submitted to the department of Molecular Biology and Biotechnology, Tezpur University, is a record of original research work carried out by me. Any text, figures, methods or results that are not of own devising are appropriately referenced in order to give credit to the original author(s). All sources of assistance have assigned due acknowledgement. I also declare that neither this work as a whole nor a part of it has been submitted to any other university or institute for any other degree, diploma or award.

Date: 29.03.2011

Place: Tezpur University, Tezpur.


(Jyoti Prasad Saikia)



**TEZPUR UNIVERSITY
SCHOOL OF SCIENCE & TECHNOLOGY
DEPARTMENT OF MOLECULAR BIOLOGY & BIOTECHNOLOGY
NAPAAM, TEZPUR – 784 028, ASSAM, INDIA**

B. K. Konwar, Ph D (London), DIC
Professor & Dean

Phone (O): 03712-267007-9 x 5402
Mobile (P) 9435380139 Fax: 03712-267005/6
Email: bkkon@tezu.ernet.in

CERTIFICATE BY THE PRINCIPAL SUPERVISOR

This is to certify that the thesis entitled ‘MOLECULAR AND BIOCHEMICAL CHARACTERIZATION OF FOUR *ARACEAE* SPECIES’ submitted to Tezpur University in the Department of Molecular Biology and Biotechnology, under the School of Science and Technology in partial fulfillment for the award of the degree of Doctor of Philosophy in Molecular Biology and Biotechnology is a record of research work carried out by Mr Jyoti Prasad Saikia under my personal supervision and guidance.

All help received by him from various sources have been duly acknowledged.

No part of the thesis has been reproduced elsewhere for award of any other degree.

A handwritten signature in black ink, appearing to be 'B K Konwar'.

(B K Konwar)

Signature of the Principal Supervisor
Professor and Dean
School of Science & Technology
Dept of Mol Biol & Biotechnology

Date: 29.03.2011
Place: Tezpur University, Tezpur

**NORTH-EAST INSTITUTE OF
SCIENCE & TECHNOLOGY**
(Formerly Regional Research Laboratory)
Council of Scientific & Industrial Research
Jorhat - 785 006, ASSAM
Tel: 91-0376-2370012, 91-0376-2371283 (Direct)
Fax : (0376) 2370011, 2370115
E mail : baruanc@rrljorhat.res.in
Website: <http://www.rrljorhat.res.in>



उत्तर पूर्व विज्ञान तथा प्रौद्योगिकी संस्थान
(सी एस आई आर की अंगीभूत इकाई)
जोरहाट 785 006, आसाम, भारत
फोन : 2371283 (Direct)
पिएविएक्स: 91-0376-2370117, 2370121, 2370139
फैक्स : 91-0376- 2370011, 2370115
ई-मेल : baruanc@rrljorhat.res.in
वेबसाइट : <http://www.rrljorhat.res.in>

Dr N.C. Barua

*Chief Scientist & Head,
Natural Products Chemistry Division &
Coordinator, Science & Technology*

CERTIFICATE FROM THE CO-SUPERVISOR

This is to certify that the thesis entitled '*MOLECULAR AND BIOCHEMICAL CHARACTERIZATION OF FOUR ARACEAE SPECIES*' submitted to Tezpur University in the Department of Molecular Biology and Biotechnology, under the School of Science and Technology in partial fulfillment for the award of the degree of Doctor of Philosophy in Molecular Biology and Biotechnology is a record of research work carried out by Mr. Jyoti Prasad Saikia under my supervision and guidance.

All help received by him from various sources have been duly acknowledged.

No part of the thesis has been reproduced elsewhere for award of any other degree.

(Dr. N. C. Barua)

Signature of the Co-Supervisor
Chief Scientist and Head
Natural Products Chemistry Division

Date: 29.03.2011

Place: NEIST, Jorhat



An ISO 9001:2000 Certified Organization
Connecting Science & Technology for Brighter Tomorrow



**TEZPUR UNIVERSITY
SCHOOL OF SCIENCE & TECHNOLOGY
DEPARTMENT OF MOLECULAR BIOLOGY & BIOTECHNOLOGY
NAPAAM, TEZPUR – 784 028, ASSAM, INDIA**

CERTIFICATE BY THE EXTERNAL EXAMINAR AND ODEC

This is to certify that the thesis entitled 'MOLECULAR AND BIOCHEMICAL CHARACTERIZATION OF FOUR *ARACEAE* SPECIES' submitted by Mr Jyoti Prasad Saikia to Tezpur University in the Department of Molecular Biology and Biotechnology under the School of Science and Technology in partial fulfillment of the requirement for the award of the degree of Doctor of Philosophy in Molecular Biology and Biotechnology has been examined by us on and found to be satisfactory.

The committee recommends for the award of the degree of Doctor of Philosophy.

Signature of:

Principal Supervisor
Date:

External Examiner
Date:

Acknowledgement

Firstly, I would like to express my heartfelt gratitude to my principal supervisor, Dr. Bolin Kumar Konwar, Professor and Dean, Department of Molecular Biology and Biotechnology, Tezpur University, Napaam, Tezpur-784028, who guided me throughout the research work and writing up of the thesis. Without his constant inspiration, encouragement and constructive criticism, the present work would not have been possible. I would also like to express my sincere gratitude once again to my principal supervisor for collaborating with different research groups for providing me the opportunity to work on the emerging area of nanobiotechnology.

I would like to express my gratitude to my co-supervisor, Dr. Nabin Chandra Barua, Scientist G, Head, Natural Product Division, NEIST, Jorhat for his constant support. I would like to express my deep sense of gratitude to Prof. S. K. Dolui, Department of Chemical Sciences and Prof. A. K. Mukherjee, Department of Molecular Biology and Biotechnology, Tezpur University, Napaam for their kind advice and guidance during the tenure of my research work.

I would like to express my sincere thanks to my friend Mr. Samrat Paul, Research Scholar, for his support and his supervisor Prof. Sanjoy Kumar Samdarshi, Department of Energy, Tezpur University for allowing me to use their laboratory and handling of various equipment for generation of research data. I also like to express my sincere thanks to Prof. Ashok Kumar, Department of Physics, Tezpur University and his research scholar Mr. Somik Banerjee for helping me in the analysis of certain parameters. I would like to specially mention the name of

Prof. Niranjan Karak, Head, Department of Chemical Sciences, Tezpur University and his research scholars Dr. Subhansu Dutta and Mr. Rocktotpal Konwarh for their assistance in analysis of various sample parameters and handling of some important equipment.

I would like to acknowledge Dr. Dhiren Chowdhury, Dr. Jitu Buragohain, Dr. Ranjan Kandali, Dr. Khanindra Ratna Barman, Dr. Naba Kumar Bordoloi, Mr. Tabaruk Husain, Mr. Sahin Sarif and Ms. Luna Barua for their help and suggestions. I will fail in my duty if I do not acknowledge my junior scholars Ms. Pinkee Phukon, Mr. Pranjal Bhorali, Mr. Mayur Mausum Phukon, Ms. Angana Ray, Ms. Krishna Gogoi, Ms. Kalpana Sagar, Ms. Shyamalima Gogoi, Mr. Salam Pradeep Singh and Mr. Yasir Basir who helped me in various ways. I would also like to acknowledge the two M.Sc. project students Ms. Nilam Nayan Borah and Ms. Priyanka Roy.

I would also like to thank Mr. Ratan Barua, Department of Physics for his expert assistance in handling the scanning electron microscope for taking various sample images.

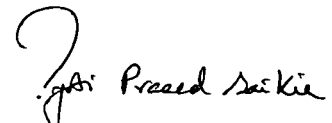
Last but not least I would like to acknowledge the moral support provided by Ms. Porimita Saikia, younger sister and Mr. Gunjan Prasad Saikia, younger brother during my entire carrier of studies.

I will fail in my duty if I do not acknowledge all the faculty members, technical staffs and office staffs of MBBT department including Shree Depak Deka and Shree Dharanidhar Bonia for their support and cooperation. At last I would like to acknowledge DBT Nodal Cell for supporting the writing up phase of the Ph.D.

work. I would also like to show my gratitude to all those who directly or indirectly helped me in my research work.

Date: 29.03.2011

Place: Tezpur University, Tezpur


(Jyoti Prasad Saikia)

Content

| Content | Page number |
|---|-------------|
| Chapter 1: Introduction | 1 |
| 1.1 General | 1 |
| 1.2 Taxonomy | 2 |
| 1.3 Phylogeny | 3 |
| 1.4 Origin | 3 |
| 1.5 Morphology | 6 |
| 1.6 Other characters | 8 |
| 1.7 Genetics of aroids | 9 |
| 1.8 <i>Amorphophallus paeoniifolius</i> | 11 |
| 1.9 <i>Xanthosoma sagittifolium</i> | 12 |
| 1.10 Food | 13 |
| 1.11 Cultivation | 15 |
| 1.12 Compounds and bioactivity | 16 |
| 1.13 Aroid Starch | 17 |
| Chapter 2: Review of literature | 21 |
| Chapter 3: Materials and methods | 32 |
| 3.1 Chemicals used | 33 |
| 3.2 Morphological study | 33 |
| 3.3 Karyotyping | 33 |
| 3.4 Biochemical composition | 34 |
| 3.4.1 Moisture | 34 |
| 3.4.2 Ash | 34 |
| 3.4.3 Crude protein | 35 |
| 3.4.4 Crude lipid | 35 |
| 3.4.5 Starch content | 35 |
| 3.4.6 Crude fiber | 35 |
| 3.4.7 Total carbohydrate | 36 |

| | |
|--|----|
| 3.4.8 Total sugar content | 36 |
| 3.4.9 Total energy | 36 |
| 3.4.10 Mineral estimation | 36 |
| 3.5 Genome size study | 37 |
| 3.5.1 Isolation of Genomic DNA | 37 |
| 3.5.2 Determination of yield and quality of DNA | 37 |
| 3.5.3 Genome size determination | 38 |
| 3.6 RAPD study | 39 |
| 3.6.1 DNA amplification | 39 |
| 3.6.2 RAPD analysis | 40 |
| 3.7 Compound isolation and identification | 40 |
| 3.7.1 Plant sample preparation | 40 |
| 3.7.2 Extract preparation | 41 |
| 3.7.3 Biochemical and bioactivity test with the crude extracts | 41 |
| 3.7.3.1 The total polyphenol content | 41 |
| 3.7.3.2 Total flavonoid estimation | 41 |
| 3.7.3.3 The blood clotting experiment | 41 |
| 3.7.3.4 The antioxidant activity | 42 |
| 3.7.3.5 Antimicrobial activity of the crude extracts | 42 |
| 3.7.4 Thin layer chromatography (TLC) | 43 |
| 3.7.5 Column chromatography | 43 |
| 3.7.6 High Performance Liquid Chromatography (HPLC) | 43 |
| 3.7.7 Fourier Transform Infrared Spectroscopy (FTIR) | 44 |
| 3.7.8 Nuclear Magnetic Resonance (NMR) | 44 |
| 3.8 Antimicrobial assessment | 44 |
| 3.8.1 Microbial strains | 44 |
| 3.8.2 Antibacterial assay | 45 |
| 3.8.2.1 Preparation of inoculum | 45 |
| 3.8.2.2 The antibacterial test | 45 |
| 3.8.3 Antifungal assay | 45 |
| 3.8.3.1 Preparation of the inoculum | 45 |

| | |
|--|----|
| 3.8.3.2 The antifungal test | 46 |
| 3.9 Anti-haemolysis test against free radicals | 46 |
| 3.10 Starch isolation, physicochemical characterization | 47 |
| 3.10.1 Starch Granule Isolation | 47 |
| 3.10.2 Proximate Composition Analysis | 47 |
| 3.10.3 Scanning Electron Microscopy of Starch Granules | 48 |
| 3.10.4 Elemental Composition Analysis using EDX of starch granules | 48 |
| 3.10.5 Amylose Content Estimation | 48 |
| 3.10.6 Apparent amylose content estimation | 48 |
| 3.10.7 Total amylose content estimation | 49 |
| 3.10.8 X-ray Diffraction Study of the Starch Granules | 49 |
| 3.10.9 Starch Granule Damage Estimation | 49 |
| 3.10.10 Functional Group Analysis Using FTIR Spectroscopy | 50 |
| 3.10.11 Analysis of Gelatinization Parameter Using Differential Scanning Calorimetry (DSC) | 50 |
| 3.10.12 Analysis of Water Binding Capacity | 51 |
| 3.10.13 Colorimetric Measurement of Amylose Leaching | 51 |
| 3.10.14 Acid Hydrolysis of Starch Granules | 51 |
| 3.10.15 Enzymatic Hydrolysis of Starch Granules | 51 |
| 3.11 Application of starch for functional composite preparation with polyaniline and its bio-efficacy assay | 52 |
| 3.11.1 Synthesis of starch/polyaniline composites | 52 |
| 3.11.2 Characterization | 53 |
| 3.11.3 Antioxidant activity | 53 |
| 3.11.4 Cytotoxicity assay by anti-haemolysis test | 54 |
| 3.12 Statistical Analysis | 55 |
| Chapter 4: Results | 55 |
| 4.1 Morphological study | 56 |
| 4.2. Biochemical study | 59 |
| 4.3. Karyotyping | 60 |
| 4.4. Molecular characterization | 62 |

| | |
|---|-----|
| 4.4.1. Genome Size (DNA C-value) determination | 62 |
| 4.4.2. Randomly Amplified Polymorphic DNA (RAPD) analysis | 65 |
| 4.5. Compound purification | 66 |
| 4.6. Isolation and characterization of the starch (polymeric compound) from aroids | 84 |
| 4.7. Composite preparation with the starch isolated from <i>C. esculenta</i> | 91 |
| Chapter 5: Discussion | 100 |
| 5.1 Morphological study | 100 |
| 5.2 Biochemical characterization | 101 |
| 5.3 Karyotyping | 103 |
| 5.4 Molecular biological study | 103 |
| 5.5 Compound purification | 105 |
| 5.5.1 Total polyphenol content | 105 |
| 5.5.2 Total flavonoid estimation | 106 |
| 5.5.3 The antioxidant capacity | 107 |
| 5.5.4 Blood clotting | 107 |
| 5.5.5 Antimicrobial activity | 108 |
| 5.5.5.1 Antibacterial activity | 108 |
| 5.5.5.2 Antifungal activity | 108 |
| 5.5.6 Thin layer chromatography (TLC) | 108 |
| 5.5.7 Column chromatography | 109 |
| 5.5.8 High Performance Liquid Chromatography (HPLC) | 109 |
| 5.5.9 Fourier transform infrared spectroscopy (FTIR) | 110 |
| 5.5.10 Nuclear magnetic resonance | 111 |
| 5.6 Antimicrobial study | 111 |
| 5.7 Compound identified | 112 |
| 5.8 Antioxidant activity of the pure compounds | 112 |
| 5.9 Starch isolation and physicochemical characterization | 113 |
| 5.9.1 Starch granule morphology | 113 |
| 5.9.2 X-ray Pattern and Crystallinity of Starch Granules | 114 |

| | |
|---|-----|
| 5.9.3 Detection of functional groups using FT-IR Spectroscopy | 114 |
| 5.9.4 Gelatinization parameter | 115 |
| 5.9.5 Recording of amylose leaching by colorimetric method | 115 |
| 5.9.6 Acid hydrolysis | 115 |
| 5.9.7 Enzymatic hydrolysis | 116 |
| 5.10 Starch and polyaniline composite | 117 |
| 5.10.1 Morphology of the polyaniline loaded starch granules | 117 |
| 5.10.2 X-ray diffraction studies | 118 |
| 5.10.3 UV-Visible spectroscopy | 118 |
| 5.10.4 FT-IR spectroscopy | 118 |
| 5.10.5 Differential scanning calorimetry (DSC) | 119 |
| 5.10.6 Antioxidant activity | 120 |
| 5.10.7 Cytotoxicity by anti-haemolysis | 121 |
| Chapter 6: Conclusion | 124 |
| References | 129 |
| List of publications | 154 |

List of tables

| Tables | Page number |
|---|--------------------|
| Table 3.1. Sequences of primer | 38 |
| Table 3.2. Composition of different starch/polyaniline composites | 51 |
| Table 4.1. Morphological characters of the aroids | 56 |
| Table 4.2. Biochemical composition of the aroids | 59 |
| Table 4.3. Time of active cell division | 61 |
| Table 4.4. Spectrophotometric determination of purity and yield of DNA from all forms of aroid species | 62 |
| Table 4.5. Genome size of the aroids | 64 |
| Table 4.6. DNA fragments generated from RAPD analysis | 65 |
| Table 4.7. Pair-wise genetic similarity matrix among the aroid species based on Jaccard similarity coefficient | 66 |
| Table 4.8. Purified fractions generated from HPLC | 73 |
| Table 4.9. Structural information generated from FTIR data | 75 |
| Table 4.10. NMR data and correlation with structures presented in Figure 4.22 | 76 |
| Table 4.11. Documentation of the results of the antimicrobial assays | 83 |
| Table 4.12. Proximate composition of the aroid starches | 85 |
| Table 4.13. DSC analysis of aroid starch | 86 |
| Table 4.14. Analysis of the XRD data | 89 |
| Table 4.15. Composition of the different Starch-polyaniline composites | 92 |

List of figures

| Figure | Page number |
|--|--------------------|
| Figure 4.1. Morphology of the aroid plants (photo) | 58 |
| Figure 4.2. Morphology of the aroid corms (photo) | 59 |
| Figure 4.3. Somatic chromosomes of aroids (photo) | 61 |
| Figure 4.4. Idiogram of chromosomes of four aroid species | 61 |
| Figure 4.5. Agarose gel electrophoresis of purified genomic DNA of the aroids (photo) | 63 |
| Figure 4.6. Photograph of the leaf sections for determining cell dimensions (photo) | 64 |
| Figure 4.7. Agarose gel electrophoresis pattern of the RAPD products (photo) | 65 |
| Figure 4.8. Dendrogram presentation among the aroids as determined from RAPD data | 66 |
| Figure 4.9. Total phenolic content of the aroid corm extracts | 67 |
| Figure 4.10. Total flavonoid content of the aroid corm extracts | 68 |
| Figure 4.11. DPPH scavenging potency of the extracts | 68 |
| Figure 4.12. Standard equivalence of the extracts with respect to antioxidant property | 69 |
| Figure 4.13. Blood coagulating property of the extracts | 69 |
| Figure 4.14. Antimicrobial activity of the extracts (photo) | 70 |
| Figure 4.15. Antifungal activity of the extracts (photo) | 70 |
| Figure 4.16. TLC profiling of the compounds (photo) | 71 |
| Figure 4.17. Polyphenolic content of the fractions from column chromatography | 71 |
| Figure 4.18. HPLC profiling of the fractions AC-I, AC-II, BC-I and BC-II | 72 |
| Figure 4.19. HPLC profiling of the fractions CC-I, CC-II and XC-I | 72 |

| | |
|--|----|
| Figure 4.20. FTIR spectra of purified compounds from <i>C. esculenta</i> and <i>X. caracu</i> | 74 |
| Figure 4.21. FTIR spectra of purified compounds from <i>A. paeoniifolius</i> and <i>X. sagittifolium</i> | 74 |
| Figure 4.22. Structures of the five different compounds isolated from the four different aroids | 79 |
| Figure 4.23. Antibacterial activities against <i>E. coli</i> (photo) | 81 |
| Figure 4.24. Antibacterial activity against <i>S. aureus</i> (photo) | 81 |
| Figure 4.25. Antibacterial activity against <i>C. albicans</i> (photo) | 82 |
| Figure 4.26. Antibacterial activity against <i>F. oxysporum</i> (photo) | 82 |
| Figure 4.27. Antioxidant activities of the compounds | 84 |
| Figure 4.28. Scanning electron microscopic images of purified aroid starch granules showing their size and morphology (photo) | 87 |
| Figure 4.29. X-ray diffraction analysis of purified starches | 88 |
| Figure 4.30. Measurement of crystallinity of the aroid starches | 88 |
| Figure 4.31. Gaussian and Lorengian linear curve fitting on the XRD data of aroid starches for calculating crystallite sizes and strains | 89 |
| Figure 4.32. FT-IR patterns of the purified aroid starches along with commercial starch from MERCK (India) showing their purity | 90 |
| Figure 4.33. Effect of temperature on amylose leaching in aroid starches | 91 |
| Figure 4.34. Acid hydrolysis of the aroid starches with respect to time (days) | 91 |
| Figure 4.35. SEM of the composites and pristine polymers showing their morphology (photo) | 93 |
| Figure 4.36. XRD pattern of (a) pure starch, (b) composite | |

| | |
|--|----|
| sample S1, (c) composite sample S2, (d) composite sample S3, and (e) pure polyaniline (PAni) | 94 |
| Figure 4.37. FT-IR spectra of the composites and pristine Polymers | 94 |
| Figure 4.38. UV-Vis spectroscopy of the composites, starch and polyaniline | 95 |
| Figure 4.39. DSC of the composites with pristine polymer | 95 |
| Figure 4.40. Comparative graph showing the antioxidant activity of the composite samples and pure components | 96 |
| Figure 4.41. UV-Vis spectra showing the weight dependent DPPH activity of the composite sample S2 synthesized with 0.5M aniline | 97 |
| Figure 4.42. Time dependent DPPH scavenging activity of 0.4 mg of the composite sample S3 | 97 |
| Figure 4.43. Comparative graphical representation of the haemolysis prevention activity of the different weights of the copposite samples S1, S2, S3 and pure polyaniline | 98 |
| Figure 4.44. Scanning electron micrograph showing morphology of the normal RBC (A), damaged RBC due to H ₂ O ₂ treatment (B) and (C) H ₂ O ₂ and S1 treated RBC (photo) | 99 |

CHAPTER 1

INTRODUCTION

1.1 General

Aroid is the common name for members of the Araceae family of plants, sometimes known as Philodendron or Arum. The beautiful and bizarre combination of spathe and spadix, well-known as the inflorescence, sometimes referred to as a "flower", is a distinguishing feature of aroids. The densely flowered spadix is subtended by a spathe, a modified leaf that protects the spadix. The flowers on the spadix are pollinated by flies and beetles that are attracted by the sometimes foul scents, or by bees attracted by sweet scents. Heat occasionally plays a role in pollination. That is, the spadix increases in temperature to volatilize scents which in turn attracts insects. Skunk cabbage (*Symplocarpus foetidus*), which may even melt its way through snow, is known for heat production in its spadix. The varying colors of spathe and spadix may also play an important role in pollination. The aroids rarely enter into the world of commerce as they are mostly grown in subsistence agriculture systems and for local markets. However, the aroids play a substantial role in the food security of millions of people in the tropics. The starch-rich corms are the main product, but leaves and flowers are also eaten. Taro (*Colocasia esculenta*) widely grown in the tropics and subtropics, but has been neglected by crop breeders and conservationists. Much of the diversity within the crop is still being maintained by farmers and local communities. Although of New World origin, today the greatest use of cocoyam (*Xanthosoma*) is in West Africa. Taro (*Colocasia*) and cocoyam form an edible aroid complex, and the two are often substituted for each other. Their uses are also very similar, the corm, cormel, petiole and leaf of both can be used. Cocoyam is the third most important root and tuber crop in West and Central Africa and probably the most important leafy vegetable. Some aroids exhibit unique thermogenic characters¹. The physiological origin of thermogenesis is confirmed as cytochrome system and dependent on the partial pressure of oxygen^{2,3}.

The intellectual appeal of aroids is matched by their aesthetic qualities. No other group of plants can compare to the excessive and exotic foliage exhibited by Araceae. Leaf blades are wide ranging in size, shape, color and

sometimes vary even from immature to mature stages. They range in size from small as a coin to as large as several meters in width as is the case in *Amorphophallus titanum*, considered a giant in the aroid world. Leaf blades may be variously lobed or divided, and in some groups window-like holes may occur naturally in the leaves. Texture of foliage varies as well, from leather-like, as in *Philodendron rugosum*, to velvety, as in *Anthurium warocqueanum*, to silky as in *Xanthosoma pubescens*.

Araceae remains to be one of the most inadequately known families of plants to science with large percentages still new. There are 104 genera and about 3,700 species if the *Lemnaceae* (the duckweed family) is not regarded as a generic synonym or 108 genera and about 3,750 species if the *Lemnaceae* are included. More aroids are tropical and include members from terrestrial, aquatic, and epiphytic habitats. But, there are many aroids which thrive in the colder Northern climates and indeed require the cold to successfully pass through their regular periods of dormancy, and only a few of the genera from America occur in the Old World. Asia has more genera than America, but America has more species, with well over half of all the species of the world.

1.2 Taxonomy

Royal Botanic Gardens, Kew (RBGK) maintains the plant exemplar group, part of the Araceae (aroids); whereas software development is led by Oxford University⁴. Aroid taxonomy requires a text description and a dichotomous key, ideally with illustrations of flower and leaf morphology⁴. The occurrence, type and location of calcium oxalate crystals in the leaves of 14 different species of aroids were reported by Genua and Hillson⁵. They also pointed out the neglected calcium oxalate crystal details in taxonomy of aroids and their potential⁵. The use of leaf mid rib for taxonomic purpose was described by Mantovani *et al.*⁶. They mentioned that the vegetative characteristics such as habit, phyllotaxy and leaf venation are important for description and identification of plant species. However the outline of plant organs in cross section is relatively less used for species diagnosis⁶. Benzing

described the use of vascular epiphytism for taxonomic as well as adaptive diversity. Aroid, by comparison with orchidoid, epiphytism is neither as advanced nor as versatile⁷.

1.3 Phylogeny

Morphological and molecular analyses resolve many aspects of vascular plant phylogeny. The role of chloroplast trnL-F sequences in phylogenetic analysis of aroids was reported by Tam *et al.*⁸. The phylogeny of the araceae with 2,500 species in 107 genera is currently in a state of flux with various taxonomists realigning genera within subfamilies based on new data⁹. Although this new molecular phylogeny does not include all aroid genera, it corroborates in general, at the subfamily level; the molecular analysis is based on chloroplast DNA restriction site data¹⁰. Other researchers are using the non coding plastid DNA for phylogenetic analysis¹¹.

1.4 Origin

The origin of aroids was described by Kuruvilla and Singh¹². They reported karyotypes and the electrophoretic banding pattern of genomic DNA of 15 cultivars (cvs) of taro; aroids collected from North-East Indian states as well as from South and North India. NE Indian cvs are diploids or triploids whereas those from plains of South India diploids and of North India triploid. The diploids had $2n=28$ and triploids showed $2n=42$ chromosomes. The protein content varied from 4.2-11.4 mg/g dry wt. The maximum protein content was found in a triploid cv (11.4 mg/g dry wt) and minimum in a wild taro cv (4.2 mg/g dry wt). The number of protein bands observed was 7 in the wild taro (diploid) and 12 in one cultivated triploid cv Meghalaya cv showed great variation with respect to leaf size and tuber shape and size. All cvs have diverged at morphological, karyotypic and genotypic levels¹². From their analysis they suggested that the dispersion of taro to the Indian subcontinent was through NE India. Yen and Wheeler¹³ reported the origin of *Colocasia esculenta* as South East Asia. The fact was further supported by the Australian

roid biodiversity research¹⁴. A commonly accepted view was that the centre of origin and domestication of taro was in South-East Asia; in particular the region occupied by Myanmar and Bangladesh, the putative area of origin of several other *Colocasia* species^{15, 16}. Matthews¹⁶ suggested the area to be somewhere within North-East India or South-East Asia. However, there is a growing consensus that domestication occurred in many places across the natural distribution of the wild relatives. A western Melanesian centre of origin and domestication has been largely accepted for several other crops like banana, coconut and sugarcane and there is now circumstantial evidence that *Colocasia* may have been domesticated in that area too. Attention has mainly focused on Papua New Guinea, with evidence of human settlement in that country as far back as 40,000 years, and of agriculture for at least 6,500-7,000 years¹⁸. This has increased speculation as to the food plants used. The discovery of fossil pollen grains thought to be those of *Colocasia* and *Alocasia* on stone tools in deposits in the Northern Solomon Islands dated at 28,000 years ago has added to the debate¹⁹. Presumably, this does not preclude later introductions of cultivars with Austronesian migrations. Thus, most cultivars found throughout Pacific were not brought by the first settlers from Indo-Malayan region as previously thought, but were domesticated from wild sources existing in Melanesia. *C. esculenta* var. *aquatilis*, a species that is a component of the natural Eastward extension of the Indo-Malaysian flora, is a possible progenitor of cultivated taro^{20, 12, 21, 22, 23, 24}. From Melanesia, cvs were taken Eastward to Polynesia during prehistoric migrations, with a progressive decline in their number and diversity^{25, 26, 27}. Thus, with domestication also occurring in South-East Asia and with the separation of the land masses of Sunda and Sahul, two genepools came out, with overlapping in Indonesia¹⁶. Within these genepools, two botanical varieties of taro have been recognized, *C. esculenta* var. *esculenta*, commonly known as dasheen and *C. esculenta* var. *antiquorum*, and commonly known as eddoe. Dasheen varieties have large central corms, with suckers and/or stolons, whereas eddoes have a relatively small central corm and a large number of smaller cormels²⁸. There are also differences in floral

morphology. The separation of the cultivated taros into two varieties has also been challenged in the recent years²⁹. Hay²⁹ argues that if the two varietal names are to remain, then there is a “nomenclature requirement” that all other taros, wild, feral and ornamental- be described as varieties too, and this can only be done if the division between var. *esculenta* and var. *antiquorum* is practical, i.e. if it works. Botanically, all taros should simply be called *C. esculenta*. This view is supported by the lack of consistent difference between two varieties on the basis of isozymes, AFLP, RAPD or SSR markers. Additionally, AFLPs showed no evidence for association between corm shape, as exemplified by var. *esculenta* and *antiquorum*, and ploidy level¹¹. In general, triploids are more common at high altitudes and latitudes, environments that are marginal for diploids, suggesting that such conditions promote the occurrence of unreduced gametes³⁰. Currently, several species of the genus *Colocasia*, *C. fallax*, *C. affinis* and *C. gigantea* are recognized, but their centres of origin are not well defined. Mathews¹⁷ reviewed the evidence and showed South or South-East Asia distribution, largest for *C. gigantean*, Eastern China, Indonesia, Myanmar, Sri Lanka, Southern Japan, Thailand, Vietnam and more restricted for *C. fallax* and *C. affinis* and arc from the Himalayas of India and Nepal to Myanmar. Three others, *C. gracilis* (Sumatra), *C. mannii* (Assam) and *C. virosa* (Eastern India) are known only from single herbarium specimen^{23, 17}. Wild taros are of considerable interest as they have more allelic diversity than the cultivated forms, which, on the other hand, are more variable in agro-morphological characteristics^{31, 32}. DNA analyses are needed on the wild types to determine their relationships, in particular with *C. esculenta*. The mitochondrial DNA tests on *C. gigantea* suggest closer affinity to *Alocasia*¹⁶. Studies on *C. esculenta* var. *aquatilis*, the putative ancestor of cultivated forms of *C. esculenta*, are likely to be particularly rewarding. First described from Java, it is found from India to China, Japan, Malaysia, Indonesia, Papua New Guinea, Northern Australia and Polynesia, although the natural range is likely to be less than its present distribution^{22, 24, 17}. *C. esculenta* var. *aquatilis* flowers profusely and sets viable seeds²². Ribosomal DNA analysis has shown diversity in Australian and Papua

New Guinea populations, suggesting “wild populations differentiated in partial isolation in diverse ecological circumstances”^{16, 22}. From DNA studies in Japan, it seems possible that *C. esculenta* var. *aqualitis* is a progenitor of the present day diploid taro from Japan and some triploids. More genetic studies are necessary to clarify the link between the living cultivars, wild types and hypothetical ancestor(s)¹⁷. Interestingly, evidence from Myanmar has shown that the wild form is used for pig feed and occasionally as human food, raising the intriguing suggestion that use of wild types as fodder was involved in the domestication of taro¹⁷. Other wild forms, apparently distinct from the wild types of Melanesia as well as local cultivars, are reported from New Caledonia. They may represent an earlier domestication before the present-day cultivars were introduced. Possibly they are endemic to New Caledonia, remnants of Gondwanaland, and therefore potentially a useful source of novel genes. What is required is a thorough DNA analysis of the diversity in wild and cultivated taro. This will provide evidence of the origin, domestication and dispersal of the crop²⁴. DNA work will also help clarify the taxonomy of wild taros, in particular decide if they are best divided in a number of species or can all be referred to *C. esculenta*. *Xanthosoma* is an important pan-tropical crop, with its centre of origin possibly in North-South America where some species were domesticated, probably from different wild forms. *Xanthosoma* is known to have been introduced to West Africa, Oceania and Asia. There are two main species, *X. sagittifolium* (L.) Schott and *X. violaceum* Schott²⁶.

1.5 Morphology

The morphology of aroids was studied from long back. Reports are also available on seed, shoot, floral and vegetative morphologies^{27, 28, 29, 11}. The fossil morphology of aroids was reported by Daghlian³⁰, fossil morphology of leaves by Wilde *et al.*³¹ and fossilized pollen morphology by Hesse and Zetter³². Diversity of the stem morphology was reported by Murata³³. Plants of the araceae have an abbreviated subterranean stem from which much information about their structure and life is obtainable. They reported the growth pattern of

stem, number of leaves per shoot, position of foliage leaf and the lateral continuation of shoot, nature of axillary bud and phyllotaxis of more than 50 species of *Arisaema*, including evergreen tropical species as well as deciduous ones. The characters are compared and related to each other resulting in the recognition of seven types of stem patterns in *Arisaema*. They also summarized the life of the evergreen and deciduous species and the significance of stem morphology for the systematics of *Arisaema*³³. Leaf types in araceae are described and classified on the basis of their morphology and functional role. Four classes are recognized on the basis of their association with the initiation of new shoot axes, the continuation of axes, the resting of axes, or the termination and renewal of axes. This represents an unconventional terminology because of the modified structures of the stem to which the leaves are attached, rather than to the form of the leaf itself. The intent is to draw attention to the impact of shoot organization on leaf form, and to develop a leaf terminology that will aid in describing the shoot organization³⁴. Cai *et al.*³⁵ described the morphological details of a new *Colocasia* species from China. They named the species as *C. yunnanensis* and compared the species with *Colocasia bicolor* with respect to tubercles, stolon, petiole, blade and distribution etc³⁵. Number of facets on starch grains and the morphology of raphides are of most use in distinguishing genera from each other in this group³⁶. *C. esculenta* is a widely distributed species, typified by very small smoothly round to sometimes angular starch grains and small and simple lath-like raphides. They can be separated from each other on the basis of mean grain size and standard deviation and by the fact that there are some very thin and long “whisker-like” raphides present in *C. gigantea* which are not found in *C. esculenta*. Four, widely distributed non *Colocasia* aroids *Cyrtosperma*, *Alocasia*, *Xanthosoma* and *Amorphophallus* have generally sub-round to ovate grain shape with a variety of well developed facets, reflecting the formation of compound grains during growth. All of them have long-well developed raphides with a variety of shapes³⁶.

1.6 Other characters

Thermogenesis in reproductive organs is known in several plant families, including araceae. Thermogenesis may ensure protection of flowers during the period of cold. The spadix of the eastern skunk cabbage is not frost-resistant, even though they can emerge from snow-covered ground³⁷. Avoiding frost damage, however, cannot be the primary function of thermogenesis. Most of the members of araceae are tropical species that would not have need to escape frost in nature, rather frost-avoidance by thermogenesis may reflect a physiological adaptation of a process that originally evolved in response to the selective pressure other than frost. Researchers have suggested that thermogenesis and thermoregulation may help to provide the optimum temperature for the flower development or pollen tube growth³⁸. Seymour and Blaylock found that warming did advance the development and early flowering of the eastern skunk cabbage but pointed out that the adaptive value of this was obscure³⁹. Many plants were observed completing their blooming beneath a layer of forest litter and sometimes a layer of snow³⁷. The thermogenesis in plants, a property which, according to the available literature, is connected with “cyanide resistance respiration”, a type of cellular respiration insensitive to inhibition by terminal inhibitors such as cyanide, azide and carbon monoxide (CO), and by inhibitors such as antimycin-A act between b and c-type cytochromes. A significant logarithmic relationship was reported between the volume of the thermogenic spadix zone and the maximum temperature difference between the spadix and ambient air⁴⁰. Four heat transfer models were reported, conductive, convective and radiative heat transfers, to test if physical (geometric and thermic) constraints apply⁴⁰. Two heat transfer models were found to be suitable and equivalent; conductive heat transfer alone and convective plus radiative heat transfers⁴⁰. The inflorescence of several members of the arum lily warm up during flowering and are able to maintain their temperature at a constant level, relatively independent of the ambient temperature. The heat is generated via a mitochondrial respiratory pathway that is distinct from the cytochrome chain and involves a cyanide-resistant

alternative oxidase (AOX). At low temperatures, the dehydrogenases are almost in full control of respiration but as the temperature increases, the flux control shifts to the AOX. Four inferences were proposed by Ito-Inaba *et al.*⁴¹; in all aroid flowers, AOX assumes almost complete control over the respiration. The temperature profile of AOX explains the reversed relationship between ambient temperature and respiration in thermoregulating *Arum* flowers. The thermoregulation process is the same in all species and variations in inflorescence temperatures could easily be explained by variations in AOX protein concentrations⁴¹.

1.7 Genetics of aroids

The genetic diversity of cultivated forms of *C. esculenta* was initially quantified by looking at morphological and cytological characters¹². There are diploid ($2n=2x=28$) and triploid ($2n=3x=42$) forms²⁴. Isozymes were used on major collections assembled in five South-East Asian countries and two Pacific countries. The results from these analyses suggested that there are two distinct gene-pools, South-East Asian and South-West Pacific. The overall diversity is low, except in Indonesia where the gene-pools overlap. The allelic diversity of wild taros included in the study was similar to that of the cultivated forms. A core sample of 168 accessions was identified based on these data^{42, 43}. Similar conclusions were drawn from further studies using RAPD, AFLP and SSR markers. Genetic variation is greater in South-East Asia than in the Pacific, with Indonesia again the most diverse, and diversity within most of the countries is low⁴⁴. These studies also showed that there is little genetic variation in Polynesian taros, in contrast to those from Asia and Malaysia. The high level of phenotypic variation in Polynesia is thought to be due to somatic mutations occurring in this vegetative propagated crop, suggesting that numerous Polynesian varieties are clones that are derived from very few original mother plants^{42, 43}. The results of a molecular study of taro genetic diversity using RAPD confirmed that although cultivars in the Pacific region exhibit remarkable morphological variation, the genetic base appears to be very

narrow⁴⁵. This is of critical concern, as a narrow genetic base is likely to leave the crop vulnerable to pests and disease attack⁴⁶. Further, studies on Pacific genetic diversity were made under TaroGen (Taro Genetic Resources: Conservation and Utilisation), a regional project funded by AusAID which, among other things, established a core collection which is maintained *in vitro* at the Regional Germplasm Centre, Secretariat of the Pacific Community, Fiji (Centre for Pacific Crops and Trees). This is representative of the genetic diversity within Pacific Island countries like Cook Islands, Fiji, New Caledonia, Niue, Palau, Papua New Guinea, Solomon Islands, Tonga, Samoa and Vanuatu⁴⁷. DNA fingerprint data using SSR markers showed that great allelic diversity exists in Papua New Guinea and Solomon Islands.

There is relatively little information on *Alocasia* as compared to the other genera. The genus contains about 65 species occurring from Sri Lanka and India, through Indo-China to China and Southern Japan, the Malaysian archipelago, Australia and Oceania⁴⁸. The main centre of diversity of the genus is Borneo, where there are estimated 23 species⁴⁸. It is not known where *Alocasia* was brought into domestication. Hay⁴⁸ considered *A. acrorrhizos* a cultigen, without wild forms, although it is possibly wild in Peninsular Malaysia⁴⁹. Probably a *macrorrhizos* has hybridised with *A. portei* to give a form with slightly wavy leaf margin in the Philippines⁵⁰. In India, *A. macrorrhiza* and *Colocasia* occur mostly in the humid tropical habitats of the Western and Eastern Ghats and in the North-East⁵¹. The crop is important, too, in some Pacific islands, notably Samoa, Tonga and Wallis and Futuna. The number of varieties is low and presumed that the species has a narrow genetic base⁴⁶. However, the crop has shown 32 potential varieties in the recent years. The production of three varieties grown in Samoa increased substantially following the devastation of *Colocasia* by taro leaf blight in the early 1990. Tonga has four varieties. There are no national collections of the edible forms of *Alocasia*, apart from India, which records seven varieties of *A. macrorrhizos*; however, there are collections of a number of ornamental species in botanic gardens and

nurseries. The Hortus Botanicus Leiden, the Netherlands, holds 42 and the Belgium National Botanic Gardens 17 accessions.

1.8 *Amorphophallus paeoniifolius*

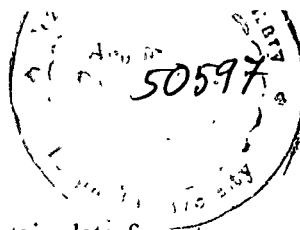
Amorphophallus is a native of tropical Asia, commonly known as elephant foot yam and its distribution was discussed by Hetterscheid and Ittenback⁵². West Africa is the western most limit, whereas the eastern limit is a line going from Japan, through Taiwan, the Philippines, and New Guinea to North-East Australia. There appears to be a high degree of endemism, with only *A. paeoniifolius*, *A. muelleri* and *A. abyssinicus* with a “fair geographic range”; this may indicate that the genus is actively speciating. Hay⁵³ put the number of species at about 100, with centers of diversity in Africa and Laurasian Malesia west of Wallace’s Line. *A. paeoniifolius* occurs in the Pacific, having reached Australia and New Guinea without human intervention. In Malaysia, it is still the practice to leave plants that are found when land is cleared for the cultivation from forest, although they are not used. However, some cultivars are still retained; others are introductions^{25, 54}. But, it is India where most of the diversity of the edible form exists and where it is relatively important among root crops. Within the network of ten research centers of the All India Coordinated Research Project on Tuber Crops, there are 195 accessions. Some selections have been made for the different regions and a hybrid released from a breeding programme^{55, 56}. In North-Eastern states, wild forms are used as vegetables as well as for medicine.

Diversity studies have been done on parts of the collection in India using morphological descriptors and isozyme markers, and further work needs to be done. Apart from India, studies are reported from Indonesia, with a collection of eight species (16 cvs known) reported from the Bogor Botanic Gardens, collected from Java, Sumatra and Kalimantan. There are two forms of *A. paeoniifolius*, one wild and the other cultivated⁵⁵. Many species have entered the nursery trade and there are many companies offering online sales of plants from Asian countries like Burma, Thailand, Vietnam, India, China and Japan.

One company advertising aroids of Yunnan has outlets worldwide. It would be a relatively simple exercise to compare the known species with those that are available commercially. It does appear, based upon a brief survey that many of these fascinating plants are well conserved, with one caveat that the genetic diversity retained by nurseries may not be representative of that in the natural populations. There are also collections at botanic gardens like 7 accessions in National Botanic Garden of Belgium; 42 accessions in Royal Botanic Gardens, Kew; 9 accessions of *A. paeoniifolius* and 7 of *A. rivieri* in Royal Botanic Gardens, Sydney and 530 accessions in Hortus Botanicus Leiden, the Netherlands. Useful notes on the geography, ecology and conservation, but mostly relating to *A. titanium*, can be found on the International Aroid Society website, adapted from Hetterscheid and Ittenbach⁵².

1.9 *Xanthosoma sagittifolium*

As with the edible species of *Colocasia*, those of *Xanthosoma* are also pan-tropical; however, the origin of the genus is tropical America, possibly in Northern part of South America, where some species were domesticated, probably from different wild forms⁵⁷. *Xanthosoma* was introduced to West Africa, Oceania and Asia in the 19th century^{58, 59}. Today, it is ranked sixth in cultivation and production and an important food for some 400 million people^{60, 61}. It has overtaken *Colocasia* as the main edible aroid in many tropical areas¹⁷. Taxonomists have described a number of edible species based on leaf shape, pigmentation and other vegetative characters. Wilson⁵⁹ listed *X. violaceum*, *X. atrovirens*, *X. caracu*, *X. jacquini*, *X. maffafa*, *X. belophyllum* and *X. brasiliense*. Clement⁵⁷ stated that the taxonomic position of the cultivated *Xanthosoma* species is unclear, and in recent years the tendency has been to give the name of *X. sagittifolium* to all cultivated *Xanthosomas*. But this distinction is based on morphological features like colour of the corm, cormels and leaves and shape of cormels that seem unconvincing as a basis to separate the species. The phylogeny of *Xanthosoma* is being studied at the Universidade Católica de Brasília, Brazil as well as the cytogenetics of more than 30 wild and



cultivated species, maintained in order to obtain data for a taxonomic revision. Crop improvement was tried in Cameroon through hybridization between the different genotypes. Some attempts were made to produce new forms through *in vitro* culture and breeding continues in the Caribbean^{61, 62}. In Cuba and Sri Lanka four species (*X. violaceum*, *X. atrovirens*, *X. caracu* and *X. sagittifolium*) were described. Studies in Cuba concluded that classification based on one or a few morphological characters does not show the true genetic variability within the genus, and that DNA markers are needed. In this regard, analyses of *X. sagittifolium* in the cocoyam collection in Florida showed very little genetic variation⁶³. Characterization would indeed seem a priority that too filled up the gaps in *Xanthosoma* collections. Major collections of *X. sagittifolium* from Cameroon, Equatorial Guinea, Gabon, Ghana, Puerto Rico, Togo and Central and South America were made between 1986 and 1991, and maintained at the Institute of Agricultural Research, Ekona, Cameroon^{61, 62}. The collections were evaluated for petiole length, yield and incidence of Pythium infection⁶¹. Over 300 accessions were assembled; many of them were considered landraces of previous introductions, especially by the Portuguese. Hybridization resulted in the production of more than 10,000 seeds from “white” x “white and “white” x “red” crosses, but few viable seeds from “white” x “yellow” or “red” x “yellow” crosses, perhaps due to ploidy differences⁶¹. Unfortunately, funding for the maintenance of the collection ended in 1994, and by 1997 there were substantial losses⁶². A collection of 70 *X. sagittifolium* accessions at the University of Ghana showed that the diversity present was of potential interest to plant breeders and those concerned with conservation⁶⁴.

1.10 Food

The food value of the different parts of edible varieties of aroids like corms, stem and leaf varies extensively. In many places, processing of corms depends on the edibility. The prospect of biotechnological application of aroids in food processing was reviewed by Jube and Borthakur⁶⁵. The composition of aroids could be used for formulating different types of processed food.

Extending the biochemical study of food materials from simple proximate composition to complete phytochemical composition is necessary to evaluate the nutraceutical properties of the food materials completely. In Assam, the corms are usually eaten boiled, mashed or sometimes pounded, frequently mixed with other staples, such as citrus fruits. Traditionally it was done to diminish acidity and enhance tests. The source of starch varies all over the world and it depends on the tradition and prevalent climatic conditions. However, it is starch and starch derivatives of maize and potato that are of commercial interest⁶⁶. World production of the crop is estimated to be 5.5 million tones annually and provides about a third of the food intake of more than 400 million people in the tropics⁶⁷. The nutritional value is the main concern when a crop is being considered as a food source. The high starch content of most root crops is considered as excellent energy source, but they are marginal to poor sources of protein^{68, 69}. Root crops contain a wide variety of minerals and trace elements, including relatively substantial quantities of iron and calcium, as well as potassium and magnesium^{70, 71, 72}. The dietary importance of root crops has led workers to devise various means to determine the composition of food commodities. Several authors have evaluated the chemical composition of the whole corm and cormels of both *X. sagittifolium* and *C. esculenta* species^{68, 73}. It has been observed that, in spite of the fact that cocoyams are neglected crops; their compositional value is high, with an average protein content of 6% and 390 calories per 100 g dry matter. Agbor-Egbe and Richard⁷⁴ compared the composition of 32 cultivars of *X. sagittifolium* species and *C. esculenta* species and reported difference among the species. This observation supports earlier work done by Coursey⁵⁸ which indicated that the composition of food commodities are dependent on the variety, location, season, method of processing and storage. Aroid corm protein was reported in detail by Shewry⁷⁵. Flour of *C. esculenta* corms are reported to increase the keeping quality of wheat based products⁷⁶. The biochemical composition of the leaf of *C. esculenta* was reported by Sahoo *et al.*⁷⁷. The oxalate composition of *C. esculenta* leaf was reported as 524.2 ± 21.3 mg in 100 gm fresh weight⁷⁸.

The biochemical composition of *X. sagittifolium* corm was reported by Omokolo and Boudjeko⁷⁹. Biochemical composition of *Amorphophallus* corm was reported by Das *et al.*⁸⁰. Recently, antioxidant activities of two aroid extracts were reported by Mandal *et al.*⁸¹. They reported two neglected species of araceae as important food and ethno-medicine in Asia and Africa (*Alocasia macrorrhiza* (Linn.) G. Don and *A. fornicata* (Roxb.) Schott). Their results suggested that two aroid species have antioxidant activity in their edible parts⁸¹.

1.11 Cultivation

The major aroids comprise taro (*Colocasia esculenta* (L.) Schott), *Xanthosoma* species and swamp taro (*Cyrtosperma merkusii* (Hassk.) Schott), syn. *C. chamissonis* (Schott) Merr.). Taro, *Colocasia esculenta* (L.) Schott (see photo below) is grown for its corm. *Xanthosoma* is vegetatively propagated from corm sets, headsets or cormels. Although flowers occur and seeds are viable, flowers are rare in most varieties and non-existent in some. In addition, seedlings may not breed true and hence are not recommended for regeneration. All four (*C. esculenta*, *X. sagittifolium*, *X. caracu* and *A. paeonifolius*) crops require moist soils and none could tolerate drought. Taro (*C. esculenta*) needs reliable rainfall throughout the growing season or irrigation, moist soils and temperatures around 25°C. *Xanthosoma* grows in lowland and upland situations, with well-distributed rainfall, 1500-2000 mm annually; a mean temperature above 20°C, and freely draining soil of pH 5.5-6.5. It tolerates light shade but grows well in the open. In the case of *C. esculenta* planting sets, suckers or cormels in tropical latitudes and dry land conditions are planted at the onset of the rainy season. Suckers could be planted in wetland tropical conditions at any time of the year as long as water is available; in temperate latitudes cormels are planted in spring, but at high altitude, during the warmer, wetter time of the year. In the case of *Xanthosoma* species if water is available, either through irrigation or well-distributed rainfall, planting could be done at any time of the year. There is no seasonality. There are variations in the regeneration techniques among *Colocasia* and *Xanthosoma* species. In the case of *Colocasia*,

regeneration is obtained after 5-15 months of one crop cycle, depending on variety and growing conditions. In many species, the time to regenerate depends on when the mother or central plant starts to die. Although *Xanthosoma* species are perennial, it is best to regenerate the crop after 9-12 months when the central or mother plant begins to die. If evaluations for yield or organoleptic qualities are not of concern, the crop can be left in the ground. Delaying the harvesting for too long period may lead to rotting of roots. The majority of *Amorphophallus* species can be grown in humus-rich, rather organic, well drained and well aerated soil at some 20°C (optimal 25°C) during summer in a semi-moist soil in a partially shaded spot with protection from direct sunlight, especially during hours at midday. Few tropical species, such as the famous *Amorphophallus titanum* from Sumatra require a higher average temperature of some 25°C throughout their growing cycle. Few species have a prolonged growing cycle which exceeds 12 months, or are even ever green; however in most species the single leaf starts to yellow in autumn. At this point plants should be kept absolutely dry at a minimum of some 10°C. The tuber in immature specimens may increase its weight threefold in a single season. Most tubers stay dormant for some 3 to 7 months. Most *Amorphophallus* species flower before the leaf unfolds, whereas some may rest for the entire year.

1.12 Compounds and bioactivity

Araceae is a large, mainly tropical family, many members of which contain bioactive substances which are often either toxic or irritating. Inflorescences frequently emit strong fragrance. The active compounds have not been adequately determined, not even the chemotaxonomy of the family. Two groups of compounds of known bioactivity are alkylresorcinols and nitrogenous sugar analogues, have been sought in representative species from most of the genera in the family⁸². Although percentage sampling was necessarily small, a few examples of species containing these substances were found and some taxonomic suggestions were made and compared with results in the literature. Compound isolation from aroid corms was reported by Agbor-Egbe and

Rickard⁷⁴. They reported the phenolic compounds present in the cormels of the edible aroids, *Colocasia spp* and *Xanthosoma spp*. Their investigation showed the presence of a range of phenolic compounds which includes gallic acid, chlorogenic acid, (+)-catechin, (-)-epicatechin and (-)-epigallocatechin and the possible presence of proanthocyanidins and flavones.

1.13 Aroid Starch

Most of the estimated 2500 million tonnes of starch crops harvested annually is consumed directly as food or used as animal feed, but there is increasing demand from nonfood industries for starch as a renewable raw material. In particular, starch is a major feedstock for first-generation biofuels due to the relative ease with which it can be converted to fermentable sugars⁸³. Amylopectin and amylose of aroids together form semicrystalline, insoluble granules with an internal lamellar structure. Amylopectin is the major component, typically making up 75% or more of the starch granules. A large branched amylopectin has an estimated molecular weight between 107-109 daltons⁸⁴. The glucosyl residues of amylopectin are linked by α -1,4-bonds to form chains of between 6 and >100 glucosyl residues in length. The α -1,4-linked chains are connected by α -1,6-bonds (branch points). Amylopectin is responsible for the granular nature of starch. Although its exact molecular architecture is not known, the combination of chain lengths, branching frequency, and branching pattern gives rise to a racemose or treelike structure in which clusters of chains occur at regular intervals along the axis of the molecule. Typically, chains within these clusters average between 12 and 15 glucosyl residues. The less abundant chains that span two clusters contain approximately 35–40 residues, while those that span three clusters contain approximately 70-80 residues^{84, 85}. Within the starch granules amylopectin molecules are radially organized such that the free (nonreducing) ends of the chains point towards the periphery. Pairs of adjacent chains within clusters form double helices that pack together in organized arrays, giving rise to concentric, crystalline layers (lamellae) within the granule. These lamellae alternate with

amorphous lamellae formed by the regions of the amylopectin molecule that contain the branch points. The lamellar organization is repeated with a 9-10 nm periodicity. This semicrystalline structure makes up the bulk of the matrix of the starch granule and is highly conserved in higher-plant starches^{86, 87}. It seems possible that the organization of amylopectin to form the granule matrix is largely a physical process.

Edible aroids are subsidiary food in tropical and subtropical countries⁸⁸. Environment influences size and distribution of starch granules⁸⁹. The starch type depends on the environmental conditions in which the plant grows. In *Hordeum spp.*, the stresses induced by high temperatures tend to reduce the number of A-type starch granules, but proportionately the effect is less in the case of B-type granules⁹⁰. Langeveld *et al.*⁹¹ hypothesized that small granules are formed in vesicles, bobbed off from the out-growth of A-type granules containing amyloplast. The hypothesis was supported by the presence of B-type granules as revealed through transmission electron microscopy and confocal laser scanning microscopy.

Starches have many deficiencies like poor antioxidant, high density and susceptibility to microbial attack. With compensation against these deficiencies, the starch will become a potent base material for many biological and non-biological industrial applications. Emergence of polymeric biomaterials in contemporary times is multidisciplinary and is challenging to the extreme as they can make the living standard of human beings one step in front. Such biomaterials are generally synthetic polymers finding applications in artificial organs, implantable devices, prostheses, ophthalmology, dentistry, wound dressings, tissue engineering and in drug delivery systems⁹². The prerequisite for a polymeric material to be applicable as an ideal biomaterial is biocompatibility which in turn depends on its mechanical properties, biodegradability as well as cytotoxicity⁹³. Bulk commodity polymers have been developed as biomaterials, among which only a few are found to be promising. Polymer nanocomposites pave a way to create the prospective for avant-garde materials by amalgamation of flexible organic polymer with stiff inorganic

components. The unison of properties of nylon 6 and clay nanocomposites led to emanation of a truck load of novel polymeric materials⁹⁴. Incorporation of layered nanofillers can significantly impact the microphase morphology of the polymers and blends by acting as templates for the structural development⁹⁵. Material properties of nanocomposites improve dramatically due to significant change in microphase domain size and shape of the polymeric structure by incorporation of the nanofillers without affecting light weight characteristic of the pristine polymer. Composite materials are synthesized with a view to compensate each others deficiencies. The idea of combining a natural biodegradable, non-toxic polymer with a synthetic functional polymer is relatively new and can bring about an entirely new direction in the research of advanced functional materials for the future. The utilization of metal oxide particles in biomedical field has attracted growing interest. These particles are now being used as carriers in various biotechnological applications. It was reported that certain iron oxide particles are efficiently internalized into cells. The uptake of these particles by macrophages was quantified by an electron spin resonance (ESR) experiment of Billotey *et al.*⁹⁶. A laboratory technique to quantify the uptake of these particles in biological cells and their kinetics was demonstrated for macrophage cells by Wilhelm *et al.*⁹⁷. The nanoparticles loaded quercetin molecules have been reported to enhance their antioxidant capacity⁹⁸. Different types of adsorbants, such as Chromosorb, Tenax, Porapak and Chezacarb were magnetically modified and used for the pre-concentration and isolation of the pollutant compounds^{99, 100}.

Starch, a natural and easily available polymer consisting of amylose and amylopectin can easily be extracted and purified from the natural sources. Plants with underground storage organs, well known for their high starch content could be used for the extraction of starch. Polyaniline, on the other hand, is a highly functional synthetic polymer which is unique among the family of π -conjugated polymers because of its ease of synthesis, good environmental stability and simple acid/base doping/dedoping chemistry. Polyaniline has found immense applications in diverse areas¹⁰¹. A range of

biomedical applications for the conducting polymers are currently being considered including the development of artificial muscles, controlled drug release and the stimulation of nerve regeneration¹⁰². Low cytotoxicity and good biocompatibility are evident from the growth of cells in conducting polymers and the low degree of inflammation seen in test animals for several weeks¹⁰³.

1.14 Objectives

In view of the above mentioned back ground information, the following objectives were taken for the present research work:

1. Morphological characterization of aroids.
2. Study on chromosome number and karyotype.
3. Genome size determination and genotyping using RAPD based marker analysis.
4. Estimation of the nutritional components like protein, carbohydrate, lipid and some essential minerals and preparation of a composite.
5. Biochemical assessment of aroids and testing their antimicrobial activity.

CHAPTER 2

REVIEW OF LITERATURE

The family Araceae, commonly known as aroids, encompasses 105 genera and more than 3,300 species, mostly being herbaceous. Though the selected species are solely grown for food, they are also used as traditional medicines in the North Eastern part of India¹⁰⁴.

Morphological data can help in phylogenetic study of plants when compared to the of fossil records¹⁰⁵. For legal protection of an economic plant the morphological record serves a lot¹⁰⁶. The morphological details of the *X. sagittifolium* were reported by Reyescastro *et al.*¹⁰⁷. Along with the morphological study the karyotyping is a good identity proof for most of the plants. The morphology of aroids was reported by different researchers¹⁰⁸, *C. esculenta* by Quero-Garcia *et al.*¹⁰⁹, Wang¹¹⁰, Kawasaki *et al.*¹¹¹, Lakhanpaul *et al.*¹¹² and Strauss¹¹³. The karyotyping of the aroid crops was reported by Chauhan and Brandham¹¹⁴ and Petersen¹¹⁵. They collected samples from throughout India for morphological as well as genetic study. The morphology of *Amorphophallus titanum* was reported by Camp¹¹⁶. The morphology of new *Amorphophallus* species from China was reported by Li and Long¹¹⁷. Bogner *et al.*¹¹⁸ reported three new species of *Amorphophallus* from Asia¹¹⁸.

Species richness of Amazonian region was reported by Leimberk and Balslev¹¹⁹. They reported that 89% of the trees carried epiphytic aroids, and there were significantly higher numbers of aroid-carrying trees on floodplains where 98% of trees had aroids, compared to 82 and 86% in transition and upland transects, respectively. Two aroid-free trees represented *Duroia hirsuta* (*Rubiaceae*), a myrmecophyte whose ants protect it from epiphytes. Most epiphytic aroids grew on the lower parts of the trunks, 90% in the first 8 m from the ground; the median epiphyte height above ground was 2.9 m. Aroids were observed up to a maximum height of 22 m above the ground. Mean tree density in all terrain types was estimated at 1312 trees per ha. Density was lowest on the floodplain (1012 trees/ha); in transition and upland forest, tree density was 1515 and 1509 trees/ha, respectively. Other variables such as phorophyte bark hardness and texture, canopy height and light did not differ significantly either. For the likelihood ratio test used, the categories of bark texture rough and

peeling, canopy height class one and two, and light intensity categories. The species diversity in Colombia was reported by Croat¹²⁰. With the possible exception of eastern Brazil, the region most poorly known floristically in South America is the slopes of the Andes in western South America. Species diversity is greatest in the wet tropical areas on both sides of the equator in Colombia, Ecuador, and Peru. The aroids are effectively eliminated from the Pacific slope of Peru and southern Ecuador owing to the Humboldt Current desertification, whereas Colombia is exceedingly rich on the very wet Pacific slope, leading to much greater overall species diversity. This fact, coupled with the high rate of endemism in the family and the much more complex mountain system in Colombia, has created a situation where the aroid flora of this country is the highest of any region in the world. Parts of Ecuador are certainly as species-rich per unit area, but the country is much smaller and geographically less complex. The South American Andes is poorly known owing to the large number of species occurring in the region and their taxonomic complexity. The genus *Philodendron* and some sections of *Anthurium* are particularly poorly known. Since these two genera may constitute 70-80% of the aroid flora, any given local flora may be very poorly known to the species level. Other complex and poorly known genera, especially at lower elevations, include *Dieffenbachia*, *Monstera*, *Rhodospatha*, and *Spathiphyllum*. *Stenospermation*, rich in species and even more poorly known, is particularly diverse at middle to high elevations in the Andes. The biodiversity of the aroids in Mexico was reported by Wolf and Flamenco¹²¹. In Costa Rica, epiphytic bromeliads are also most common in mountain areas. Above 2000 m, the number of epiphytic aroids and orchids decreases rapidly. After an initial rise in species richness, the number of epiphytes decreases again when rainfall exceeds 2500 mm annually. All species-rich groups exhibit this pattern, except the aroids that remain comparatively stable. Again in important plant groups such as ferns, the bromeliads and orchids, the number of epiphytes decreases when annual rainfall exceeds 2500 mm, while aroids remain stable. Coast in Colombia (annual

rainfall of 5100–7150 mm), aroids were with 100 species even the largest plant family, comprising over 10% of the total vascular flora.

The plant-parasitic nematodes associated with various aroid species are reported by Amsing *et al.*¹²². Species of *Meloidogyne*, particularly *M. incognita* and *M. javanica*, are the most widely reported nematode pests of both *Colocasia* and *Xanthosoma* but the severity of crop damage varies widely, depending on plant cultivar, growing conditions, nematode population, and geographical location. *Rotylenchulus reniformis* is also widely reported on the aroids, and low initial populations built up to high levels on *Xanthosoma caracu*, *X. atrovirens*, *X. violaceum* and *Colocasia esculenta*. Reports are also available with preplant populations of 56 *R. reniformis*/100 cm³ of soil and final populations of about 400/100 cm³ of soil, a significant (P = 0.05) reduction of 26% in marketable dry cormel weight of *X. caracu* occurred in non-treated plots when compared to fumigated plots, but yield of *X. atrovirens* was not affected. Yield of *C. esculenta* grown under plastic mulch culture was not increased by fumigation treatment, even though very high levels of *R. reniformis* built up in non-treated control plots. Other plant parasitic nematodes reported to associate with taro are *Criconeimidae spp.*, *Longidornis siddiqi*, *Helicotylenchus spp.*

Chromosomal variation in the *C. esculenta* was reported by Coates *et al.*²². Chromosome number of the cultivated types of *Colocasia esculenta* from China was reported by Zhenhua¹²³. A review on the variation of chromosome number in Araceae was reported by Marchant¹²⁴. The mitotic index study of the edible cocoyam visibly *Colocasia* and *Xanthosoma* species were reported by Ekanem and Osuji¹²⁵. The chromosome number of *Amorphophallus zengianus* was reported by Chunlin and Heng¹²⁶. Karyotyping of *Amorphophallus* from China was reported by Li *et al.*¹²⁷.

The amount of nuclear DNA and size of the genome (C-value) are two important biodiversity parameters. Study on them provides a strong unifying element in biology with practical and predictive uses. The C-value stands for 'constant'; the constant amount of DNA which could be a characteristic of a

particular genotype¹²⁸. Hinegardner¹²⁹ described genome size as an important biodiversity parameter. Till date, flow cytometry and fuelgen densitometry are the standard methods for the determination of genome size. But, these established techniques need sophisticated instruments, which is not possible in all situations. Although, the flow cytometry yields almost accurate and reproducible amount of 2C DNA content of plant species, the problem starts with expeditions to more distant areas, when the transport and maintenance of the material become an issue. Moreover, the cost of establishing a flow cytometry laboratory may be prohibitive in certain areas¹³⁰. The North Eastern region like many other region of the country, regarded to be the biodiversity hotspot, is yet to establish a flow cytometry laboratory. Another easy method for estimation of genome size was described by Konwar *et al.*¹³¹.

The RAPD analysis of *C. esculenta* and *X. sagittifolium* were reported by Irwin *et al.*⁴⁵ and Lakhanpaul *et al.*¹¹². Ochiai *et al.*¹³² reported RAPD analysis of *Colocasia esculenta* and *Xanthosoma sagittifolium* from different geographical locations. The RAPD analysis of the Amorphophallus species were also reported by Wenbing *et al.*¹³³ and Zhen and Jia-yi¹³⁴.

The flours prepared from the edible part of *C. esculenta* and *X. sagittifolium* did not show significant difference in moisture, crude protein, total sugars, amylose, and amylopectin contents. *C. esculenta* flour showed higher crude fat, total, soluble, and insoluble dietary fiber, and mineral (P, Ca, Fe, and Zn) contents, whereas *X. sagittifolium* flour showed higher starch, ash, and reducing sugar content than *C. esculenta*. With regard to physical and physicochemical characteristics, *X. sagittifolium* flour showed higher titratable acidity and relative density, being darker and more yellowish than its counterpart. *X. sagittifolium* flour showed higher gelatinization temperature as compared to *C. esculenta* flour. Parameters such as viscosity setback and consistency were lower in *C. esculenta* flour than *X. sagittifolium* flour. They also proposed from their study that the flour prepared from the aroid corm powder could be considered as dry food and self stable food because of their low moisture content and water activity¹³⁵. Meija and Soukup¹³⁶ reported the

presence of phenyl terminated fatty acids in different aroid seed oils. Huang *et al.*¹³⁷ reported a study on the peels of *C. esculenta*. They reported that breaking the peels in to micro-particles using different millings will lead to change in the physicochemical properties. The contrasting differences reported were increase in the soluble fiber percentage, particles solubility and water holding capacity. Micronization would expected to be helpful in the preparation of dietary fiber supplement from food waste in the food processing industries. The oxalate content of some edible *C. esculenta* leaves was reported¹³⁸. Glycemic index (GI) has been widely used in the management of blood sugar level among diabetics however; in the South Pacific region very little information regarding the GI of local foods is made available. Lako *et al.*¹³⁹ reported the glycemic index and the glycemic load of *X. sagittifolium* is of moderate range³⁸. Bahado-Singh *et al.*¹⁴⁰ reported from their research on glycemic index that *C. esculenta* and *X. sagittifolium* GI depends on the processing methods³⁹. In the study they found that the roasting and baking increases the GI, boiling and frying decreases the GI value of the corms. The micronutrient estimation of *C. esculenta* and *X. sagittifolium* was equally important not only to establish them as good source of minerals but also to find out the level of toxicity in the soil. The detailed study on the higher levels of arsenic, mercury and cadmium like toxic metals was reported to exist by Essumang *et al.*¹⁴¹. Dilworth *et al.*¹⁴² reported that availability of Ca, Fe and Mg etc minerals in the cooked and uncooked tubers (*C. esculenta* and *X. sagittifolium*) crops upon digestion showed a similar pattern. They suggested that consumption of these tuber crops in the Caribbean might not be responsible for the reported cases of iron deficiency in the region. However, the availability of minerals from these tuber crops when consumed with other foods needs further investigation. *C. esculenta* and *X. sagittifolium* though popular as food, many biologically active compounds with the potential antifungal activity were reported by Schmourlo *et al.*¹⁴³. The presence of different types of secondary amines in *X. sagittifolium* and their quantification were reported by Uhegbu¹⁴⁴. They reported the presence of diethylamine, dimethylamine, morpholine, ethylaniline and praline in *X. sagittifolium*. Use of

X. sagittifolium as the substrate for the production of beer was reported by Onwuka and Eneh¹⁴⁵. They found *X. sagittifolium* have more potential in the beer production as compared to barley and sorghum because of its potentially higher carbohydrate content (71-78%) as compared to barley (65%) and sorghum (70-73%). The natural defense mechanism of *X. sagittifolium* is more than *C. esculenta*. Crude aqueous extract from peripheral rot zone of cocoyam tubers infected by *Sclerotium rolfsii* Sacc. were shown to be inhibitory to be dialysed *in vivo* polygalacturonase (PG) of the pathogen. PG inhibitory action, phenol oxidase and peroxidase activities were higher in cocoyam tubers of *X. sagittifolium* than those of *C. esculenta* cultivars. The levels of phenol oxidase, peroxidase and PG inhibition also decreased as the postharvest age of tubers increased¹⁴⁶. The vitamin composition of the edible aroids was reported by Rashid and Daunicht¹⁴⁷. The chemical composition of *C. esculenta* corms was reported by Hussain *et al.*¹⁴⁸. Nutritional quality of *C. esculenta* (L.) Schott cultivar *Guavir* corms with respect to starch and unavailable carbohydrates (cellulose, hemicellulose and pectin) were 54 and 15% of the dry matter respectively. Lipid accounted for less than 1% of the dry matter. Palmitic, oleic and linoleic acids were the main fatty acids in the lipids, with linoleic acid predominating. Crude protein amounted to 10.4% of the dry matter. This protein was low in the sulphurcontaining amino acids and tryptophan, but contained adequate levels of the other essential amino acids. The high starch content of most of the root crops is considered to be an excellent energy source, but they are marginal to poor sources of protein^{68, 69}. Root crops contain a wide variety of minerals and trace elements, including relatively substantial quantities of iron and calcium, as well as potassium and magnesium^{70, 71, 72}. The dietary importance of the root crops has helped workers to devise various means to determine the composition of food commodities. Several authors have evaluated the chemical composition of whole corms and cormels of both *X. sagittifolium* and *C. esculenta*^{68, 73}. Cocoyams are neglected crops but their compositional value is high, with an average protein content of 6% and 390 calories per 100 g dry matter. Agbor-Egbe and Richard⁷⁴ compared the composition of 32

cultivars of *X. sagittifolium* and *C. esculenta* species⁵⁴. They reported difference among the species. This observation supports earlier work done by Coursey⁵⁸ which indicated that the composition of food commodities are dependent on the variety, location, season, method of processing and storage⁵⁵. The detail report on aroid corm protein was reported by Shewry⁷⁵. The flour of *C. esculenta* corms was reported to increase the keeping quality of the wheat based products⁷⁶. Traditional food items were prepared like achu, poi etc by processing *C. esculenta* corms¹⁵⁰. The biochemical composition of the leaf of *C. esculenta* was reported by Sahoo *et al.*⁷⁷. The oxalate composition of *C. esculenta* leaf was reported as 524.2 ± 21.3 mg in 100 gm fresh weight⁷⁸. The biochemical composition of *X. sagittifolium* corm was reported by Omokolo and Boudjeko⁷⁹. The biochemical composition of *Amorphophallus* corms was reported by Das *et al.*⁸⁰. The biochemical composition and nutrient content of the edible parts of *C. esculenta* was described by Hussain *et al.*¹⁴⁸. Nutrient composition of *C. esculenta* cultivars from Papua New Guinea was reported by Wills *et al.*⁷³. The mineral composition of leaves of *Colocasia* and *Xanthosoma* species was reported by Barminas *et al.*¹⁵¹. Agbor-Egbe and Rickard⁷⁴ compared the chemical composition of fresh and stored *Colocasia* and *Xanthosoma* species⁵⁴. The biochemical composition of the *Amorphophallus paeoniifolius* was reported by Chattopadhyay *et al.*¹⁵².

Raeker *et al.*¹⁵³ reported the presence of significant difference in amylose content among aroid cultivars. The negative correlation between amylose content and starch granule size explain, at least in part, cultivar dependency of granule size. Starch being a low-cost and renewable resource, could be used as fillers in the development of biodegradable polymer products¹⁵⁴. Starch with smaller granules show slightly higher viscosity in the starch filled poly-hydroxyl-ester-ether composites¹⁵⁵. Plastic film-incorporated starch produce porous structures enhancing accessibility of plastic molecules to oxygen and microorganisms^{156, 157}. Starch morphology and granule size are genetically controlled. It is also known that genetic variation and environmental condition influence structure and properties of starch^{158, 90}. Therefore, an effort

has been made to determine the granule size, crystallinity, composition and physicochemical properties of starch present in *C. esculenta* var. *Ghe Kochu* grown in NE India. The physico chemical properties of four different starches were reported in our published paper¹⁵⁹.

A. campanulatus species is analgesic and used in the treatment of piles^{160, 161}. Traditionally, the stem sap of aroids has been applied on cuts and ear infections. Very scanty information is available on aroids of this moderate and humid geographical region of uneven topology. Researchers from other places of the world reported the presence of amylase inhibitor in the aroid corms¹⁷. Sakano *et al.*¹⁶² reported the presence of human lenosterol synthase inhibitor from *C. esculenta* species. Six different flavonoid glycosides were reported from *C. esculenta* shoot¹⁶³. Kim *et al.*¹⁶⁴ reported several compound from *Colocasia* species having antioxidant as well as antimelanogenic activity. Lewu *et al.*¹⁶⁵ reported the presence of toxic compounds in *Xanthosoma* leaf which reduces the body weight¹⁶⁶. Antifungal activity of the aqueous extracts of *X. sagittifolium* was reported by Schmourlo *et al.*¹⁴³. The tubers of *Amorphophallus* species were reported to contain betulinic acid, beta-sitosterol, stigmasterol, lupeol, triacontane and beta -sitosterol palmitate⁸⁰. Some Chinese medicinal formulations prepared from *Amorphophallus* species were reported to prevent fatness in rats¹⁶⁷. In traditional Chinese medicine (TCM), a gel prepared from the flour has been used for detoxification, tumour-suppression, blood stasis alleviation and phlegm liquefaction etc¹⁶⁸. The detoxification property of *Amorphophallus* species is supported by an inhibition of DNA damage as reported by Yeh *et al.*¹⁶⁹. Some of the Indian medicinal formulations used in the treatment of piles known to contain *Amorphophallus* species corms as a constituent¹⁶¹. The antioxidant activity of the *C. esculenta* leaf was reported by Tarwadi and Agte¹⁷⁰. Many aroids were used in different traditional medicine reported to contain anti-inflammatory, anti-cholinesterase and antioxidant property¹⁷¹. Flavonoid glycosides from the shoot system of *C. esculenta* was reported by Leong *et al.*¹⁶³. Kim *et al.*¹⁶⁴ reported lignans from the tuber-barks of *C. antiquorum* having antimelanogenic Activity. Many other medicinal

properties of *Colocasia* species were reported by Fawole *et al.*¹⁷¹. Mollik *et al.*¹⁷² reported the use of *X. sagittifolium* in many different folk medicines in Bangladesh. Volpato *et al.*¹⁷³ reported the use of *X. sagittifolium* in the traditional medicines of Cuba. Antibacterial, antifungal and cytotoxic activities of amblyone isolated from *A. campanulatus* was reported by Khan *et al.*¹⁷⁴. Chua *et al.*¹⁶⁸ reported the traditional uses and potential health benefits of *A. konjac*. Freedman¹⁷⁵ reported that the polyphenolic antioxidants protect tissues from intensive pulse light therapy. Yang *et al.*¹⁷⁶ reviewed the cancer prevention by antioxidant beverages like tea. Rushworth and Micheau¹⁷⁷ reported the use of natural antioxidants in the treatment of resistant cancer cells.

Phenolics display a wide variety of structures, ranging from simple moieties containing a single hydroxylated aromatic ring to highly complex polymeric substances^{178, 179}. The biosynthetic pathways of phenolic compounds in plants are quite well known^{180, 181, 182}. The biosynthesis and accumulation of secondary compounds can be an endogenously controlled process during the developmental differentiation or it can be regulated by exogenous factors such as light, temperature and wounding. Phenylalanine, produced in plants via the shikimate pathway, is a common precursor for most of the phenolic compounds in higher plants. Similarly, hydroxycinnamic acids, and particularly their coenzyme A esters, are common structural elements of phenolic compounds, such as cinnamate esters and amides, lignin, flavonoids and condensed tannins. The phenylalanine hydroxycinnamate pathway is defined as general phenylpropanoid metabolism. It includes reactions leading from L-phenylalanine to the hydroxycinnamates and their activated forms. The enzymes catalysing the individual steps in general phenylpropanoid metabolism are phenylalanine ammonia-lyase (PAL), cinnamic acid 4-hydroxylase (CA4H), and hydroxycinnamate: coenzyme A ligase (C4L). These three steps are necessary for the biosynthesis of phenolic compounds. A growing body of evidence indicates that phenylpropanoid and flavonoid pathways are catalysed by several membrane-associated multienzyme complexes¹⁸³.

Starch based materials has been extensively used both in biological and non-biological applications. Starch enforced rubber composites have been prepared for potential applications in the tyre industry. Starch-based materials called BioTRED have been used by Goodyear Tire Co., in order to reduce tire weight and rolling resistance and simultaneously to decrease the energy consumption in the production processes¹⁸⁴. The Goodyear GT3 is claimed to be the first tire in the market using BioTRED which is expected to be used in the fuel-economic version of the Ford Fiesta. There has also been a report on applications of starch and starch-based materials in different biomedical applications¹⁸⁵, paper and pulp industry¹⁸⁶, food packaging industry^{187, 188}. Santander-Ortega *et al.*¹⁸⁹ reported the use of modified starch nanoparticles in trans-dermal drug delivery. Freire *et al.*¹⁹⁰ reported the starch based colon specific drug delivery. Sun *et al.*¹⁹¹ reported a novel drug delivery system using nanoparticles. Nanoparticle based targated drug delivery was also reported by Singh and Lillard¹⁹². Nanoparticles decorated with multiple magnetite nanocrystals for the simultaneous enhanced magnetic resonance Imaging, Fluorescence Imaging, and drug delivery was reported by Lee *et al.*¹⁹³. Victor *et al.*¹⁹⁴ reported the mitochondria-targeted antioxidant delivery for the treatment of sepsis and septic shock¹¹⁵. A composite of polyaniline and corm starch from corn was reported by Egashira *et al.*¹⁹⁵ to prepare a drug-coating nanoparticle.

Free radicals are generated and induced in the biological systems due to daily activities. The free radical damage to the living tissue is already well established and prolonged hazards of it lead to the development of some sever diseases. In particular cancer, inflammation, infection, cardiac and cerebral ischemia-reperfusion injury neurodegenerative diseases, cardiovascular diseases and aging¹⁰¹. External factors like high-energy radiation, xenobiotics and oxidative stress are the inducing factors for the above mentioned diseases. Prevention of many oxidant-dependent diseases is possible by supplementing antioxidants externally. As such there is an increasing interest in antioxidants, particularly in those intended to prevent the presumed deleterious effects of free radicals in the human body, and to prevent the deterioration of fats and other

constituents of food stuffs. It has been reported that the conjugated polymers have very good antioxidant properties¹⁰³. But, to use these properties practically biocompatibility of conjugated polymers has to be enhanced and toxicity reduced. The idea of synthesizing a composite comprising of a biodegradable polymer with polyaniline can provide the path for applying the tremendous potential of these materials. A first hand report on the antioxidant and the enhanced haemolysis prevention activity of starch/polyaniline composite has been presented for future use in biomedical applications.

CHAPTER 3

MATERIALS AND METHODS

The investigation was carried out using the following materials. The necessary methods and procedures were used for obtaining comprehensive results.

3.1 Chemicals used

All chemicals and reagents were of analytical grade and procured from Merck India Ltd., M/S Sigma, USA, Bengal Chemical and Pharmaceutical Ltd. and Himedia Lab.

3.2 Morphological study

For the present study *Colocasia esculenta*; Assamese: *panchmukhia kochu*, *Xanthosoma sagittifolium*; Ass: koladohi kochu; *Xanthosoma caracu*; Ass: bogadohi kochu and *Amorphophallus paeoniifolius*; Ass: *Ool kochu* were selected. The morphological data collection was with respect to corm or tuber shape and dimension, petiole length, diameter and color, leaf blade color and dimensions, number of primary lateral veins. All measurements were done using the standard instruments. Leaf area was measured with a Portable Laser area meter (Model-CL-203, make CID, Inc, USA) and diameter from the periphery measured with non elastic thread. All length-measurements were completed with the slide calipers. The length of leaf *Colocasia* and *Xanthosoma* species was taken from the bottom of the V to the tip of the leaf, and for *Amorphophallus* it was the length from the origin of bifurcation of the leaf mid vein to its apex. The corm diameter of *Colocasia* and *Amorphophallus* species was the maximum usually towards the upper side, whereas, in *Xanthosoma* species it was the average of five uniformly separated regions on the corm. The leaf breadth was the breadth through the point of attachment of the petiole. Identification up to the genus level was done according to keys provided by Acevedo-Rodríguez and Strong¹⁹⁶, Llamas¹⁹⁷, Santosa *et al.*¹⁹⁸ and Boyce *et al.*¹⁹⁹.

3.3 Karyotyping

The karyotyping of the aroid species was done by cytological study on the root tips of plants. Newly growing plantlets of all four selected aroids were selected for the purpose. The root tips were collected from morning 4 to 7 am.

The root tips of 7-15 mm length were collected and pretreated with saturated paradichlorobenzene for 6 h and then fixed with 1:3 (v/v) acetic-acid: ethyl-alcohol after washing with distilled water. The root tips were hydrolyzed with 1 N HCl for 10 minutes at 60°C. After washing with distilled water the tips were stained with actocarmine for 1-3 h. The root tips were then squashed between the glass slide and a cover slip by thumb pressure and then observed under the microscope. Slides having good revelation of chromosomes were photographed for record and reference.

3.4 Biochemical composition

3.4.1 Moisture

Thermal drying method was used in the determination of moisture content of the samples. Dried biomass sample of 1.0 g was weighed in triplicate and placed in a clean pre-weighted crucible. The crucible with the dried biomass was dried in an oven at 105°C to constant weight. The percentage moisture content (%MC) was computed as:

$$MC(\%) = \frac{W_o}{W_i} \times 100$$

where W_o = loss in weight (g) on drying and W_i = initial weight of sample (g).

3.4.2 Ash

The ash content was determined using the ignition method. The crucible used was thoroughly cleaned and pre-heated in a muffle furnace to about 600°C. The oven-dried biomass sample 10 g used in moisture determination were weighed in triplicate and placed in the pre-heated crucible. The crucible was covered with its lid and placed in a cold muffle furnace. The temperature of the muffle furnace was allowed to rise to 600°C and the ash preparation was carried on for eight hours at the temperature. The crucibles were removed and cooled in a desiccator and weighed. The percentage ash content was calculated using the formulae:

$$Ash(\%) = \frac{M_a}{M_s} \times 100$$

where M_a = Mass of ash (g) and M_s = Mass of sample used (g).

3.4.3 Crude protein

Protein was extracted from the corm following the method described by Cameiro *et al.*²⁰⁰ and estimated using the method of Lowry *et al.*²⁰¹.

3.4.4 Crude lipid

Determination of crude lipid content of the biomass was done using the direct solvent extraction method. The solvent used was petroleum ether (boiling temperature range 40-60°C). The dried sample 10.0g was weighed in triplicate and secured in soxhlet extraction thimble. The boiling range (40-60°C) petroleum ether 250 ml was added to the biomass and extracted for four hours. At the end of extraction, the solvent was evaporated and the flask dried in the oven (60°C). The percentage crude lipid (CL) was calculated using the formulae:

$$Lipid(\%) = \frac{M_{ex}}{M_s} \times 100$$

where M_{ex} = mass of extract (g) and M_s = Mass of sample used (g).

3.4.5 Starch content

Extraction of starch in the corm of aroids and determination of its content were done following the anthrone method described by Rose *et al.*²⁰².

3.4.6 Crude fiber

The fiber content in the corm was estimated using the gravimetric method. Corm pieces 20 g were treated with 2 N hydrochloric acid (HCl) for an hour in a boiling water bath. Then filtered through Whattman number-1 filter paper and washed with distilled water to neutralize the pH. The remainder was treated with 2 N sodium hydroxide (NaOH) solution in the same way, again filtered and washed to get pH 7. The remainder was dried at 100°C for an hour

to remove the moisture and then weighted. The fiber percentage was calculated using the formulae:

$$\text{Crude fibre(\%)} = \frac{[(W_2 - W_1) - (W_3 - W_1)]}{(W_2 - W_1)} \times 100$$

where, W1 = weight of empty dry crucible, W2 = weight of crucibles with dry mass, W3 = final weight of the crucible with the crude fiber of the dry mass.

3.4.7 Total carbohydrate

Total carbohydrate content of the biomass was estimated following the difference. In this method, the sum of the percentage of all the other proximate components was subtracted from 100.

Total carbohydrate (%) = 100 – (% moisture + % crude protein + % crude lipid + % ash).

3.4.8 Total sugar content

Fresh biomass was homogenized with 80% ethanol (3 x 30 min, 50°C). Extracts were evaporated to dryness and the rest re-dissolved in 50% ethanol. Total soluble sugar was quantified by the anthron method.

3.4.9 Total energy

Total energy was calculated using the formulae:

The total energy (per 100 g fresh weight) = (Total carbohydrate X 4) + (Total crude protein X 4) + (Total crude lipid X 19.9).

3.4.10 Mineral estimation

Ash was first dissolved in 4 ml concentrated hydrochloric acid. The acid was then evaporated on a boiling water bath. After evaporation again dissolved in 2 ml of the above acid and then filtered through Whatman No.1 filter paper and the final volume was adjusted to 100 ml in a volumetric flask. Na and K were estimated using flame photometer as described by Toth *et al.*²⁰³. Ca and Mg were estimated using compleximetric titration with ethylenediamine tetraacetic acid (EDTA) described by Ringbom *et al.*²⁰⁴.

3.5 Genome size study

3.5.1 Isolation of Genomic DNA

Genomic DNA was isolated using the method described by Ronning *et al.*²⁰⁵. One gram leaf frozen in liquid nitrogen was ground using mortar and pestle. The extraction buffer 10 ml [100mM Tris-HCl, pH 8.0; 250mM NaCl; 25 mM ethylenediaminetetraacetic acid (EDTA); 0.1% (v/v) 2-mercaptoethanol; 100 mM diethyldithiocarbamic acid (DEDTC); 2% (w/v) polyvinylpyrrolidone (PVPP)] was added and grinding continued. The tissue homogenate was filtered through four layers of cheese cloth. Sodium dodecyl sulfate (SDS) was added to a final concentration of 1.25% shaken vigorously and incubated at 65°C for 10 min. Potassium acetate was added to the final concentration of 1.2 M, shaken vigorously and incubated at 0°C for 20 min, followed by centrifugation at 25,000 g for 20 min at 4°C. The supernatant was filtered through two layers of mira-cloth, combined with 2/3 volume ice cold isopropanol and precipitated overnight at -20°C. DNA was pelleted at 20,000 g for 15 min at 4°C. The pellet was dried and resuspended in 400 µl Tris-EDTA (TE) pH 7.4. Each DNA sample was treated with ribonuclease A (RNase A, Bangalore Gene, India) with a concentration of 50 µg ml⁻¹ and incubated at 37°C for 30 min. Organic extraction was performed adding an equal volume of phenol : chloroform : isoamyl alcohol (25:24:1), shaken vigorously and then centrifuged at 12,000 g for 10 min. The process was repeated with chloroform: isoamylalcohol. The DNA was then precipitated by adding NaCl to a final concentration of 0.2 M and two volumes of ice cold 95% ethanol, incubated at -20°C for 30 min and centrifuged for 15 min at 12,000 g to pellet the DNA. The pellet was dried and resuspended in 100 µl TE (pH 7.4).

3.5.2 Determination of yield and quality of DNA

The yield and quality of DNA was determined using the method described by Gallagher²⁰⁶. The isolated DNA 50 µl was evaporated to dryness using Maxi Dry Plus under 1mbar atm pressure at 35°C. The dried DNA was dissolved in 1 ml 1X TNE buffer containing 0.01 M Tris base, 1 mM EDTA

and 0.2 M NaCl (pH adjusted to 7.4 with concentrated HCl). Both blank and samples were analyzed at 325 nm for confirming the cleanliness of cuvettes. Absorption at 230 nm for detecting any phenol contamination was also measured. The purity level of the DNA was estimated from absorption at 260:280 nm. The quantification of the DNA was done putting the absorption value at 260 nm in the following formulae:

$$\text{Concentration of dsDNA } (\mu\text{g/ml}) = A_{260}/0.020$$

Where, A_{260} - absorption value of DNA in TNE after subtracting TNE blank absorption value; ds, double stranded; 0.020- molar extinction coefficient with a unit of $\text{M}^{-1}\text{cm}^{-1}$.

3.5.3 Genome size determination

Genome size determination was done using the method of Konwar *et al*¹³¹. The method can be divided in to two parts, (a) determination of number of cells in the leaf tissue and volume of intercellular space, and (b) determination of genome size.

(a) Determination of number of cells in the leaf tissue and volume of intercellular space

Fine transverse and longitudinal cross sections of the pre-weighed leaf tissue of 1 cm^2 size were obtained with a sharp sterile blade and observed under a microscope (Carl Zeiss microlmaging, Germany) at 400x magnification. The volume of the whole tissue section (1 cm^2) was determined (length×breath×thickness). The length, breath and thickness of rectangular cells; length and radius of the cylindrical cells and radius of spherical cells were measured with a micro scale having 400x magnifications. Data generated from five randomly selected cells of five random sections as well as cell volumes were recorded with the specific formulae. The intercellular spaces in the leaf tissue of the aroid were measured in five small leaf sections of known dimensions by measuring with a micro scale at 400x magnification.

(b) Determination of genome size

Genome size of the plant species was determined using the following calculations:

Average volume of a single cell ($l \times b \times t$) = $x \mu^3$

where, l = length, b = breath and t = thickness

Volume of a tissue ($l \times b \times t$) = $t \mu^3$

Volume of the intercellular space = $s \mu^3$

Actual cell mass = $(t-s) = v \mu^3$

Total number of cells in the cell mass = $v \mu^3 / x \mu^3 = y$

Now, weight of the tissue section = wg

wg tissue contains = y cells

So, 1g tissue will contain cells = y/w

DNA yield per gram of leaf tissue = $d \mu g = d \times 10^6$ pg

So, one cell contains DNA = $(d \times 10^6) / (y/w)$ pg = $(d \times 10^6) / (y/w) \times 978$ Mbp

3.6 RAPD study

3.6.1 DNA amplification

The primers used in the experiment were OPW-04, OPW-05, OPW-08, OPW-10, OPW-15 and OPW-16. The sequences of the primers are presented below:

Table 3.1. Sequences of the primer

| Sl. No. | Primers |
|---------|-------------------------|
| 1 | OPW-04 (5-CAGAAGCGGA-3) |
| 2 | OPW-05 (5-GGCGGATAAG-3) |
| 3 | OPW-08 (5-GACTGCCTCT-3) |
| 4 | OPW-10 (5-TCGCATCCCT-3) |
| 5 | OPW-15 (5-ACACCGGAAC-3) |
| 6 | OPW-16 (5-CAGCCTACCA-3) |

PCR amplification was carried out using RAPD decamer primers (Operon Technologies, USA). The reaction mixture (25 μ l) consists of 100 ng

template DNA, 1X reaction buffer (10 mM Tris-HCl pH 9.0, 50 mM KCl and 1.5 mM MgCl₂), 100 μM of each of the dATP, dTTP, dCTP and dGTP, 5 pM primer and 0.5 U of *Taq* DNA polymerase (Bangalore gene, India). Amplification was performed using the thermal cycler Gene Amp PCR system 9700 (Applied biosystems) with a heated lid to reduce the evaporation under the conditions of an initial 1 min denaturation at 94°C, followed by 45 cycles of 1 min at 94°C, 1 min at 35°C, and 2 min at 72°C, with a final 5 min extension step at 72°C.

Approximately, 15 μl of the amplified products were loaded on a 2% agarose gel and separated by electrophoresis in TAE buffer (Tris 1.6 M, acetic acid 0.8 M, EDTA 40 mM) at 100 volts. A 100 bp ladder (Bangalore gene, India) was loaded in all gels used as the molecular marker. After electrophoretic separation for 90 min, the gel was stained with ethidium bromide and visualized by UV light. Following electrophoresis, the gel was photographed using Geldoc 1000 (Biorad).

3.6.2 RAPD analysis

The images of DNA bands in the electrophoresed gel were analyzed using Biorad software for the estimation of molecular weight of the bands. The pairwise genetic similarity matrix between the genotypes was generated using Jaccard's coefficients.

3.7 Compound isolation and identification

3.7.1 Plant sample preparation

The corms of the selected aroids were cut in to small pieces of about 1.0 cm² and soaked in water for an hour. The corm pieces were ground using a Mixture-Grinder to produce slurry. The slurry was allowed to dry under reduced pressure. The powder was passed through a 100 μm sieve to get free flowing powder. The powder was dried under vacuum and then stored in air tight containers for future use.

3.7.2 Extract preparation

The extracts were prepared in water, methanol and methanol: water (80:20). For the extract preparation, 100 g of dry powder was extracted with 1.0 l solvent at the ambient temperature (25°C) for 24 hours. The extraction procedure was repeated three times more with the fresh solvents and all extracts were pooled together. The procedure was repeated 10 times to collect sufficient crude extract for the further study.

3.7.3 Biochemical and bioactivity test with the crude extracts

3.7.3.1 The total polyphenol content

The total polyphenol content of the corm powder was estimated by using the method of Cordenunsi *et al.*²⁰⁷. The prepared extract 500 µl was mixed with 2.5 ml 0.2 N Folin's reagent and incubated at room temperature for 5 min. Saturated Na₂CO₃ (75 g/l) 2.0 ml was added to the mixture and incubated for 90 min at 30°C. Absorption of the mixture was taken at 765 nm against a reagent blank. Standard curves were prepared using gallic acid, BHT, tannic acid and quercetine dehydrate.

3.7.3.2 Total flavonoid estimation

For total flavonoid estimation extracts were subjected to total flavonoid estimation following the method of Chang *et al.*²⁰⁸. To an aliquot 500 µl of the extract, 1.5 ml of 95% ethanol, 100 µl of 10% aluminium chloride, and 2.8 ml milli-Q water were added. After 40 min of incubation at 25°C, the light absorption was measured at 415 nm against the reagent blank. Standard curves were prepared using quercetine dihydrate in the extraction solvent.

3.7.3.3 The blood clotting experiment

The blood clotting experiment was performed using platelet poor plasma of goat blood by following the method of partial thromboplastin time. The solvent free extract (20 mg) was dissolved in 500 µl of 20 mM potassium

phosphate buffer. A 20 µl aliquot of the solution was used in calculating the blood clotting time. The experiment was repeated thrice.

3.7.3.4 The antioxidant activity

The antioxidant activities of the aroid corm extracts were determined using the method of Chen and Ho²⁰⁹. Butylated hydroxytoluene (BHT), gallic acid and quercetin dihydrate were used as standards with the concentration similar to flavonoid estimation in different solvents. The scavenging abilities of the extracts were determined using the formulae:

$$\text{DPPH scavenging (\%)} = [(OD_{t=0} - OD_{t=30}) / OD_{t=0}] \times 100$$

OD_{t=0}, is the optical density at time t=0 min

OD_{t=30}, is the optical density at time t= 30 min

3.7.3.5 Antimicrobial activity of the crude extracts

Antimicrobial activity was tested using disc diffusion method (for bacteria) and well diffusion method (for fungus). The assay was performed against four different microorganisms, two bacterial and two fungal species. The bacterial species selected were *Escherichia coli* (MTCC 739) and *Staphylococcus aureus* (MTCC 96) and fungal species *Candida albicans* (MTCC 3017) and *Fusarium oxysporum* (NCIM 1281). The bacterial species were grown on Muller Hilton agar whereas the fungal species on potato dextrose agar by spread plate culture. The crude extracts were dried and 50 mg of the same was dissolved in 500 µl of 1% DMSO in sterile water. From the above stock 40 µl of the solution was loaded on sterile paper disc (diameter 5 mm). The discs were applied on the spread plate culture of the two bacteria to test antibacterial property. Ampicillin loaded discs were purchased from Himedia lab (India) containing 25 µg was used as positive control and a blank paper disc loaded with 40 µl of 1% DMSO was used as negative control for the experiment. For the determination of antifungal activity, wells were prepared on the potato dextrose agar medium and 100 µl of the extract (50 mg/500 µl of 1% DMSO) were poured to it. Bacterial plates were inoculated at 37°C (for 24 h)

and fungal plates at 25°C (for 48 h). The culture plates were obtained after incubation period and photographed. Stock solutions of antimicrobial (cell culture tested 100X) was diluted to 1X solution (Himedia) with 1% DMSO and tested as positive controls.

3.7.4 Thin layer chromatography (TLC)

Before TLC profiling, the methanolic extract was fractionated with equal volume of diethyl ether using a separating funnel. The diethyl ether soluble fraction was dried to concentrate and developed in a silica gel G (Merck) plate using n-hexane/ethyl acetate/formic acid (100/50/0.5 v/v/v) as mobile phase. The developed spots were stained in an iodine chamber to locate positions of compounds.

3.7.5 Column chromatography

Column chromatography was done using silica gel G (Merck) as the stationary phase with the dimension of 16 cm X 2 cm in a glass column. The column was packed and run with n-hexane/ethyl acetate/formic acid (100/50/0.5 v/v/v). The ethyl acetate extract prepared for the TLC was loaded to it. The eluted volumes were collected as 20 ml fractions in 40 different tubes. The fractions were dried and re-dissolved in methanol (10 ml) and the total polyphenol content was estimated by using the method of Cordenunsi *et al.*²⁰⁷. The highest polyphenol containing fractions were subjected to HPLC analysis and purification.

3.7.6 High Performance Liquid Chromatography (HPLC)

HPLC analyses of the extracts were done using Waters HPLC system. The column was an Ascentis Reverse Phase-Amide Column with the dimension of 10 cm X10 mm I.D. and the particle size of 10 µm (Supelco, USA) was used for the purification of compounds. The absorption of the compounds was measured at 280 nm for the purification purpose. The compounds were separated using two different solvent system gradients; solvent A, 0.085%

orthophosphoric acid in Mili Q water (with 18 mega ohm); solvent B, acetonitrile (HPLC grade). The gradient was run as follows: at t=0 min A was 85% and B was 15%; at t= 30 min A was 65% and B 35%; at t=35 min A was 15 % and B 85% and runs up to 40 min. The separated compounds were collected by repetitive injections. The collected compounds were then run in the same gradient to confirm their elution time.

3.7.7 Fourier Transform Infrared Spectroscopy (FTIR)

The FTIR characterization of the purified compounds was done using Nicolet FTIR instrument to evaluate the functional groups of the compounds. Dry compounds were ground with KBr (Potassium bromide, FTIR grade, Merck) using a clean and smooth mortar and pestle. After mixing for three minutes, the mass was transferred to a pellet preparation instrument, and a solid pellet was prepared using hydraulic pressure. The pellet was transferred to the holder of the Nicolet FTIR spectrometer. The transmission peaks were obtained from wave number 400-4,000 cm^{-1} . Data were recorded for analysis.

3.7.8 Nuclear Magnetic Resonance (NMR)

The pure compounds of 40 mg was dissolved in the 0.5 ml of DMSO- d_6 (NMR grade) and loaded into the NMR tube. Total scans of about 1000 cycles were done to obtain the H^1 and C^{13} NMR spectra. The spectra were recorded for analysis purpose.

3.8 Antimicrobial assessment

3.8.1 Microbial strains

Bacterial and fungal strains were used for the test. The same were obtained from MTCC, IMTECH, Chandigarh, India and NCIM, NCL, Pune (National collection of industrial microorganisms). Bacterial species used in the study were *Escherichia coli* (MTCC 739) and *Staphylococcus aureus* (MTCC 96) and the two fungal strains *Candida albicans* (MTCC 3017) and *Fusarium*

oxysporium (NCIM 1281). The compounds were dissolved in 5% of dimethyl sulphoxide (DMSO) to prepare a solution of 5 mg/ml.

3.8.2 Antibacterial assay

3.8.2.1 Preparation of inoculum

Escherichia coli and *Staphylococcus aureus* were cultured in Muller Hilton broth (MHB, Himedia, India). The bacterial species were incubated at 37°C to obtain a microbial population of about 10^6 ml⁻¹ of culture medium. Before carrying out the assay, the population of each bacterial species was adjusted using the sterile Muller Hilton broth.

3.8.2.2 The antibacterial test

Muller Hilton agar (MHA) medium was prepared by dissolving the prescribed amount of commercially available (Himedia, India) dry powder in 100 ml distilled water in 1,000 ml conical flask. The medium was autoclaved along with Petri dishes (90 mm). MHA was poured in to the Petri dishes (about 20 ml) and allowed to solidify under the laminar air hood.

Each plate was now inoculated with 1.0 ml of inoculum prepared in MHB and spread all over the plate using a sterile glass spreader. Wells were bored on the plate using sterile steel borer and 50 µL of the prepared solutions of 3 different concentrations of the isolated compounds poured in to each of the wells using digital pipette. The plates were incubated in 37°C for 24 h. Ampicillin (25µg/ml) was used as the positive control with an applied volume of 50 µl.

3.8.3 Antifungal assay

3.8.3.1 Preparation of the inoculum

The inoculum for the antifungal test was prepared using the potato dextrose broth (PDB) obtained from Himedia, India Pvt. Ltd. The stock inoculum was prepared on day 2 and for *Candida albicans* grown on potato dextrose agar at 28°C. Potato dextrose agar was added to the agar slant and the

cultures were gently swabbed to dislodge conidia. The suspension of conidia with blastoconidia of *Candida albicans* was transferred to a sterile tube and adjusted by turbidimetry to obtain an inoculum of 10^6 cfu ml⁻¹. The optical density of suspensions was spectrophotometrically determined at 530 nm.

3.8.3.2 The antifungal test

Petri dishes with a diameter of 90 cm were prepared with PDA. The wells of diameter 6 mm were prepared in the agar and 50 µl of the compound solution and also the positive control were poured in to them, respectively. Stock solutions of antimicrobial compounds (cell culture tested 100X) were diluted to 1X solution (Himedia) with 1% DMSO and tested as positive controls. Each fungal suspension was inoculated in the surface of the agar. After incubation for 3-5 days for *Candida albicans* at 28°C, all dishes were examined for the zone of growth inhibition.

3.9 Anti-haemolysis test against free radicals

Haemolysis prevention activity was studied following the procedure of Miki *et al.*²¹⁰. Blood was collected from slaughterhouse and diluted using 3.8% sodium citrate of 1/10th volume. Blood was then centrifuged in a 50 ml centrifuge tube using an MPW centrifuge at 3000 rpm for 5 min. The supernatant containing platelet-poor plasma was discarded and the pellet containing RBC was suspended in 10 volumes of phosphate buffer saline (PBS) of pH 7.4. The process was repeated two more times to completely remove the buffy coat of RBC. Finally the cells were suspended in PBS to get a uniform suspension of cells. The isolated compounds were suspended in PBS at a concentration of 1 mg.ml⁻¹. An aliquot of 100 µl was pipetted out into several test tubes. H₂O₂ was added to get 100 µM concentrations in 3 ml. After allowing the reaction to occur for 5 min, the tubes were subjected to 3 ml blood and incubated for 1 h at 37°C. After incubation, the samples were centrifuged at 3,000 rpm for 5 min to pellet out RBC cells. The supernatants were carefully

separated using 1 ml micropipette and used for the absorption studies at 540 nm. The percentage of haemolysis prevention was calculated using the formulae:

$$\text{Haemolysis - prevention (\%)} = \frac{(A_B - A_S)}{A_B} \times 100$$

Where, A_B is the absorption of the blank and A_S is the absorption of the sample.

3.10 Starch isolation, physicochemical characterization

3.10.1 Starch Granule Isolation

Mature corms were collected from the uprooted plants. Corms were washed thoroughly to remove the dirt and subsequently the outer cover was removed. The corms were then cut in to squares of about 1-3 cm³, weighted 100 g and soaked in double volume of potassium-metabisulfite at the concentration 50 mg.l⁻¹. Starch isolation was done following the method of Jayakody *et al.*²¹¹ with minor modifications. The blended corm paste was suspended in a double volume of extraction solution. The suspension was filtered through a double layered cheese cloth. The process was repeated twice. The filtrate was centrifuged at 1,000 x g for 30 min at room temperature. The process was repeated four more times with double distilled water. The upper brown layer contaminating proteins- polysaccharides was removed. The lower whitish part containing starch was isolated and washed with distilled water three more times to obtain pigment free white starch.

3.10.2 Proximate Composition Analysis

The proximate composition of moisture, ash and lipids was analyzed using AACC methods²¹². Free lipids were extracted using chloroform: methanol (2:1, v/v) at 25⁰C. The bound lipid was extracted from the chloroform/methanol treated starch using *n*- propanol: water (3:1, v/v) as solvent for 7 h at 50⁰C. Total lipid was estimated by hydrolyzing starch in 24% HCL and then extracted thrice with equal volume of chloroform: methanol (2:1, v/v) at 25⁰C. Total phosphorus was estimated by the method described by Morrison²¹³.

3.10.3 Scanning Electron Microscopy of Starch Granules

To determine the starch granule size, scanning electron microscopy (SEM) of the starch was done using JOEL model no. JSM-6390LV (Oxford Instrumentation Ltd., Tokyo, Japan). For the analysis, the dried starch powder was sprinkled on the carbon tape and then coated with 30 nm of platinum using JOEL auto fine coater (model no. JFC-1600). The SEM was operated at 15-20 KV (15 KV for *A. paeonifolius*, *X. caracu* and *X. sagittifolium*; and 20 KV for *C. esculenta*) and under 1 Pascal.

3.10.4 Elemental Composition Analysis using EDX of Starch granules

Atomic composition of starch with respect to C, O and P was determined using Energy Dispersive X-ray diffraction (EDX, micro-analysis). Samples were visualized under the scanning electron microscope (2,000-4,000x magnifications) using X-ray source 0-20 KV for starch surface analysis, which was conducted with EDX software.

3.10.5 Amylose Content Estimation

Apparent and total amylose content was determined using the method described by Gunaratne and Hoover²¹⁴.

3.10.6 Apparent amylose content estimation

Starch (20 mg, dry weight) was dissolved in 90% dimethylsulfoxide (DMSO, 8ml) in screw cap reaction vials. The content of each vial was vigorously mixed for 30 min and then heated in a water bath (shaking intermediately) at 85°C for 20 min. Vials were then cooled to ambient temperature and the content of each was diluted with water to 25 ml in a volumetric flask. One ml of diluted solution was mixed with water (40 ml) and 5 ml of I₂/KI solution (0.0025 M KI) and then adjusted to a final volume of 50 ml. After allowing the content to stand at ambient temperature, absorption was measured at 600 nm.

3.10.7 Total amylose content estimation

The total amylose content of the sample was determined by the above procedure, following removal of lipid with hot n-propanol: water (3:1, v/v) for 7 h. In order to correct the over-estimation of the apparent and total amylose contents were calculated from a standard graph prepared using potato amylose (0-100 %) and amylopectin (100-0 %).

3.10.8 X-ray Diffraction Study of the Starch Granules

The aroid starches were analyzed by the powder X-ray diffraction method for the quantitative phase identification. The X-ray powder-diffraction pattern was obtained using Miniflex goniometer (Rigaku Corporation, Japan) with scanning mode 2θ ; scanning type being continuous; X-Ray 30 KV/15mA; divergence slit being variable; scattering slit 4.2° ; receiving slit 0.3 mm; step 0.02 and using K β filter from 10- 40° . The starch was equilibrated at 100% relative humidity for 24 h at 25°C prior to analysis. The equation of the degree of crystallinity is as follows:

$$X_C = \left[\frac{A_C}{(A_C - A_A)} \right] \times 100$$

Where,

X_C refers to the degree of crystallinity in percentage; A_C refers to the crystallized area on the X-ray diffractogram; A_A refers to the amorphous area on the X-ray diffractogram.

Further analysis of XRD data were done to find out the strain of the starch copolymer using the Voigt-function model described by de-Keijser *et al.*²¹⁵.

3.10.9 Starch Granule Damage Estimation

The method followed for the estimation of starch damage was based on the principle that amylose leached more rapidly from the damaged starch granules when extracted by sodium sulphate as compared to the sound starch granules.

Starch (1 g) was extracted with 25 ml of extraction solution (sulphosalicylic acid 2 g/1000 ml 1.41 M sodium sulphate) for 15 min at 50°C with thorough shaking at 5 min intervals. Celite (0.25 g) was added to the suspension followed by brief stirring. The mixture was allowed to stand for 1-2 min and later filtered through whatman no. 1 filter paper. Aliquot of 10 ml from the above suspension was mixed with 10 ml diluting solution (gelatin 50 g and 2.5 ml of H₂O₂ in 500 ml boiled distilled water) and 0.5 ml of iodine reagent (0.55 g I₂ and 1.10 g KI in 25ml distilled water) was added. The mixture was kept in a water bath at 30°C for 15 min. The absorbance was measured at 560 nm against reagent blank. Iodine absorbance value 50 units corresponding to 9% starch damage was used as the standard for the necessary calculations²¹⁶.

3.10.10 Functional Group Analysis Using FTIR Spectroscopy

The FTIR spectra of the purified starch were assessed in the wave length range of 4000-400 cm⁻¹. A pure grade commercial starch sample (Merck, India Lid.) was used as the control.

3.10.11 Analysis of Gelatinization Parameter Using Differential Scanning Calorimetry (DSC)

Gelatinization parameter was measured using DSC equipped with thermal analysis data recording software. Water (11 µl) was added with a microsyringe to starch (3.0 mg) in the DSC pan, which were then sealed, reweighed and allowed to stand for 2 h at room temperature in order to attain an even distribution of water. The scanning temperature range and heating rates were 20-120°C.min⁻¹, respectively. An empty aluminium pan thermogram was taken as the reference in all measurements. The transition temperature reported was at the onset (T_o), peak (T_p), and conclusion (T_c). The enthalpy of gelatinization (delta H) was estimated by integrating the area between the thermogram and baseline under the peak and expressed in joule per unit weight of dry starch (J.g⁻¹).

3.10.12 Analysis of Water Binding Capacity

The procedure described by Sugimoto *et al.*²¹⁷ was used with slight modification. Starch (5.0 g) was added to 75 ml distilled water in 100 ml centrifuge bottle. The bottle was stoppered and agitated on a magnetic stirrer for 1 h, centrifuged for 10 min at 2,200×g. The water was decanted and the bottle was allowed to further drain for 10 min and weighed. The amount of water held by starch was determined. The binding capacity was calculated from the formulae:

$$\text{Water binding capacity (\%)} = \left[\frac{(\text{Final weight of the starch} - \text{Initial weight of the starch})(g)}{\text{Initial weight of the starch}(g)} \right] \times 100$$

3.10.13 Colorimetric Measurement of Amylose Leaching

Amylose leaching was assessed by heating the isolated starch (2mg ml⁻¹ deionised water) at 50, 60, 70 and 80°C for half an hour²¹¹. The tubes were centrifuged at 2000×g for 10 min. The supernatant (4 ml) was used to determine amylose content by the method of Gunaratne and Hoover²¹⁴.

3.10.14 Acid Hydrolysis of Starch Granules

Starch was hydrolyzed in triplicate with 2.2 M HCl (1 g starch/40 ml, 2.2 M HCl) at 35°C in a water bath (Pharmacia, Biotech, USA) for a period of 15 days. The starch slurry was vortexed daily to re-suspend the deposited starch granules. Aliquots taken for analysis during the interval were neutralized with 2.2 M NaOH and centrifuged (2,000 × g, 10 min). The amount of total reducing sugar (glucose equivalent) in the supernatant was determined by Somogyi-Nelson method²¹⁸. The extent of hydrolysis was calculated by using the formulae given by Jayakody *et al.*²¹¹:

$$\text{Hydrolysis (\%)} = \frac{\text{Reducing sugar (as glucose)} \times 0.95 \times 100}{\text{Initial starch weight (g)}}$$

3.10.15 Enzymatic Hydrolysis of Starch Granules

Enzymatic digestibility of starch was assessed using an amorphous suspension of α-amylase in 2.9 M sodium chloride and 3.0 mM calcium

chloride (Himedia, India), in which the concentration of α -amylase was 32 mg protein.ml⁻¹ and specific activity 1,122 U.mg⁻¹ protein. Starch granules (20 mg dry weight) were suspended in 10 ml 0.02 M phosphate buffer (pH 6.9) containing 0.006 M NaCl. α -Amylase 5.5 μ l was added, the mixture was gently mixed and digested at 37^oC in a water bath (New Brunswick Scientific) for 72 h. The reaction mixture was vortexed regularly at an interval of 12 h to suspend the deposited granules. The digestion reaction was terminated by adding 5.0 ml absolute ethanol. The hydrolysate was recovered by centrifugation at 2,000 x g for 5 min. Aliquots of the supernatant were analyzed for reducing sugar (maltose) content following the method of Somogyi-Nelson²¹⁸.

$$\text{Hydrolysis (\%)} = \frac{\text{Reducing sugar (as maltose)} \times 0.95 \times 100}{\text{Initial starch weight (g)}}$$

3.11 Application of starch for functional composite preparation with polyaniline and its bio-efficacy assay

3.11.1 Synthesis of starch/polyaniline composites

The isolated starch from *C. esculenta* (*Pochmukhia kochu*) was used to prepare the following composites. Starch (4%, w/v) was suspended in cold water and rapidly stirred to form a uniform dispersion. Aniline was added to the dispersion, followed by the addition of HCl. The pH was maintained at 2.5. Ammonium peroxodisulphate (APS) was used as the oxidant and added dropwise to the starch/aniline dispersion with a continuous stirring at 50 rpm. The temperature was maintained at 0^oC (273 K) using a ice bath to maximize the yield of polyaniline. The composites were obtained by *in situ* polymerization with the varying amount of aniline 0.1-1.0 M. The aniline:oxidant ratio was maintained at 2:1 for all the composites.

Table 3.2. Composition of the different Starch-polyaniline composites

| Sample code | Starch (w/v) | Aniline (M) | Oxidant (M) |
|-------------|--------------|-------------|-------------|
| S1 | 4% | 0.1 | 0.05 |

| | | | |
|----|----|-----|------|
| S2 | 4% | 0.5 | 0.25 |
| S3 | 4% | 1.0 | 0.5 |

3.11.2 Characterization

Scanning electron micrographs of the composites were acquired using a JEOL JSM-6390LV model (Oxford Instrumentation Ltd.). The starch/polyaniline composite samples were mounted on a carbon-tape to obtain a uniform layer. About 6 nm platinum coating was done using JOEL auto fine coater (Model No. JFC-1600) prior to characterization.

X-ray diffraction pattern of the pristine and composites were carried out using Miniflex X-ray diffractometer (Rigaku Corporation, Japan) with scanning mode 2θ ; scanning type being continuous; X-ray 30 kV/15mA; divergence slit being variable; scattering slit 4.2° ; receiving slit 0.3mm; step 0.02 and using K α filter from 10 to 40° .

UV-Vis absorption pattern of the composite dispersed in water was done using UV-Vis spectrophotometer (Shimadzu-1700, Japan) from 200 to 1100 nm. Differential scanning calorimetry was carried out using DSC (Shimadzu, Japan) from 0-300°C with a rate of 10°C.min⁻¹.

3.11.3 Antioxidant activity

The antioxidant activity was performed using the method of Serpen *et al.*²¹⁹. The assay was done with different concentrations and compositions of the material. The material weighing 0.2-1.0 mg was applied to 3.0 ml of 100 μ M DPPH (1'-1'-Diphenylpicryl-hydrazyle) solutions in HPLC grade MeOH. The reaction mixture was vortexed for 30 sec (seconds) and incubated in darkness for 15 min (minutes); after which the wavelength scanning was performed using a Shimadzu UV-Vis spectrophotometer. In order to study the time dependence of the antioxidant activity, the maximum concentration of each sample was applied to 3.0 ml DPPH solution in a cuvette and the spectra were recorded within the time limit of $t = 0-60$ min. The DPPH degradation was calculated using the formulae:

$$\% \text{ of DPPH scavenging} = \left[\frac{(A_S - A_B)}{A_B} \right] \times 100$$

where, A_B is the absorption of the blank (DPPH + MeOH) and A_S is the absorption of the sample (DPPH + Sample + MeOH).

3.11.4 Cytotoxicity assay by anti-haemolysis test

The methodology of Miki *et al.*²¹⁰ was used to analyze the haemolysis prevention activity of the composites. Goat blood was collected and prepared in 1/10th volume of sodium citrate (3.8%, w/v). Blood was centrifuged at 3000×g for 10 min. The platelet poor plasma containing-supernatant was discarded and the pellet containing RBC were suspended in 10 volume of phosphate buffer saline (PBS) of pH 7.4. Washing was repeated twice to remove completely the buffy coat of RBC. Finally the cells were suspended in 10 volumes of PBS to get a uniform suspension of cells.

The starch-polyaniline composite samples were suspended in PBS at a concentration 5.0 mg.ml⁻¹. From the suspension 20, 40, 60, 80 and 100 µl of the material was pipetted out into the test tubes. H₂O₂ was added to get 100 µM concentrations in a volume of 3.0 ml. A time frame of 5.0 min is allowed to the reaction. Tubes were subjected to 3 ml blood and then incubated for 90 min at 37°C. Samples were centrifuged at 3,000×g for 5.0 min to pellet RBC cells. The supernatants were carefully separated using 1 ml micropette and used for recording the absorption at 540 nm. The increasing absorption corresponds to more haemolysis. The percentage of haemolysis prevention was calculated using the formulae:

$$\% \text{ of haemolysis prevention} = \left[\frac{(A_S - A_B)}{A_B} \right] \times 100$$

where, A_B is the absorption of the blank (RBC + H₂O₂) and A_S is the absorption of the sample (RBC + H₂O₂ + Sample).

3.12 Statistical Analysis

All experiments were repeated thrice. The mean of three experiments was considered. The statistical analysis was done using the origin 6.1-Scientific Graphing and Data Analysis Software (Origin Lab Corporation) as well as Microsoft excels 2007. The standard error was calculated using the formulae:

$$SE = \frac{s}{\sqrt{n}}$$

Where, SE is the standard error; s is standard deviation and n is the number of observation.

CHAPTER 4

RESULTS

The investigation was carried out to explore aroids *Amorphophallus paeoniifolius*, *Xanthosoma caracu*, *Colocasia esculenta* and *Xanthosoma sagittifolium* with respect to their morphology, biochemical characteristics, karyotyping, molecular characterization, antimicrobial and antioxidant activities of the purified compounds, isolation and characterization of the starch (polymeric compound) from corms and to develop a composite from one of the starch sources and its characterization and bioassay as antioxidant.

4.1 Morphological study

The morphological data of the plants were recorded during the period May 2006 to January 2007 and mean data are presented along with the standard errors in Table 4.1, however ranges are shown. The photographic plates of all four plants, their leaves and corms are presented in Figure 4.1 and Figure 4.2. The characters studied were dimensions of corms, petioles, leaf and surface area. The venation details of leaves were also recorded.

Table 4.1. Morphological characters of the aroids

| Character ↓ | Aroids → | <i>C. esculenta</i> | <i>X. caracu</i> | <i>X. sagittifolium</i> | <i>A. paeoniifolius</i> |
|-------------|----------------|---------------------|------------------|-------------------------|-------------------------|
| Corm/tuber | Shape | Round elongated | Cylindrical | Cylindrical | Round flatten |
| | no/plant | 3-5 | 1 | 1 | 1 |
| | Cormlet/plant | 0 | 8-12 | 5-15 | 2-5 |
| | Dimension (cm) | Height | 8-16 | 3.2-5.5 | 12.3-18.6 |
| Diameter | | 6-11 | 7.6-8.2 | 8.0-9.6 | 10-15 |

| | | | | | |
|--------------------------------|-------------------------|------------------|-------------------|-------------------|---------------------------|
| Petiole | Colour | Faded green | Green | Black | Green with creamy patches |
| | Number | 5.2 | 3.4 | 4.1 | 1.0 |
| | Surface | Smooth | Smooth | Smooth | Rough due to blunt spines |
| | Length (cm) | 92.32 - 164.23 | 80.25 - 135.6 | 84.43 - 116.60 | 41.37-60.54 |
| | Diameter (cm) | Top | 1.95 - 4.22 | 0.39 - 0.7 | 0.97 - 4.40 |
| Middle | | 4.55 - 7.56 | 0.91 - 2.65 | 2.990 - 8.600 | 2.56 - 3.13 |
| Base | | 5.54 - 15.65 | 1.40 - 3.81 | 5.390 - 16.250 | 3.732 - 5.57 |
| Leaf (cm and cm ²) | Length | 38.25 - 60.23 | 28.5 - 35.6 | 29.8 - 45.59 | 7.23 - 12.66 |
| | Breadth | 30.27 - 53.96 | 16.3 - 24.3 | 35.200 - 59.100 | 1.23 - 5.06 |
| | Leaf Surface Area (LSA) | 805.54 - 1779.66 | 1213.10 - 1423.99 | 956.23- 1541.84 | 13.45 - 20.95 |
| | LSA/plant | 1165.41- 2564.21 | 1333.14 - 1533.63 | 1215.25 - 1936.75 | 418.44 - 727.21 |
| | Colour (upper surface) | Green | Green | Dark green | Green |
| | Shape | Symmetric Heart | Symmetric Heart | Symmetric Heart | Symmetric Ovate |
| | Primary lateral | no Fusion site | 18-24 | 10-16 | 24-29 |
| | Fusion site | At edge | At edge | Near border | Near border |

| | | | | | |
|---------------|------------|-----|-----|-----|-------|
| vein | Bifurcated | No | No | No | Yes |
| Venation type | Opposite | Yes | Yes | No | Mixed |
| | Alternate | No | No | Yes | Mixed |

Data presented are mean \pm Standard error except for those which are shown as range

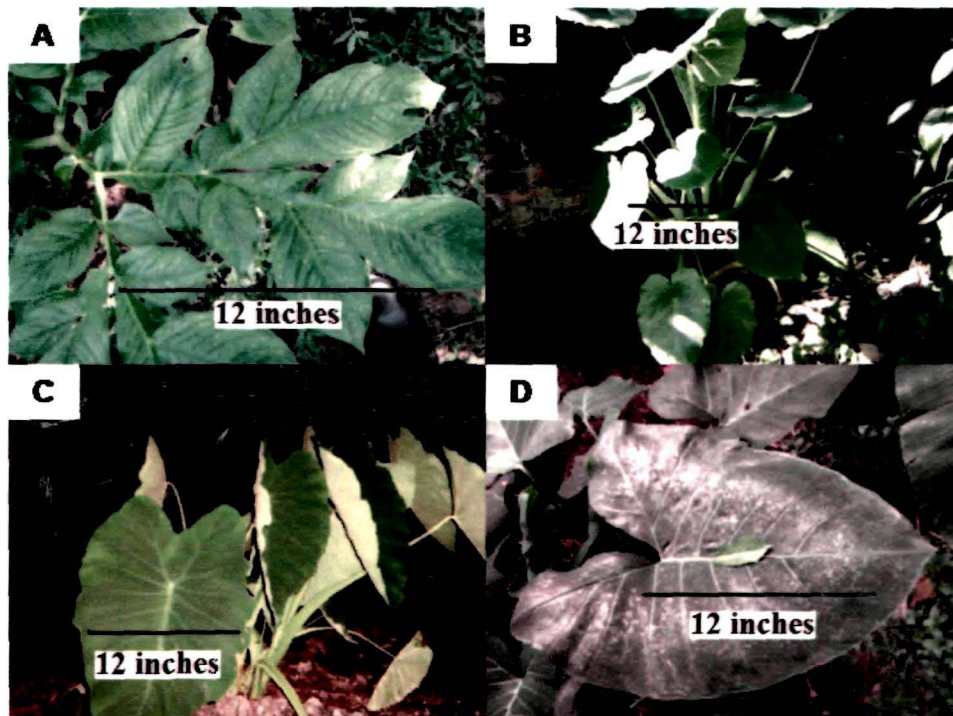


Figure 4.1. Morphology of the aroid plants, (A) *A. paeoniifolius*, (B) *X. caracu*, (C) *C. esculenta*, (D) *X. sagittifolium*. The photographs were taken with 1X magnification

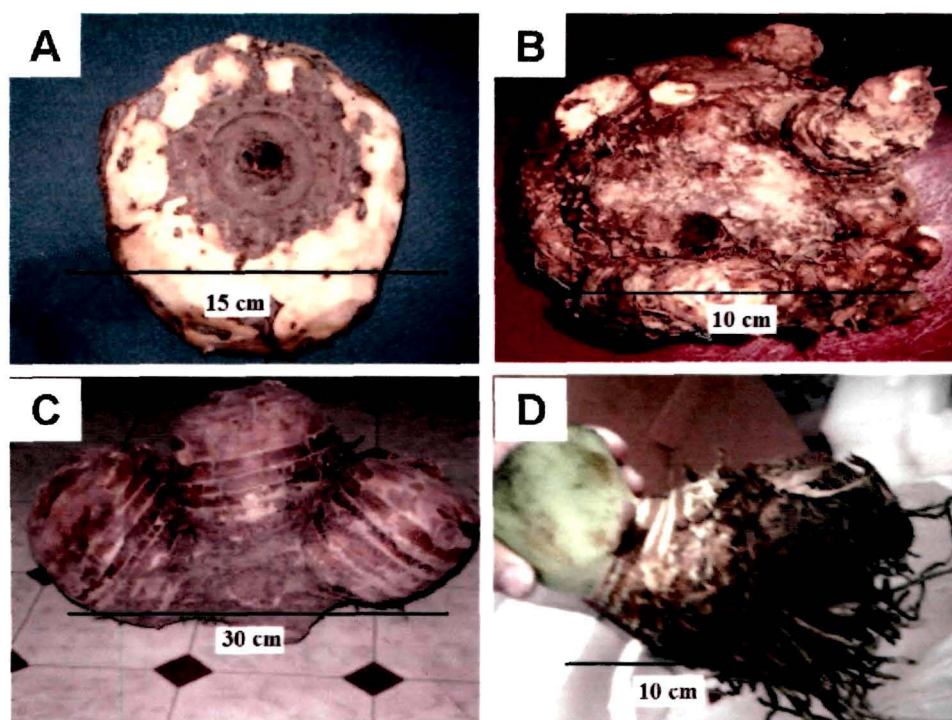


Figure 4.2. Morphology of the aroid corms, (A) *A. paeoniifolius*, (B) *X. caracu*, (C) *C. esculenta*, (D) *X. sagittifolium*. The pictures were captured with 1X magnification

4.2. Biochemical study

The biochemical data recorded for the corms are presented in Table 4.2. Characters recorded were moisture, ash, crude protein, crude lipid, starch, crude fibre, soluble sugar, total energy, Na, K, Ca, Mg contents as well as starch granule size.

Table 4.2. Biochemical composition of the aroids

| Aroids → | <i>A. paeoniifolius</i> | <i>X. caracu</i> | <i>C. esculenta</i> | <i>X. sagittifolium</i> |
|-------------------|-------------------------|------------------|---------------------|-------------------------|
| Moisture (%) | 81.64 ± 3.49 | 80.36 ± 3.26 | 77.25 ± 3.42 | 80.95 ± 3.44 |
| Ash (%) | 2.85 ± 0.11 | 2.652 ± 0.11 | 2.865 ± 0.08 | 3.91 ± 0.16 |
| Crude protein (%) | 2.49 ± 0.05 | 1.261 ± 0.10 | 2.89 ± 0.04 | 2.43 ± 0.09 |

| Aroids → | <i>A. paeonifolius</i> | <i>X. caracu</i> | <i>C. esculenta</i> | <i>X. sagittifolium</i> |
|-----------------------------|------------------------|------------------|---------------------|-------------------------|
| Crude lipid (%) | 1.06 ± 0.12 | 0.25 ± 0.05 | 1.24 ± 0.03 | 0.90 ± 0.01 |
| Starch (%) | 10.23 ± 0.44 | 14.15 ± 0.58 | 14.81 ± 0.60 | 12.36 ± 0.50 |
| Crude fiber (%) | 1.56 ± 0.06 | 1.98 ± 0.05 | 0.80 ± 0.05 | 1.36 ± 0.05 |
| Soluble sugar (%) | 1.20 ± 0.06 | 1.40 ± 0.08 | 1.80 ± 0.06 | 1.50 ± 0.05 |
| Energy (cal./100g) | 78.85 | 71.92 | 103.25 | 74.86 |
| Na (mg/100 g of dry weight) | 33.91 ± 0.18 | 14.9 ± 0.09 | 26.71 ± 0.12 | 22.41 ± 0.11 |
| K (mg/100 g of dry weight) | 40.91 ± 1.69 | 16.28 ± 0.69 | 27.1 ± 1.15 | 24.1 ± 1.15 |
| Ca (mg/100 g of dry weight) | 3.76 ± 0.17 | 1.72 ± 0.08 | 2.6 ± 0.12 | 1.72 ± 0.08 |
| Mg (mg/100 g of dry weight) | 1.3 ± 0.06 | 0.72 ± 0.03 | 1.44 ± 0.07 | 0.7 ± 20.96 |
| Starch granule size (µm) | 4.86 - 7.20 | 1.68 - 2.87 | 0.93 - 1.24 | 2.41 - 4.93 |

Data presented are mean ± Standard error except for those which are shown in range

4.3. Karyotyping

An experiment was carried out to find out the actual time of cell division having chromosomal movements in the somatic cells of aroids through fixation of root tips from early morning 4 to 7 am with 30 min interval. The time period of active cell division of four aroid species was recorded and the same are presented in Table 4.3.

Table 4.3. Time of active cell division

| Aroids | 4.00 am | 4.30 am | 5.00 am | 5.30 am | 6.00 am | 6.30 am | 7.00 am |
|-------------------------|---------|---------|---------|---------|---------|---------|---------|
| <i>A. paeoniifolius</i> | none | none | none | few | maximum | few | none |
| <i>X. caracu</i> | none | none | none | few | maximum | few | none |
| <i>C. esculenta</i> | none | none | few | maximum | few | none | none |
| <i>X. sagittifolium</i> | none | none | none | few | maximum | few | none |

The actively dividing cells were observed using a Zeiss microscope and the photographs taken are presented in Figure 4.3. The ideograms of chromosomes are depicted in Figure 4.4.

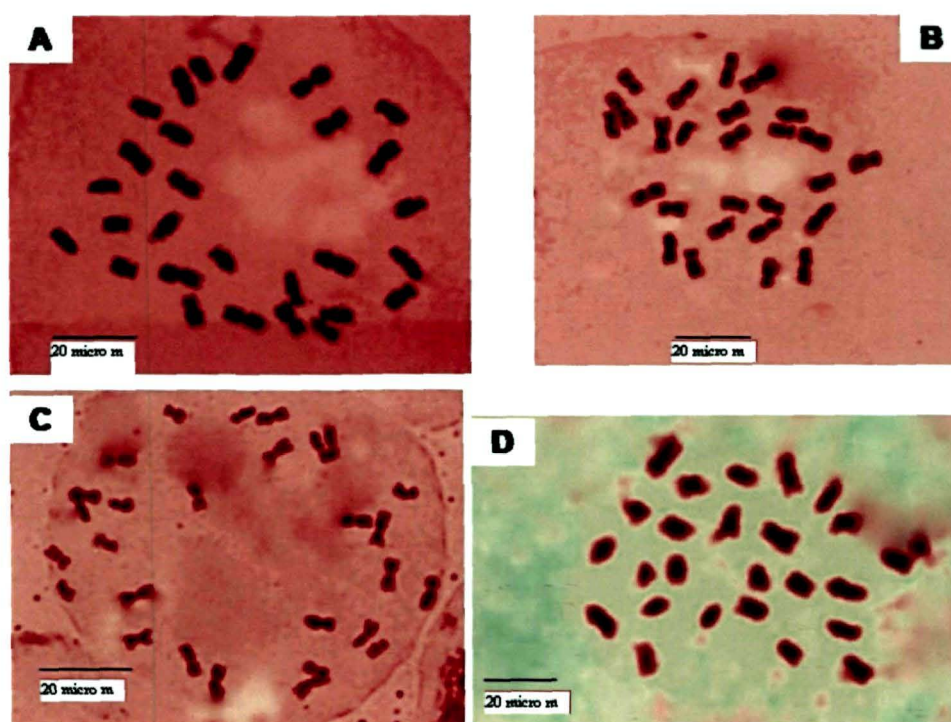


Figure 4.3. Somatic chromosomes of aroids (A) *A. paeoniifolius*, (B) *X. caracu*, (C) *C. esculenta* and (D) *X. sagittifolium*. The pictures were captured with 1000X optical magnification. All figures are metaphase stage of mitotic division.

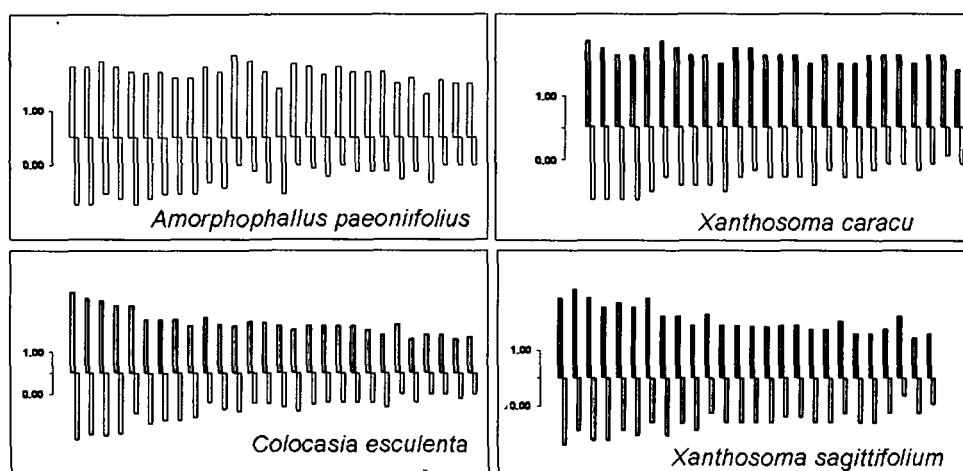


Figure 4.4. Idiogram of chromosomes of four aroid species. The scale shown is in μm ($2n=28$ in *A. paeoniifolius* and *C. esculenta* whereas in *X. caracu* and *X. sagittifolium* $2n=26$)

4.4. Molecular characterization

4.4.1. Genome Size (DNA C-value) determination

The genome size (DNA C-value) of an organism is the amount of nuclear DNA present in the haploid or single set of chromosomes present in the nucleus. For determining the amount of DNA in the nucleus of the aroid cells and genome size were determined following the method of Konwar *et al.*¹³¹. The genomic DNA was purified and its purity and yield were determined and data so obtained are presented in Table 4.4.

Table 4.4. Spectrophotometric determination of purity and yield of DNA from all forms of aroid species

| Aroids | 230 nm | 260 nm/280nm | DNA $\mu\text{g/gm}$ leaf (fresh weight) |
|-------------------------|-----------------|-------------------|--|
| <i>A. paeoniifolius</i> | 0.31 ± 0.03 | 1.735 ± 0.213 | 183.5 ± 10.5 |
| <i>X. caracu</i> | 0.30 ± 0.05 | 1.814 ± 0.124 | 159.21 ± 12.8 |
| <i>C. esculenta</i> | 0.29 ± 0.06 | 1.754 ± 0.245 | 175.21 ± 5.23 |
| <i>X. sagittifolium</i> | 0.32 ± 0.03 | 1.916 ± 0.322 | 207.24 ± 8.29 |

The isolated DNA samples of the aroid species were electrophoresed and the agarose gel photograph is presented in Figure 4.5 to visualize their purity. The leaf sections of the aroid leaves are presented in Figure 4.6.

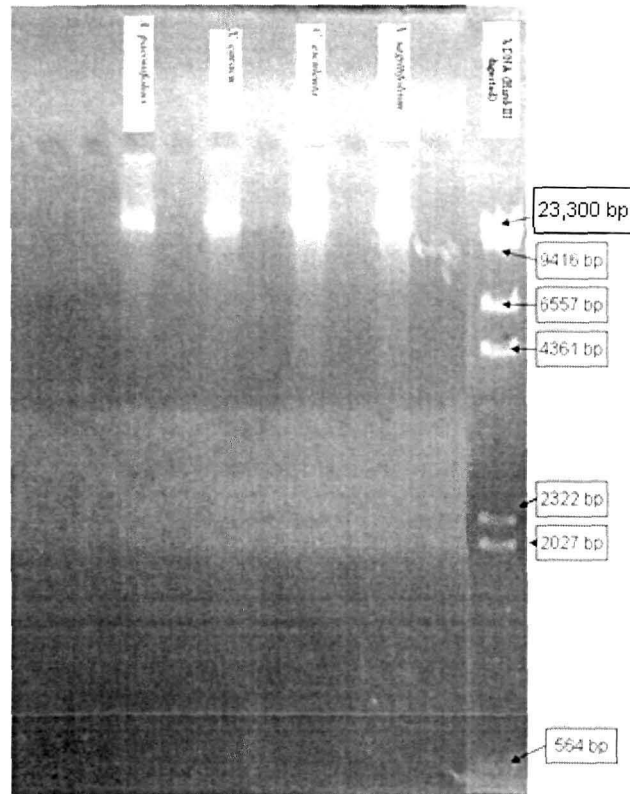


Figure 4.5. Agarose gel electrophoresis of purified genomic DNA of the aroids

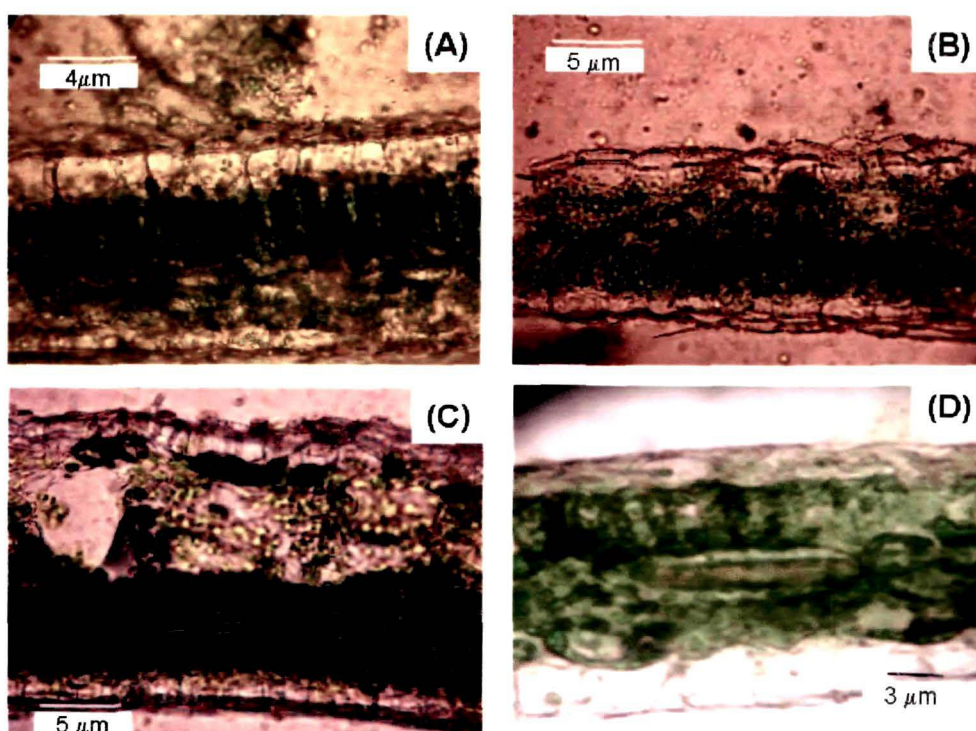


Figure 4.6. Photograph of the leaf sections for determining cell dimensions of (A) *A. paeoniifolius*, (B) *X. caracu*, (C) *C. esculenta* and (D) *X. sagittifolium* at (400X optical magnification)

The genome size in pico gram (pg) as well as in mega base-pairs (Mbp) of all four aroid species are shown in Table 4.5.

Table 4.5. Genome size of the aroids

| Aroid species | Genome size in pg (C) | Genome size in Mbp (C) |
|-------------------------|-----------------------|------------------------|
| <i>A. paeoniifolius</i> | 5.04 | 4929.12 |
| <i>X. caracu</i> | 8.21 | 8029.38 |
| <i>C. esculenta</i> | 14.1 | 13789.8 |
| <i>X. sagittifolium</i> | 8.04 | 7863.12 |

The standard error was not shown as the genome size was calculated from the mean values

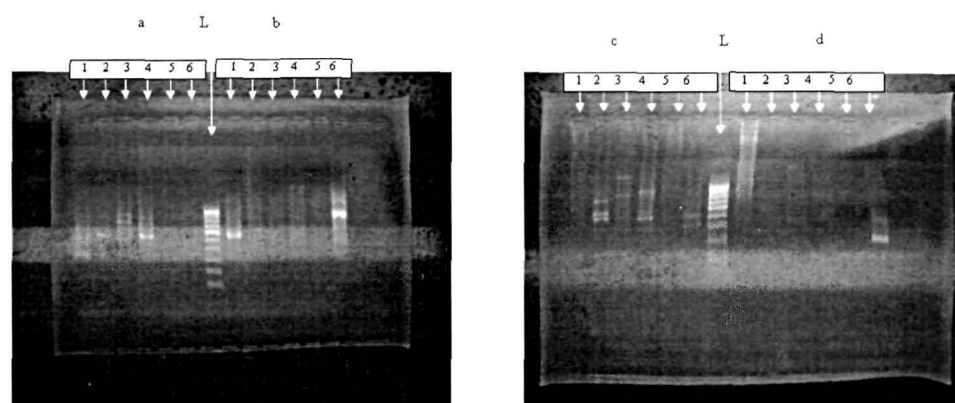
4.4.2. Randomly Amplified Polymorphic DNA (RAPD) analysis

The RAPD analyses of the aroid species were done using six different decamers having high polymorphism in the selected aroids. The result of the RAPD analysis is presented in Table 4.6. The agarose gel electrophoresis of the amplified products is shown in Figure 4.7.

Table 4.6. DNA fragments generated from RAPD analysis

| Sl. No. | Primers | Base pair length (bp) |
|---------|---------------------------|---|
| 1 | OPW-04 (5-CAGAAGCGGA-3) | 327 ^a , 571 ^b , 636 ^a , 1264 ^a . |
| 2 | OPW-05 (: 5-GGCGGATAAG-3) | 471 ^c , 542 ^c , 610 ^a , 812 ^c . |
| 3 | OPW-08 (: 5-GACTGCCTCT-3) | 903 ^a , 924 ^c , 1244 ^a , 1992 ^c |
| 4 | OPW-10 (5-TCGCATCCCT-3) | 454 ^a , 460 ^c , 1027 ^c , 1047 ^a , 1153 ^a , 4473 ^b . |
| 5 | OPW-15 (5-ACACCGGAAC-3) | 1224 ^c . |
| 6 | OPW-16 (5-CAGCCTACCA-3) | 297 ^d , 386 ^c , 461 ^d , 505 ^c , 1149 ^b , 2043 ^b . |

^a *A. paeoniifolius*, ^b *X. caracu*, ^c *C. esculenta* and ^d *X. sagittifolium*



RAPD profiling of *A. paeoniifolius* (a) and *X. caracu* (b)

RAPD profiling of *C. esculenta* (c) and *X. sagittifolium* (d)

Figure 4.7. Agarose gel electrophoresis pattern of the RAPD products (a, *A. paeoniifolius*; b, *X. caracu*; c, *C. esculenta*; d, *X. sagittifolium*. The 1-6 are the serial no. of the primers as presented in Table 4.6

The genetic relationship as determined by the RAPD analysis is depicted in Figure 4.8. The Jaccard similarity coefficient calculated from the RAPD data are presented in Table 4.7.

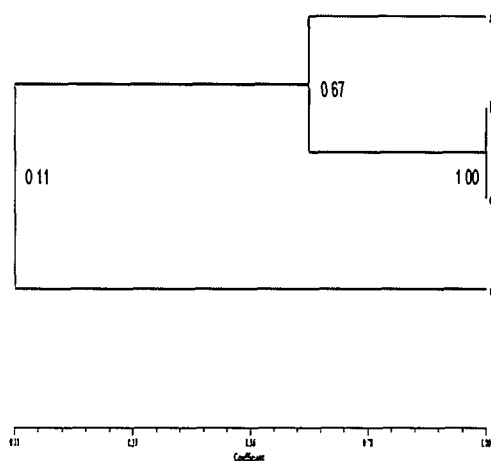


Figure 4.8. Dendrogram presentation among the aroids as determined from RAPD data, a, *A. paeoniifolius*; b, *X. caracu*; c, *C. esculenta*; d, *X. sagittifolium*

Table 4.7. Pair-wise genetic similarity matrix among the aroid species based on Jaccard similarity coefficient

| Aroids | <i>A. paeoniifolius</i> | <i>X. caracu</i> | <i>C. esculenta</i> | <i>X. sagittifolium</i> |
|-------------------------|-------------------------|------------------|---------------------|-------------------------|
| <i>A. paeoniifolius</i> | 1.0 | | | |
| <i>X. caracu</i> | 0.5 | 1.0 | | |
| <i>C. esculenta</i> | 0.5 | 0.33 | 1.0 | |
| <i>X. sagittifolium</i> | 0.0 | 0.66 | 0.33 | 1.0 |

4.5. Compound purification

The major part of the dry biomass composition of the aroid corm was starch (polymeric compound) but a minor amount of phenolic compound was also present. For estimating the phenolic compounds, there was a need to confirm their presence in the crude extract. For the convenience of compound isolation, the total phenolic content (TPC), total flavonoid content, DPPH

scavenging assay, antimicrobial assay and blood coagulation assays were performed with the crude extract. An effort was made to estimate the potency of the crude extract to reveal the presence of antibacterial compounds. The result obtained for TPC is presented in Figure 4.9, flavonoid estimation in Figure 4.10, DPPH scavenging in Figure 4.11 and Figure 4.12 and blood coagulation assay in Figure 4.13.

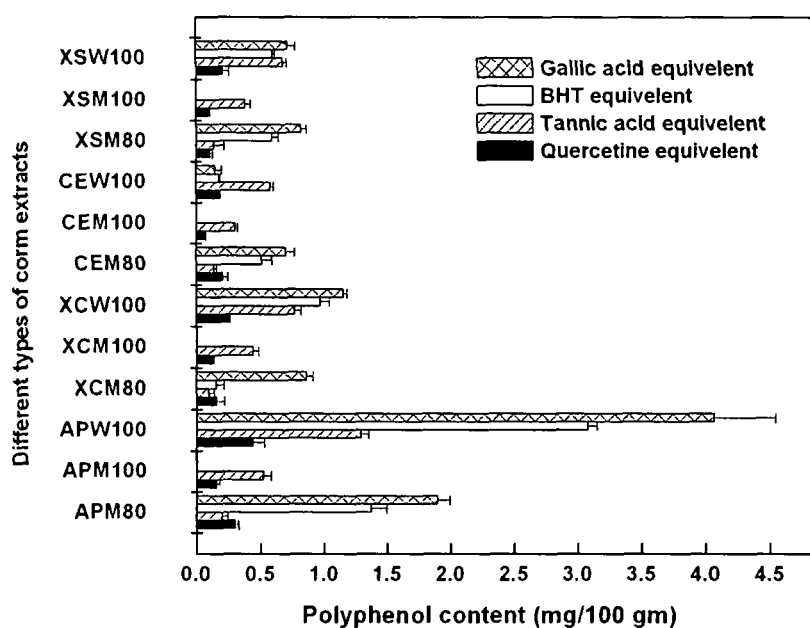


Figure 4.9. Total phenolic content of the aroid corm extracts (APM80, XCM80, CEM80 and XSM80 are 80% methanol extracts; APM100, XCM100, CEM100 and XSM100 are 100% methanol extracts; APW100, XCW100, CEW100 and XSW100 are water extracts in the order of *A. paeoniifolius*, *X. caracu*, *C. esculenta* and *X. sagittifolium*)

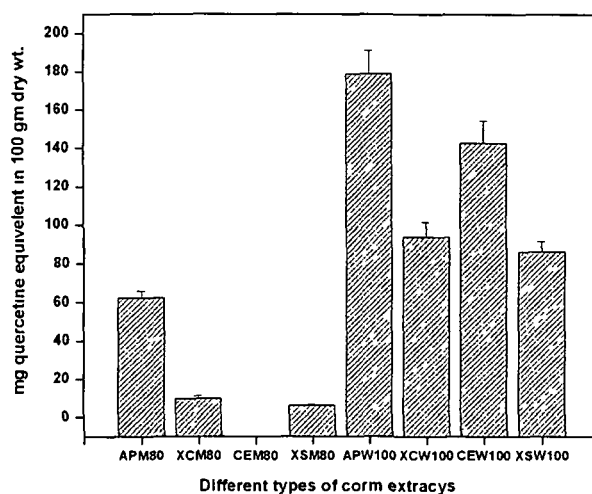


Figure 4.10. Total flavonoid content of the aroid corm extracts (APM80, XCM80, CEM80 and XSM80 are 80% methanol extract; APW100, XCW100, CEW100 and XSW100 are water extracts in the order of *A. paeoniifolius*, *X. caracu*, *C. esculenta* and *X. sagittifolium*)

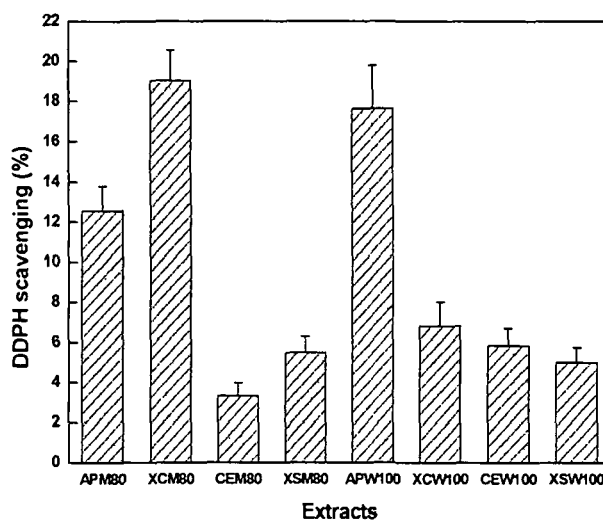


Figure 4.11. DPPH scavenging potency of the extracts (APM80, XCM80, CEM80 and XSM80 are 80% methanol extract; APW100, XCW100, CEW100 and XSW100 are water extracts in the order of *A. paeoniifolius*, *X. caracu*, *C. esculenta* and *X. sagittifolium*)

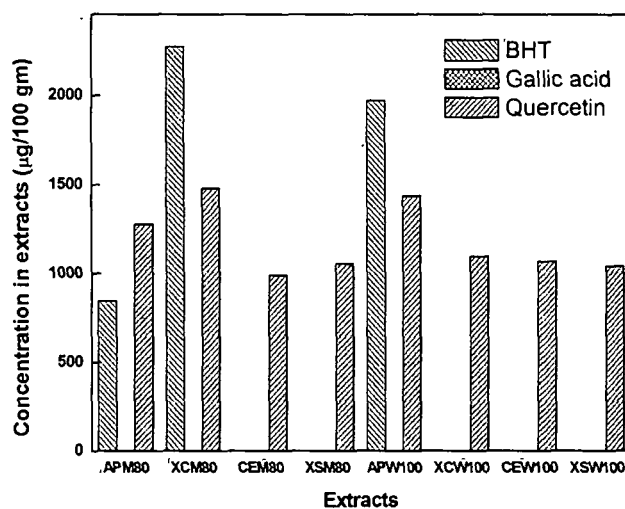


Figure 4.12. Standard equivalence of the extracts with respect to antioxidant property (APM80, XCM80, CEM80 and XSM80 are 80% methanol extract; APW100, XCW100, CEW100 and XSW100 are water extracts in the order of *A. paeoniifolius*, *X. caracu*, *C. esculenta* and *X. sagittifolium*)

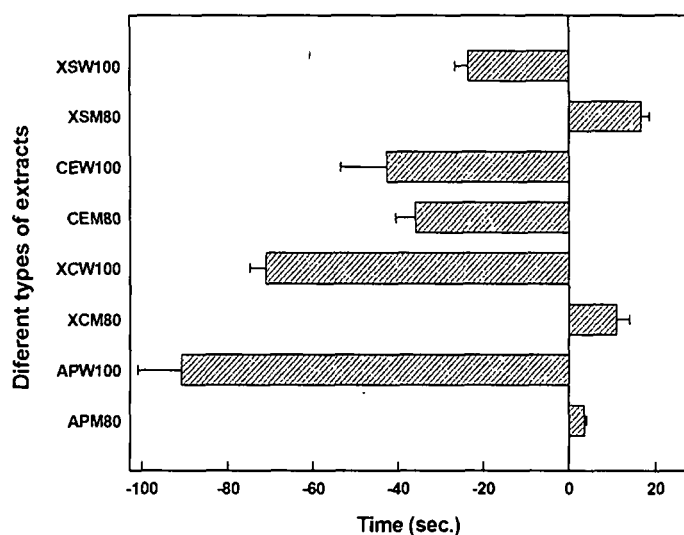


Figure 4.13. Blood coagulating property of the extracts (APM80, XCM80, CEM80 and XSM80 are 80% methanol extract; APW100, XCW100, CEW100 and XSW100 are water extracts in the order of *A. paeoniifolius*, *X. caracu*, *C. esculenta* and *X. sagittifolium*)

The antimicrobial activity of the compounds was observed and is shown in Figure 4.14 and Figure 4.15.

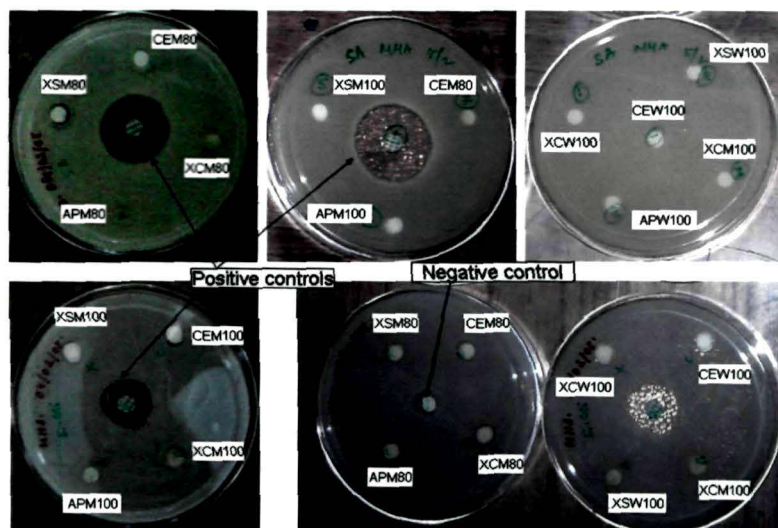


Figure 4.14. Antimicrobial activity of the extracts (APM80, XCM80, CEM80 and XSM80 are 80% methanol extract; APW100, XCW100, CEW100 and XSW100 are water extracts in the order of *A. paeoniifolius*, *X. caracu*, *C. esculenta* and *X. sagittifolium*)

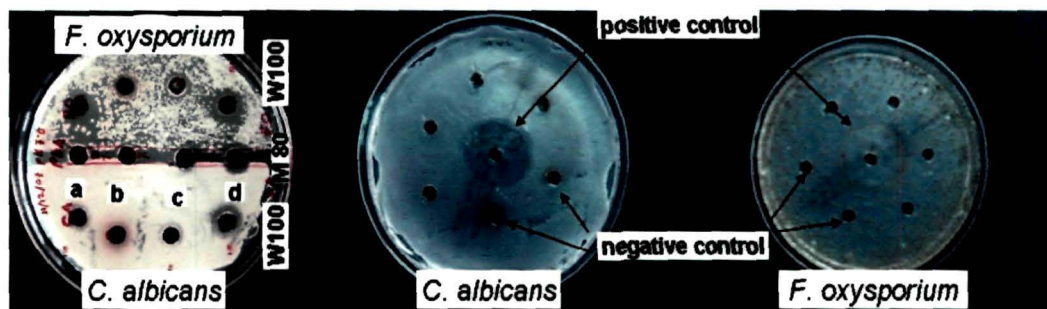


Figure 4.15. Antifungal activity of the extracts (on left), positive and negative control against *C. albicans* and *F. oxysporium* (a, *A. paeoniifolius*; b, *X. caracu*; c, *C. esculenta*; d, *X. sagittifolium*; W100 water extract and M80 80% methanolic extract of the corm)

In view of the positive results, 80% methanol extract was selected as the source for resolving the antibacterial polyphenolic compounds. Thin layer chromatography (TLC) profiling of 80% methanolic extract is shown in Figure 4.16. Further, the column chromatography (CC) was done in the same solvent

having the same polarity and the polyphenolic content was estimated for each fraction. The results observed are presented in Figure 4.17.

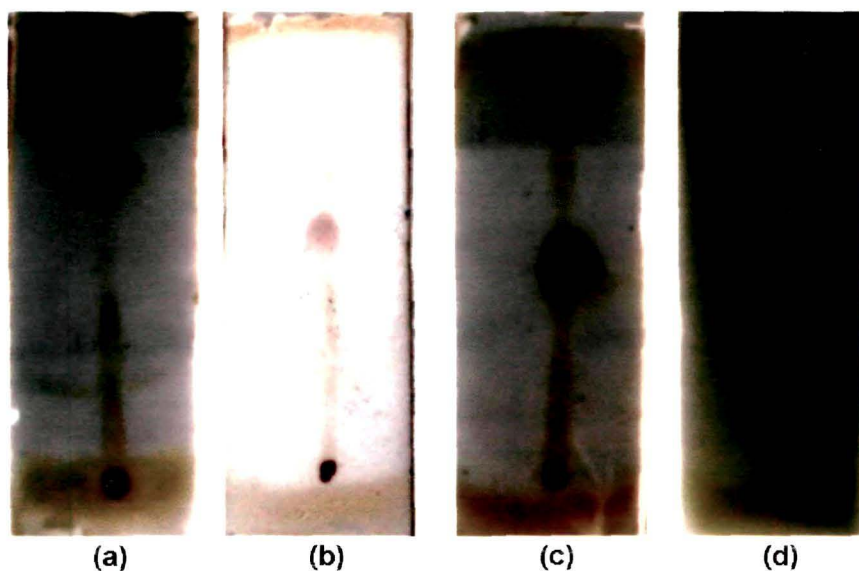


Figure 4.16. TLC profiling of the compounds, (a) *A. paeoniifolius*, (b) *X. caracu*, (c) *C. esculenta* and (d) *X. sagittifolium*

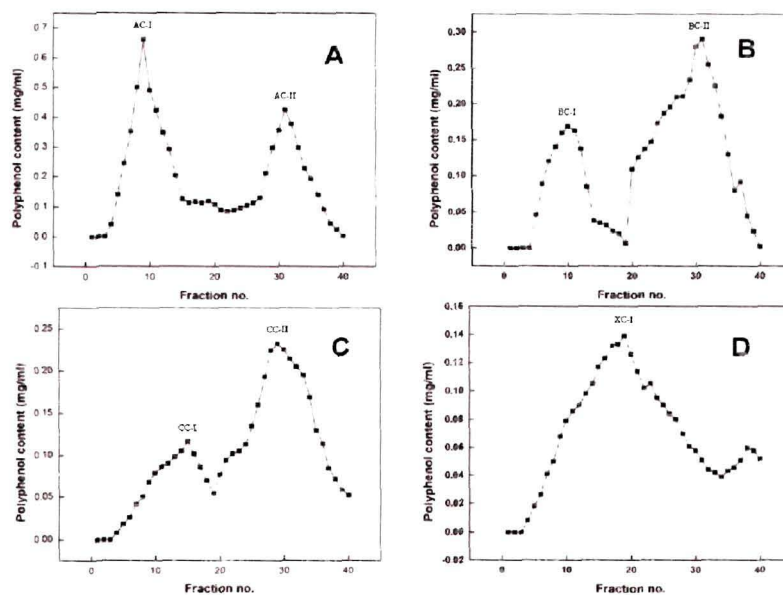


Figure 4.17. Polyphenolic content of the fractions from column chromatography, (A) *A. paeoniifolius*, (B) *X. caracu*, (C) *C. esculenta* and (D) *X. sagittifolium*

The highest polyphenol containing fractions as revealed by column chromatography were labeled as AC-I, AC-II, BC-I, BC-II, CC-I, CC-II and XC-I. These fractions were selected for further purification using the high performance liquid chromatography (HPLC). HPLC profiling of the compounds with the standardized method is shown in Figure 4.18 and Figure 4.19.

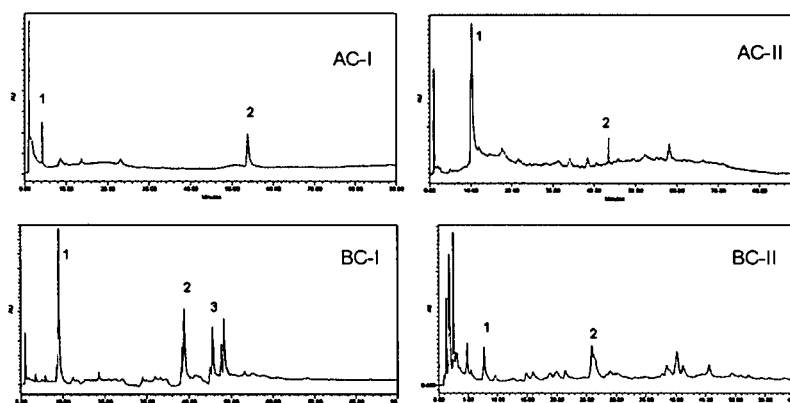


Figure 4.18. HPLC profiling of the fractions AC-I, AC-II, BC-I and BC-II

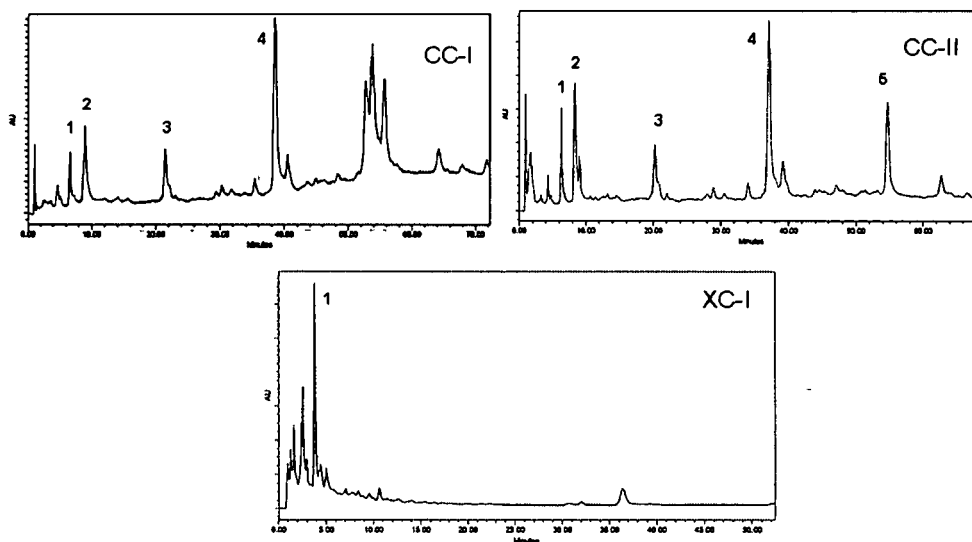


Figure 4.19. HPLC profiling of the fractions CC-I, CC-II and XC-I

Table 4.8. Purified fractions generated from HPLC

| Aroid species | Fractions generated |
|-------------------------|---------------------|
| <i>A. paeoniifolius</i> | AC-I(1) |
| | AC-I(2) |
| | AC-II (1) |
| | AC-II(2) |
| <i>X. caracu</i> | BC-I (1) |
| | BC-I (2) |
| | BC-I (3) |
| | BC-II (1) |
| | BC-II (2) |
| <i>C. esculenta</i> | CC-I (1) |
| | CC-I (2) |
| | CC-I (3) |
| | CC-I (4) |
| | CC-II (1) |
| | CC-II (2) |
| | CC-II (3) |
| | CC-II (4) |
| | CC-II (5) |
| <i>X. sagittifolium</i> | XC-I (1) |

The separated fractions as labeled in Figure 4.18 and Figure 4.19 were collected and used for characterization using furrier transformed infrared (FTIR) spectroscopy and nuclear magnetic resonance (NMR) analysis except for CC-I (1) and CC-II (1) (amount being negligible). The FTIR spectral patterns of the compounds were depicted in Figure 4.20 and Figure 4.21. The NMR spectra of the compounds are analyzed and the results obtained are presented in Table 4.10 and the predicted structures of the compounds were shown in Figure 4.22.

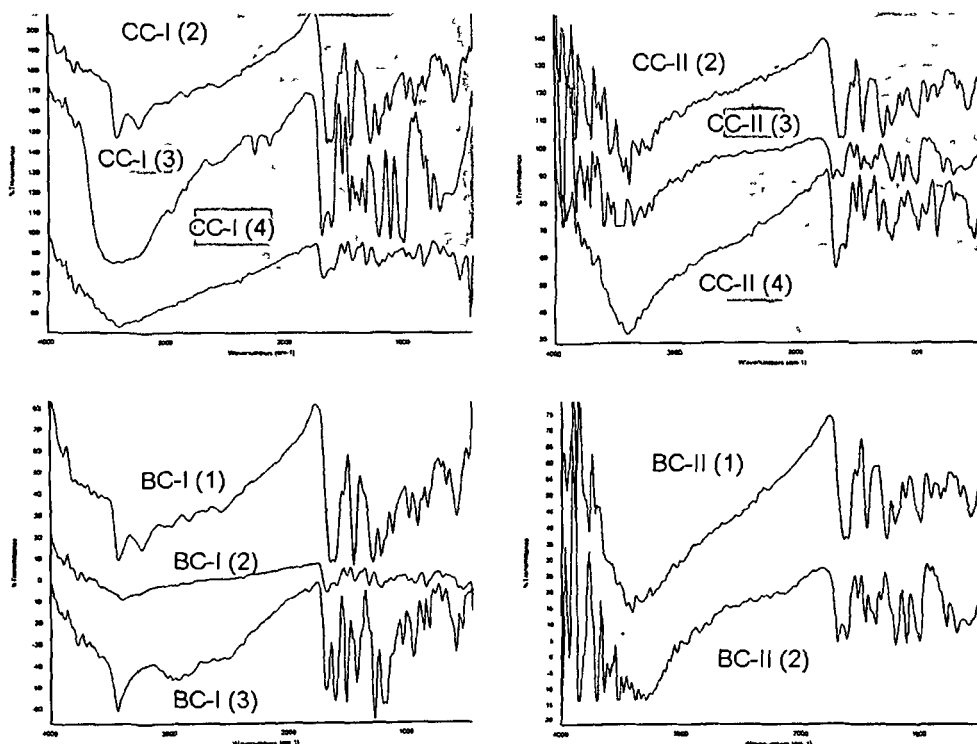


Figure 4.20. FTIR spectra of purified compounds from *C. esculenta* and *X. caracu*

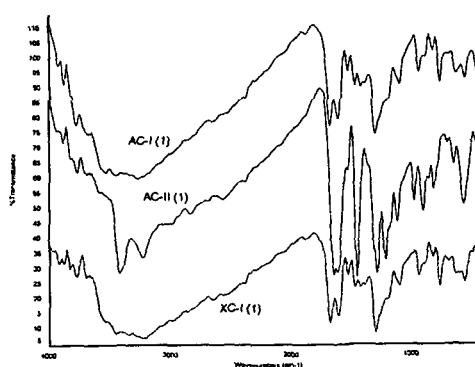


Figure 4.21. FTIR spectra of purified compounds from *A. paeoniifolius* and *X. sagittifolium*

Table 4.9. Structural information generated from FTIR data

| Sl. No. | Fractions | FTIR peaks (cm ⁻¹) | Structural information revealed |
|---------|--|--|--|
| 1 | AC-I (1) and XC-I (1) | 1400-1500 and 1585-1600 | C=C stretching of an aromatic ring |
| | | 3231-3657 | O-H bond stretching of -COOH |
| | | 3231-3657 broadening | Overlap of C-H stretching of aromatic ring |
| | | 1294 broadening | C-O of COOH group |
| | | 693 | aromatic C-H loop bending |
| | | 693 and 761 | mono-substituted benzene |
| 2 | AC-II (1), BC-I (1), BC-II (1), CC-I (2) and CC-II (2) | 1400-1500 and 1585-1600 | C=C stretching of an aromatic ring |
| | | All above features are present except peaks at 693 and 761 | |
| | | 696, 808 and 896 | meta-disubstituted benzene |
| | | 850 low intensity | para-disubstituted benzene |

| | | | |
|--|-----------------------------------|-------------------------|---|
| | | 3422 | O-H stretch of -OH |
| | | 1213 | C-O stretch of COH group of benzene |
| It was concluded that the structure could be a benzene ring substituted with three different functional groups in three different positions. These three functional groups are -OH and -COOH. One of them substituted the ring in two places (Elegir <i>et al.</i> ²³¹). | | | |
| 3 | CC-II (4), BC-I (2) and CC-I (4) | 1400-1500 and 1585-1600 | C=C stretching of an aromatic ring |
| Similar to Sl. No. 2 except the substitution pattern evidences were prominent for a meta-di-substitution only. | | | |
| 4 | BC-I (3) | 1400-1500 and 1585-1600 | C=C stretching of an aromatic ring |
| The spectrum of BC-I (3) was almost similar with Sl. No. 2 but there is a narrow and intensive band at 3430 cm ⁻¹ referring to in the spectrum of ferulic acid (Markovi ²³²). | | | |
| 5 | BC-II (2), CC-II (3) and CC-I (3) | 1400-1500 and 1585-1600 | C=C stretching of an aromatic ring |
| | | 1462 | CH stretching of methyl or methylene groups |
| The FT-IR spectra of were found to be similar with the data provided by Surowiec <i>et al.</i> ²³³ . The comparisons suggested that the compounds might be syringic acid. | | | |

Table 4.10. Prediction of compounds based on NMR data and correlation with structures presented in Figure 4.22

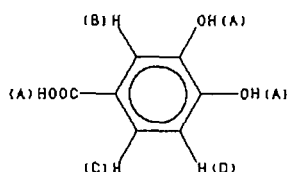
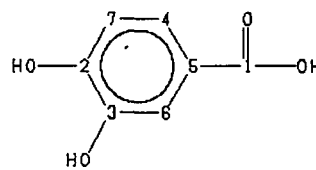
| Name of the | H ¹ NMR (ppm) | C ¹³ NMR (ppm) | Sl. No. as | Structure elucidated from FTIR and NMR |
|-------------|--------------------------|---------------------------|------------|--|
|-------------|--------------------------|---------------------------|------------|--|

| pure fraction | | | depicted in the Figure 4.22 | spectra |
|---------------|--|---|-----------------------------|--|
| AC-I (1) | 6.86 (D), 7.39 (C), 7.40 (B), 9.58 (A) | 117 (C7), 118 (C6), 123 (C5), 123 (C4), 146 (C3), 151 (C2), 168 (C1). | 1 | 3,4-dihydroxy benzoic acid (Protocatechuic acid) |
| AC-II (1) | 6.21 (F), 6.25 (E), 6.82 (D), 7.08 (C), 7.08 (B), 7.44 (A). | 115 (C9), 115 (C8), 116 (C7), 121 (C6), 126 (C5), 145 (C4), 146 (C3), 148 (C2), 168 (C1). | 2 | Caffeic acid (3,4-dihydroxycinnamic acid) |
| BC-I (1) | 6.21 (F), 6.25 (E), 6.83 (D), 7.08 (C), 7.09 (B), 7.45 (A). | 115 (C9), 115 (C8), 116 (C7), 121 (C6), 126 (C5), 145 (C4), 146 (C3), 148 (C2), 168 (C1). | 2 | Caffeic acid (3,4-dihydroxycinnamic acid) |
| BC-I (2) | 6.32 (J), 6.36 (G), 6.83 (F), 6.85 (E), 7.53 (D), 7.55 (C), 7.57 (B), 10.05 (A). | 115 (C9), 116 (C8), 119 (C7), 125 (C6), 130 (C5), 135 (C4), 144 (C3), 160 (C2), 168 (C1). | 3 | Coumaric acid (trans-in-hydroxycinnamic acid) |
| BC-I (3) | 6.40, 6.44, 6.84, 6.86, 7.14, 7.34, 7.53, 7.57, | 56, 111, 116, 116, 123, 126, 129, 145, 148, 149, 167, 168. | 4 | Ferulic acid (4-hydroxy-3-methoxycinnamic acid) |

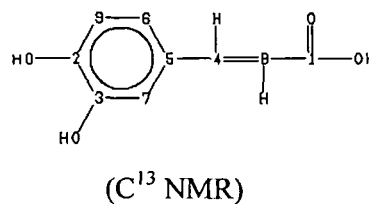
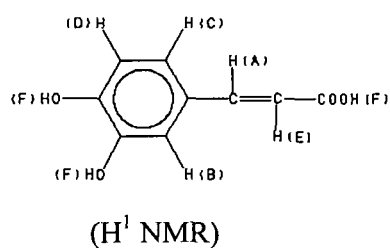
| | | | | |
|--------------|---|--|---|--|
| | 7.75, 7.77, 9.64. | | | |
| BC-II (1) | 6.22 (F), 6.26 (E), 6.83 (D), 7.01 (C), 7.09 (B), 7.45 (A). | 115 (C9), 115 (C8), 116 (C7), 121 (C6), 126 (C5), 145 (C4), 146 (C3), 148 (C2), 168 (C1). | 2 | Caffeic acid (3,4- dihydroxycinnamic acid) |
| BC-II (2) | 3.85 (D), 4.19 (C), 7.25 (B), 9.30 (A). | 56 (C6), 107 (C5), 120 (C4), 140 (C3), 147 (C2), 167 (C1). | 5 | Syringic acid (4- hydroxy-3,5- dimethoxybenzoic acid) |
| CC-I (2) | 6.20 (F), 6.24 (E), 6.81 (D), 7.07 (C), 7.07 (B), 7.47 (A). | 115 (C9), 115 (C8), 116 (C7), 121 (C6), 126 (C5), 145 (C4), 146 (C3), 148 (C2), 168 (C1). | 2 | Caffeic acid (3,4- dihydroxycinnamic acid) |
| CC-I (3) | 3.87 (D), 4.20 (C), 7.27 (B), 9.30 (A). | 56 (C6), 107 (C5), 120 (C4), 140 (C3), 147 (C2), 167 (C1). | 5 | Syringic acid (4- hydroxy-3,5- dimethoxybenzoic acid) |
| CC-I (4) | 6.32 (J), 6.36 (G), 6.83 (F), 6.85 (E), 7.52 (D), 7.55 (C), 7.58 (B), 10.06 (A). | 115 (C9), 116 (C8), 119 (C7), 125 (C6), 130 (C5), 135 (C4), 144 (C3), 160 (C2), 168 (C1). | 3 | Coumaric acid (trans- in-hydroxycinnamic acid) |
| CC-II (2) | 6.21 (F), 6.25 (E), 6.80 (D), 7.08 (C), 7.08 | 115 (C9), 115 (C8), 116 (C7), 121 (C6), 126 | 2 | Caffeic acid (3,4- dihydroxycinnamic acid) |

| | | | | |
|--------------|---|--|---|--|
| | (B), 7.48 (A). | (C5), 145 (C4), 146 (C3), 148 (C2), 168 (C1). | | |
| CC-II (3) | 3.85 (D), 4.18 (C), 7.25 (B), 9.32 (A). | 56 (C6), 107 (C5), 120 (C4), 140 (C3), 147 (C2), 167 (C1). | 5 | Syringic acid (4- hydroxy-3,5- dimethoxybenzoic acid) |
| CC-II (4) | 6.32 (J), 6.36 (G), 6.83 (F), 6.85 (E), 7.52 (D), 7.55 (C), 7.57 (B), 10.06 (A). | 115 (C9), 116 (C8), 119 (C7), 125 (C6), 130 (C5), 135 (C4), 144 (C3), 160 (C2), 168 (C1). | 3 | Coumaric acid (trans- in-hydroxycinnamic acid) |
| XC-I (1) | 6.85 (D), 7.39 (C), 7.39 (B), 9.37 and 9.74 (A) | 115 (C7), 117 (C6), 122 (C5), 122 (C4), 145 (C3), 150 (C2), 167 (C1). | 1 | 3,4-dihydroxy benzoic acid |

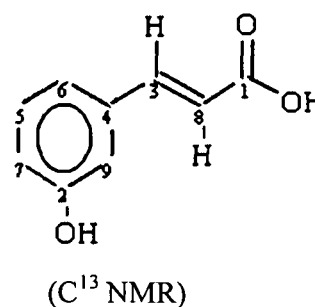
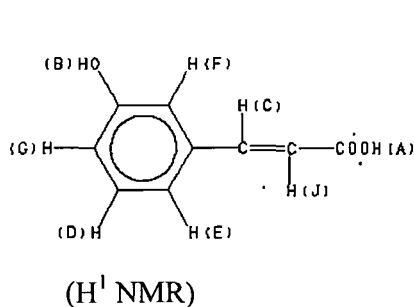
Compound 1: 3, 4-dihydroxy benzoic acid

 $(H^1 \text{ NMR})$  $(C^{13} \text{ NMR})$

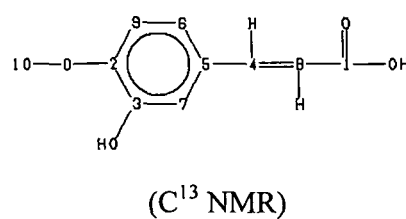
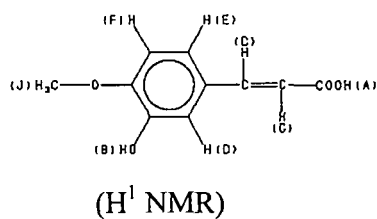
Compound 2: Caffeic acid (3, 4-dihydroxycinnamic acid)



Compound 3: Caumaric acid (trans-in-hydroxycinnamic acid)



Compound 4: Ferulic acid (4-hydroxy-3-methoxycinnamic acid)



Compound 5: Syringic acid (4-hydroxy-3, 5-dimethoxybenzoic acid)

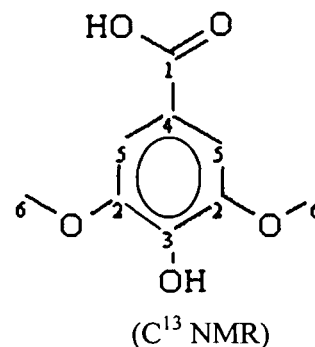
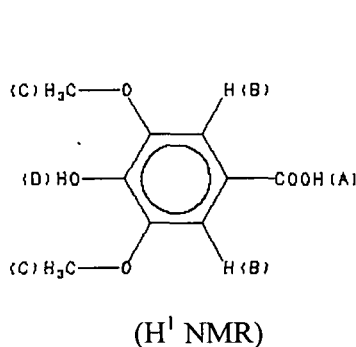


Figure 4.22. Structures of the five different compounds isolated from the four different aroids

The antimicrobial tests were performed against *E. coli*, *S. aureus* (bacteria), *C. albicans* and *F. oxysporum* (fungi). The results obtained are shown in Figure 4.23, Figure 4.24, Figure 4.25 and Figure 4.26 and data are shown in Table 4.11.

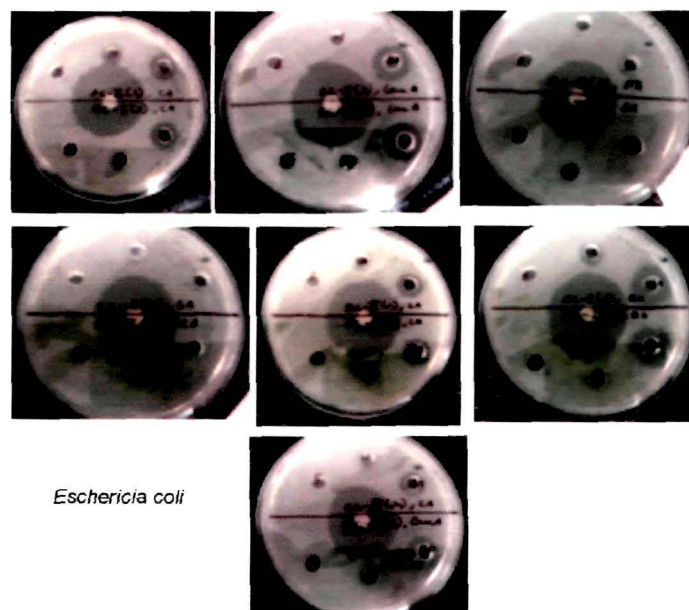


Figure 4.23. Antibacterial activities against *E. coli*

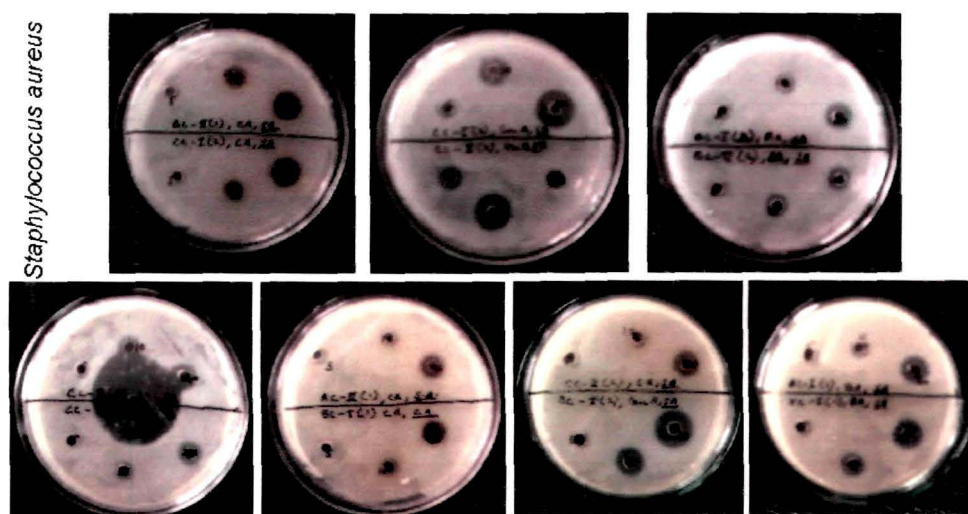


Figure 4.24. Antibacterial activity against *S. aureus*

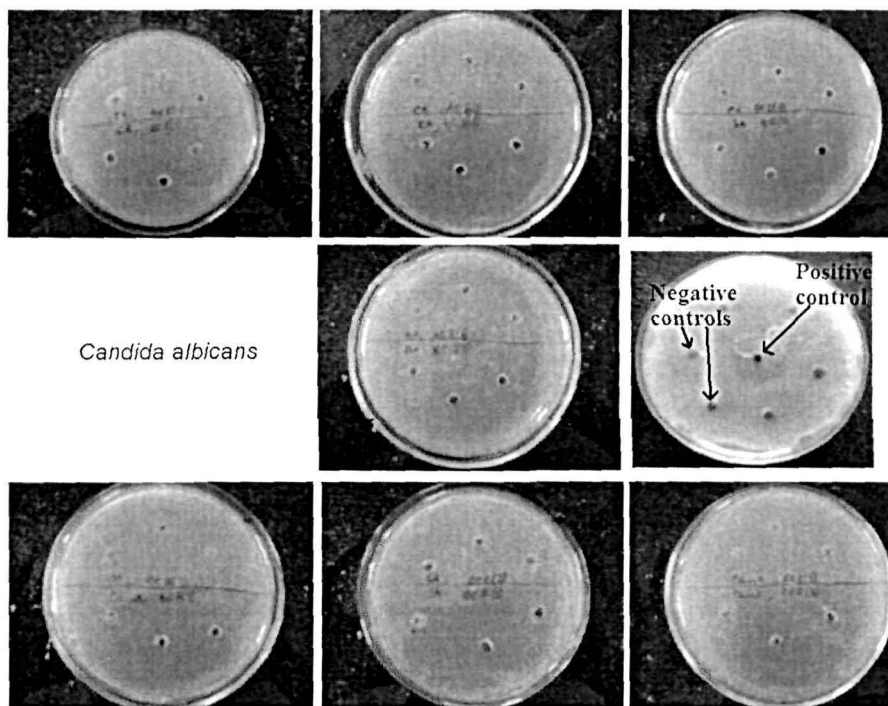


Figure 4.25. Antibacterial activity against *C. albicans*

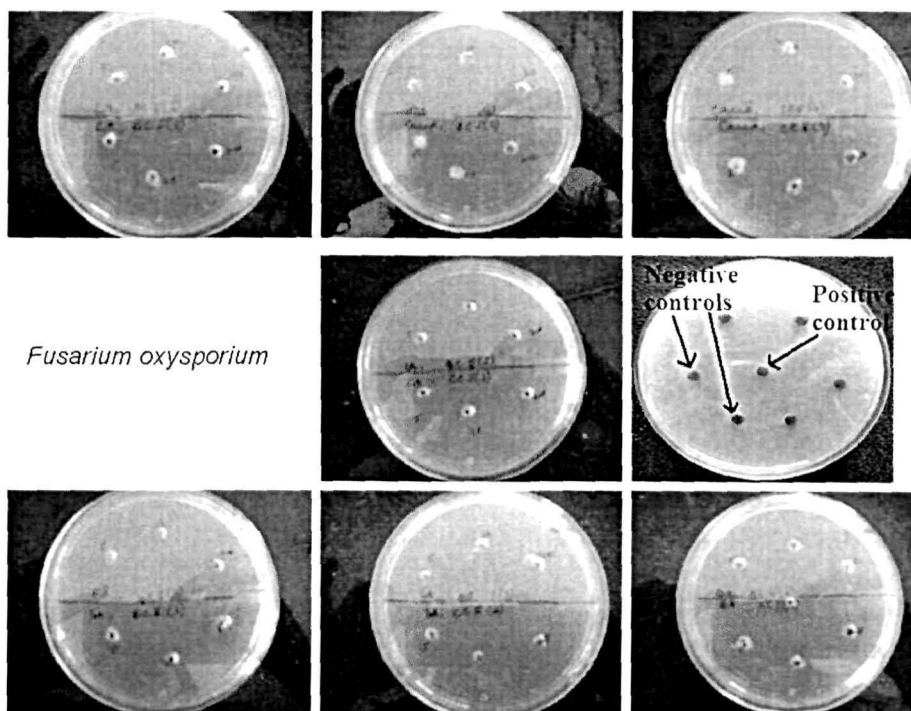


Figure 4.26. Antibacterial activity against *F. oxysporium*

Table 4.11. Documentation of the results of the antimicrobial assays

| Sl no. | Compound name | <i>E. coli</i> | <i>S. aureus</i> | <i>C. albicans</i> | <i>F. oxisporium</i> |
|--------|--------------------------------|----------------|------------------|--------------------|----------------------|
| 1 | AC-II (1) | ++ | ++ | - | - |
| 2 | BC-I (1) | ++ | ++ | - | - |
| 3 | CC-I (4) | ++ | +++ | - | - |
| 4 | CC-II (4) | ++ | +++ | - | - |
| 5 | BC-I (2) | - | + | - | - |
| 6 | BC-II (2) | - | + | - | - |
| 7 | CC-I (2) | - | + | - | - |
| 8 | CC-II (2) | - | + | - | - |
| 9 | CC-I (3) | + | + | - | - |
| 10 | BC-II (1) | + | + | - | - |
| 11 | AC-I (1) | +++ | ++ | - | - |
| 12 | XC-I (1) | +++ | ++ | - | - |
| 13 | CC-II (3) | + | ++ | - | - |
| 14 | BC-I (2) | ++ | +++ | - | - |
| 15 | Ampicillin | +++++ | +++++ | NN | NN |
| 16 | Himedia antifungal solution | NN | NN | +++ | +++ |

NN, Not Necessary; +, antimicrobial activity present and -, antimicrobial activity absent

The antioxidant activity of the compounds is shown in Figure 4.27 as the anti-haemolysis activity against H₂O₂ induced haemolysis.

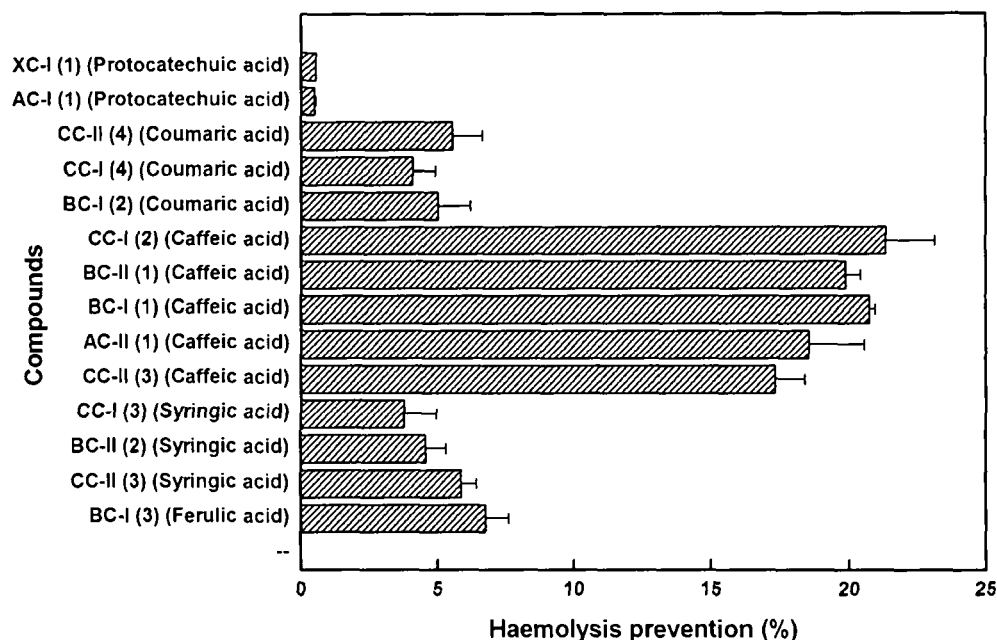


Figure 4.27. Antioxidant activities of the compounds

4.6. Isolation and characterization of the starch (polymeric compound) from aroids

The isolated starch from each aroid species was characterized with respect to granule morphology and amylose content. Fourier transformed infrared spectroscopy (FT-IR), X-ray diffraction analysis (XRD) and differential scanning calorimetry (DSC) were performed for biochemical analysis of aroid starch. Amylose leaching, acid cum enzymatic hydrolysis and water binding capacity were done for biochemical characterization of the aroid starch. The proximate composition of starch from aroids was done with respect to moisture, ash, amylase and lipid contents, starch damage, water holding capacity, α -amylase hydrolysis, total carbon, phosphorus and oxygen content. Data obtained are presented in Table 4.12. The gelatinization parameters were assessed using DSC and data obtained are presented in Table 4.13.

Table 4.12. Proximate composition of the aroid starches

| Aroids | <i>A. paeonifolius</i> | <i>X. caracu</i> | <i>C. esculenta</i> | <i>X. sagittifolium</i> |
|---|----------------------------|------------------|-------------------------|-----------------------------|
| Moisture content (%) | 9.5 ± 1.4 | 10.2 ± 0.85 | 11.2 ± 0.74 | 12.2 ± 1.2 |
| Total ash content (%) | 1.2 ± 0.9 | 1.5 ± 0.5 | 1.3 ± 0.6 | 1.2 ± 0.8 |
| Apparent amylose content (%) | 12.54 ± 0.6 | 12.84 ± 0.8 | 17.54 ± 1.2 | 18.25 ± 0.54 |
| Total amylose content (%) | 14.24 ± 2.1 | 16.6 ± 3.4 | 22.4 ± 4.5 | 20.4 ± 1.6 |
| Lipid content with chloroform: Methanol | 0.05 ± 0.01 | 0.04 ± 0.02 | 0.04 ± 0.01 | 0.06 ± 0.01 |
| Lipid content with n-propanol: water | 0.01 ± 0.005 | 0.02 ± 0.01 | 0.02 ± 0.008 | 0.03 ± 0.01 |
| Lipid content with HCl hydrolysis | 0.13 ± 0.02 | 0.2 ± 0.04 | 0.09 ± 0.02 | 0.17 ± 0.05 |
| Starch damage (%) | 4.54 ± 0.24 | 1.42 ± 0.14 | 2.17 ± 0.08 | 2.54 ± 0.11 |
| Water binding capacity (%) | 86.2 ± 4.5 | 82.1 ± 5.1 | 87.7 ± 3.5 | 79.5 ± 4.3 |
| Total carbon content (%) | 62.35 ± 9.2 | 70.18 ± 11.2 | 80.53 ± 14.5 | 80.84 ± 15.5 |
| Total oxygen content (%) | 37.75 ± 5.6 | 29.73 ± 12.3 | 11.74 ± 5.2 | 14.69 ± 5.2 |
| Granule size (µm) | 5-12 | 1.25-2.21 | 0.71-1.25 | 2.1-2.84 |
| Granule shape | Polygonal | Polygonal | Polygonal | Polygonal |
| Fissures | Absent | Absent | Absent | Absent |

| | | | | |
|---|-------------|-------------|-------------|-------------|
| Concentric rings | Absent | Absent | Absent | Absent |
| Total phosphorus content (mg/100g) from EDX | 0.08 ± 0.05 | 0.04 ± ND | 0.07 ± 0.02 | 0.05 ± 0.04 |
| Relative degree of the crystallinity (%)* | 48.84 | 46.91 | 35.77 | 41.30 |
| α-amylase hydrolysis (%) | 30.49 ± 0.3 | 42.54 ± 1.5 | 56.15 ± 1.9 | 36.04 ± 1.4 |

Data presented are mean ± Standard error; * calculated value

Table 4.13. DSC analysis of aroid starch

| Sl no | Aroids | T _o (°C) | T _c (°C) | T _p (°C) | ΔH (mJ/g) |
|-------|-------------------------|---------------------|---------------------|---------------------|---------------------|
| 1 | Starch soluble | 57.42 ± 2.4 4 | 72.44 ± 1.87 | 70.49 ± 2.63 | 9,122.00 ± 237 |
| 2 | <i>A. paeonifolius</i> | 95.94 ± 3.1 5 | 112.77 ± 1.2 8 | 104.22 ± 2.7 7 | 95,326.66 ± 54 3 |
| 3 | <i>X. caracu</i> | 97.55 ± 2.1 | 106.50 ± 3.3 1 | 103.49 ± 3.8 9 | 14,660.00 ± 23 8 |
| 4 | <i>X. sagittifolium</i> | 85.44 ± 3.8 5 | 118.01 ± 3.3 3 | 102.40 ± 3.1 5 | 24,083.33 ± 34 9 |
| 5 | <i>C. esculenta</i> | 95.45 ± 3.1 9 | 118.01 ± 2.8 4 | 106.97 ± 2.6 4 | 44,000.00 ± 45 5 |

Data presented are mean ± Standard error. T_o, temperature at starting of gelatinization; T_c, temperature at completion of gelatinization and T_p, maximum temperature during gelatinization.

The morphology of starch granules of all four aroids is shown in Figure 4.28. The other morphological features are described in Table 4.12. Sharp variation in the size and type of starches was observed in SEM analysis.

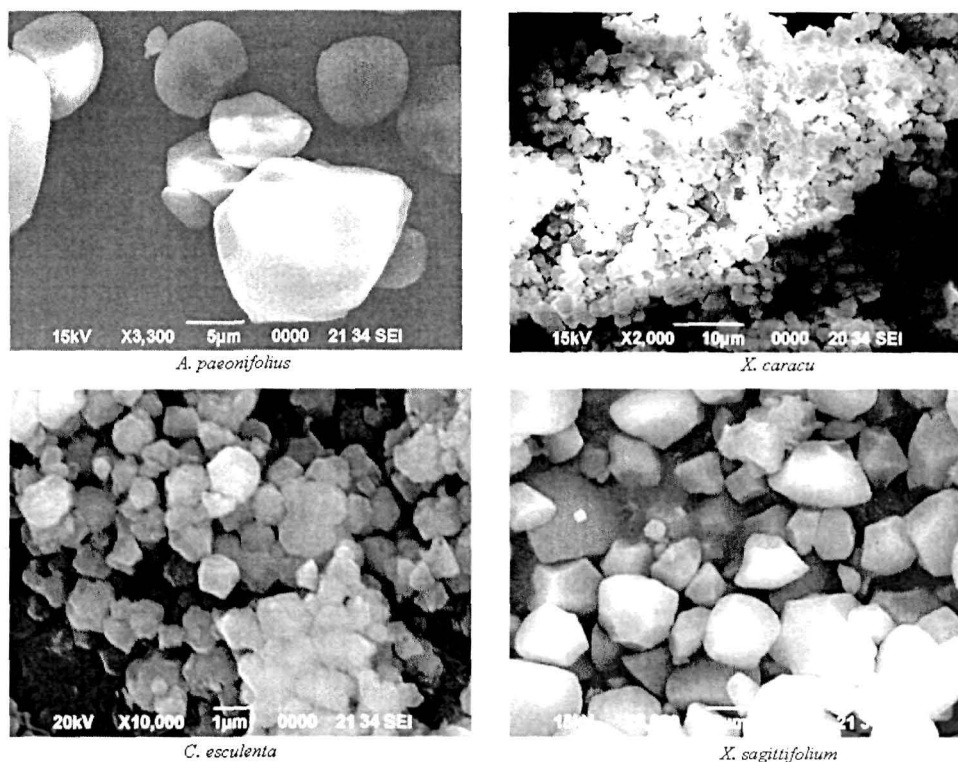


Figure 4.28. Scanning electron microscopic images of purified aroid starch granules showing their size and morphology

The X-ray diffraction analysis was performed on corm starches and data obtained are shown in Figure 4.29. The calculation on crystallinity of the aroid starches is presented in Table 4.12. The evidence for the same is presented in Figure 4.30. The size of crystal-size (in Å) and lattice strains (in %) are presented in Table 4.14. The linear curve fitting on XRD data using Gaussian and Lorengian method are shown in Figure 4.31.

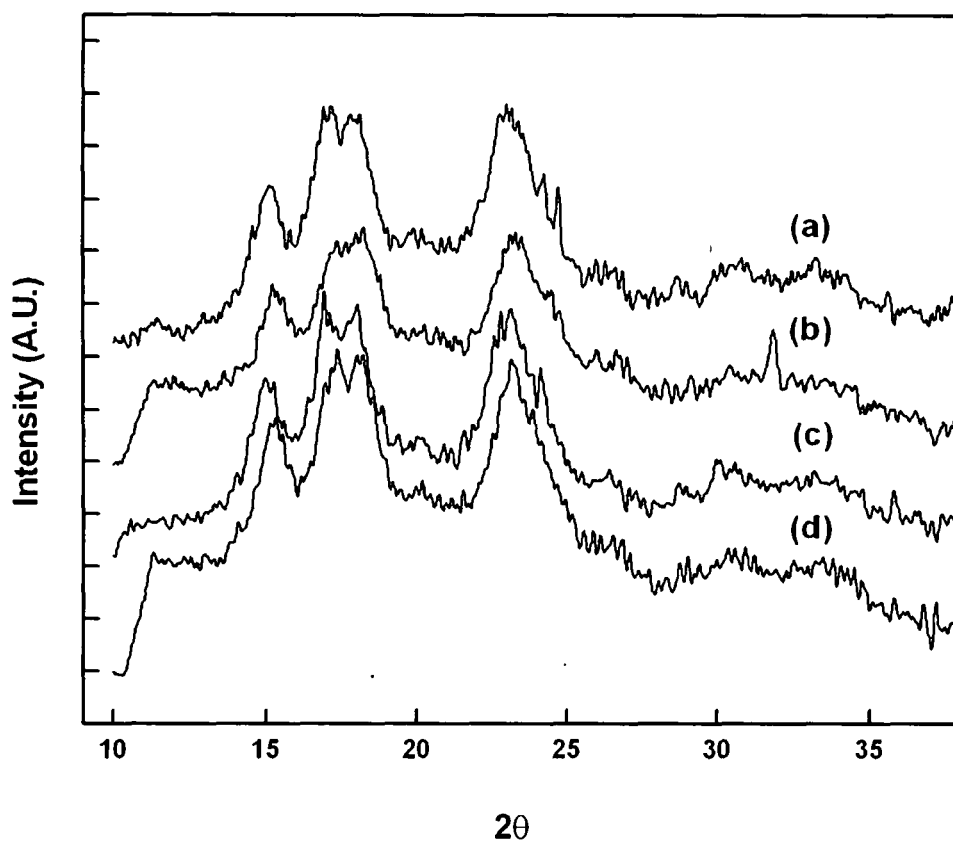


Figure 4.29. X-ray diffraction analysis of (a) *A. paeoniifolius*, (b) *C. esculenta*, (c) *X. sagittifolium* and (d) *X. caracu* purified starches

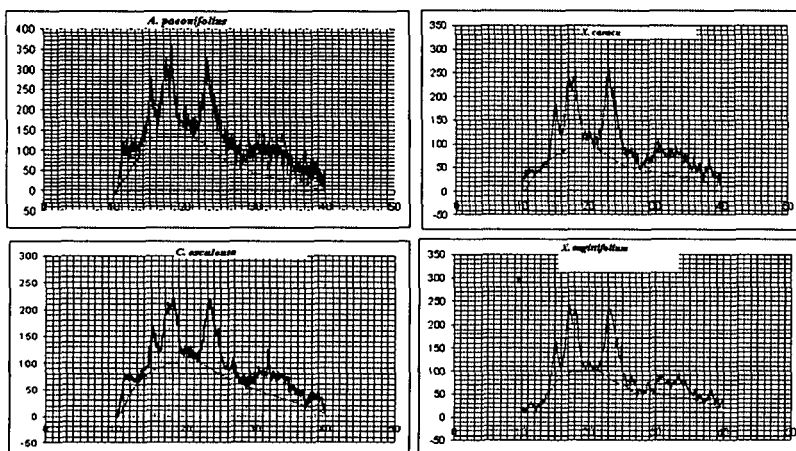


Figure 4.30. Measurement of crystallinity of the aroid starches

Table 4.14. Analysis of the XRD data

| Sl. No. | Starch from the aroid species | Lattice strain (%) | Size of the crystal (Å) |
|---------|-------------------------------|--------------------|-------------------------|
| 1 | <i>A. paeoniifolius</i> | 29.43 | 3.14 |
| 2 | <i>X. caracu</i> | 29.69 | 3.15 |
| 3 | <i>C. esculenta</i> | 23.92 | 4.12 |
| 4 | <i>X. sagittifolium</i> | 28.46 | 3.13 |

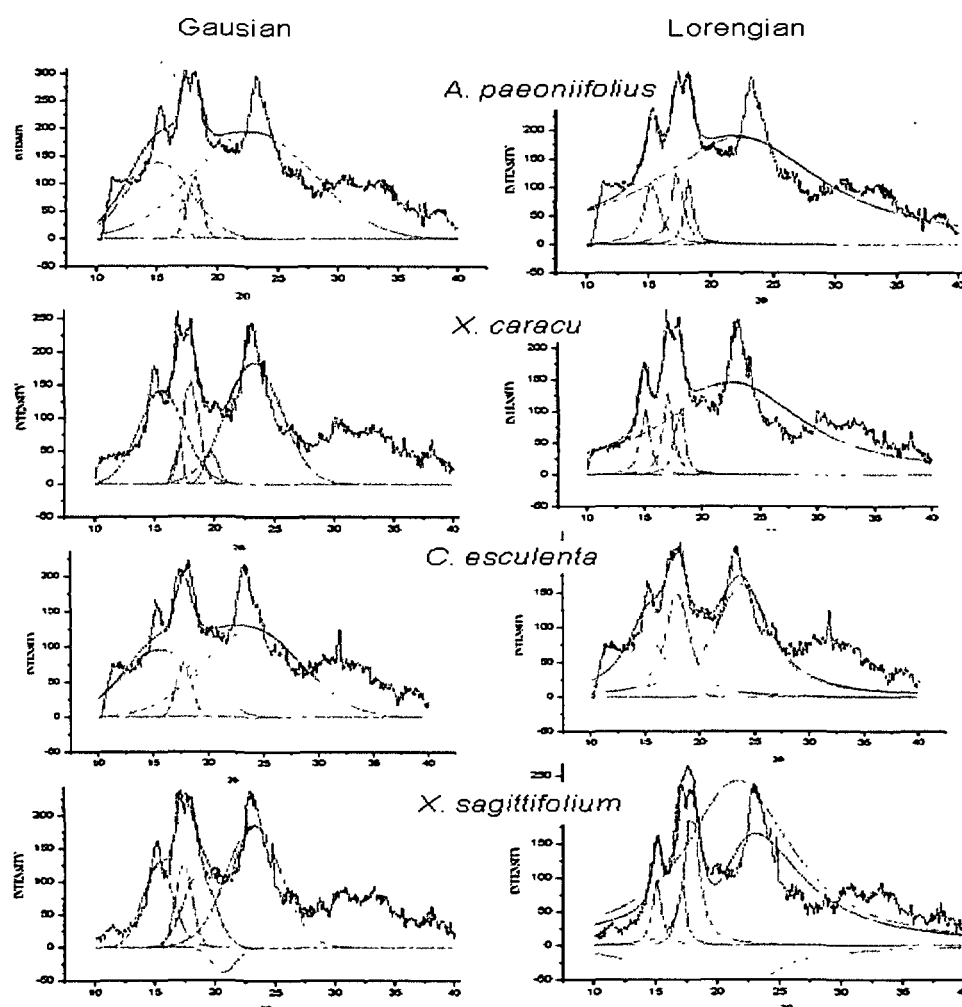


Figure 4.31. Gaussian and Lorentzian linear curve fitting on the XRD data of aroid starches for calculating crystallite sizes and strains

The FTIR analysis of the aroid starches is presented in the Figure 4.32. To verify the purity of the isolated starch, a commercial soluble starch from MERCK (India) was used as the positive control.

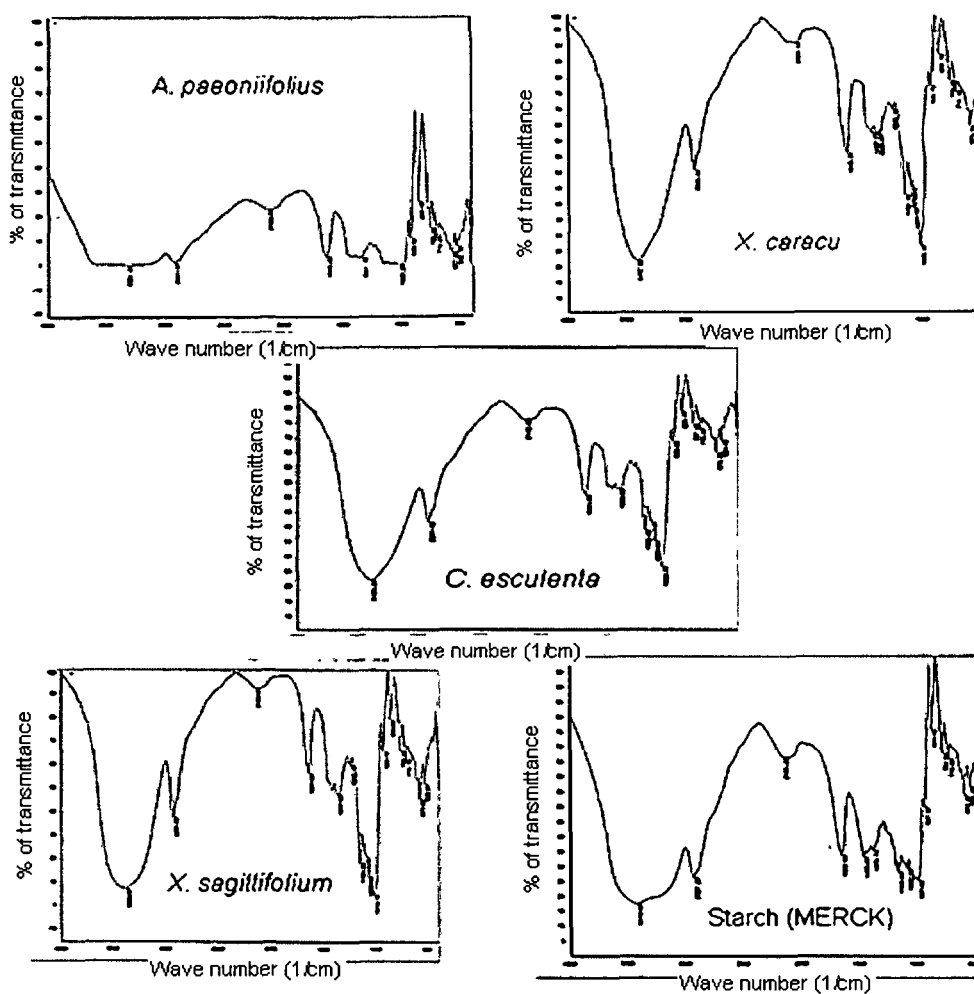


Figure 4.32. FT-IR patterns of the purified aroid starches along with commercial starch from MERCK (India) showing their purity

The results recorded for the leaching of amylose and acid hydrolysis of the starch samples are shown in Figure 4.33 and Figure 4.34, respectively. The amylose leaching of the starch isolated from all the aroid species was done at four different temperatures and the acid hydrolysis was carried out for a fortnight.

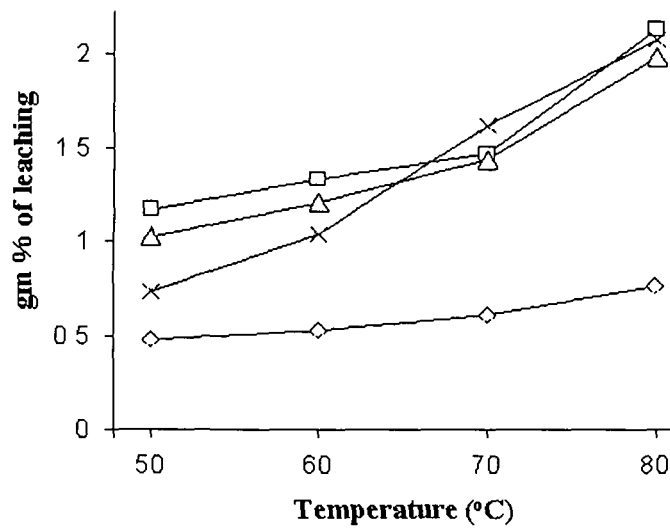


Figure 4.33. Effect of temperature on amylose leaching in aroid starches (*A. paeoniifolius* ◇, *X. sagittifolium* ×, *X. caracu* □, *C. esculenta* △). The size of the legend represent standard error

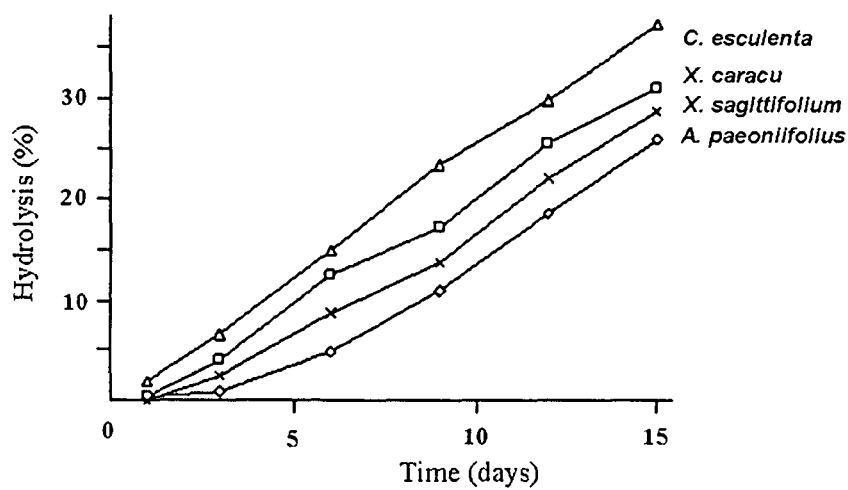


Figure 4.34. Acid hydrolysis of the aroid starches with respect to time (days). The size of the legend represent standard error

4.7. Composite preparation with the starch isolated from *C. esculenta*

Scanning electron microscopy (SEM) as presented in Figure 4.35 revealed the smallest starch granule size in *C. esculenta*. The starch could be more suitable for the industrial processing. High starch yield as presented in Table 4.2, good acid hydrolysis, high amylase content and bigger size of the

crystals of starch from *C. esculenta* make it a potent candidate for *in situ* composite preparation with polyaniline (PAni) which is a polymer and could be used for the preparation of composite due to high electrical conductivity, low density, mechanical changes due to doping-dedoping and high antioxidant potency. The composite was prepared with the objective to make a novel base material for the biomedical application.

The composition details of S1, S2 and S3 for the same are described in Table 4.15. The scanning electron micrograph (SEM) images of the composites and pristine materials are provided in Figure 4.35. The images confirmed the effective polymerization of aniline on the surface of starch granules along with the increasing concentration of polymerization which was established by the vanishing surface of the starch granules.

Table 4.15. Composition of the different Starch-polyaniline composites

| Sample code | Starch (w/v) | Aniline (M) | Oxidant (M) |
|-------------|--------------|-------------|-------------|
| S1 | 4% | 0.1 | 0.05 |
| S2 | 4% | 0.5 | 0.25 |
| S3 | 4% | 1.0 | 0.5 |

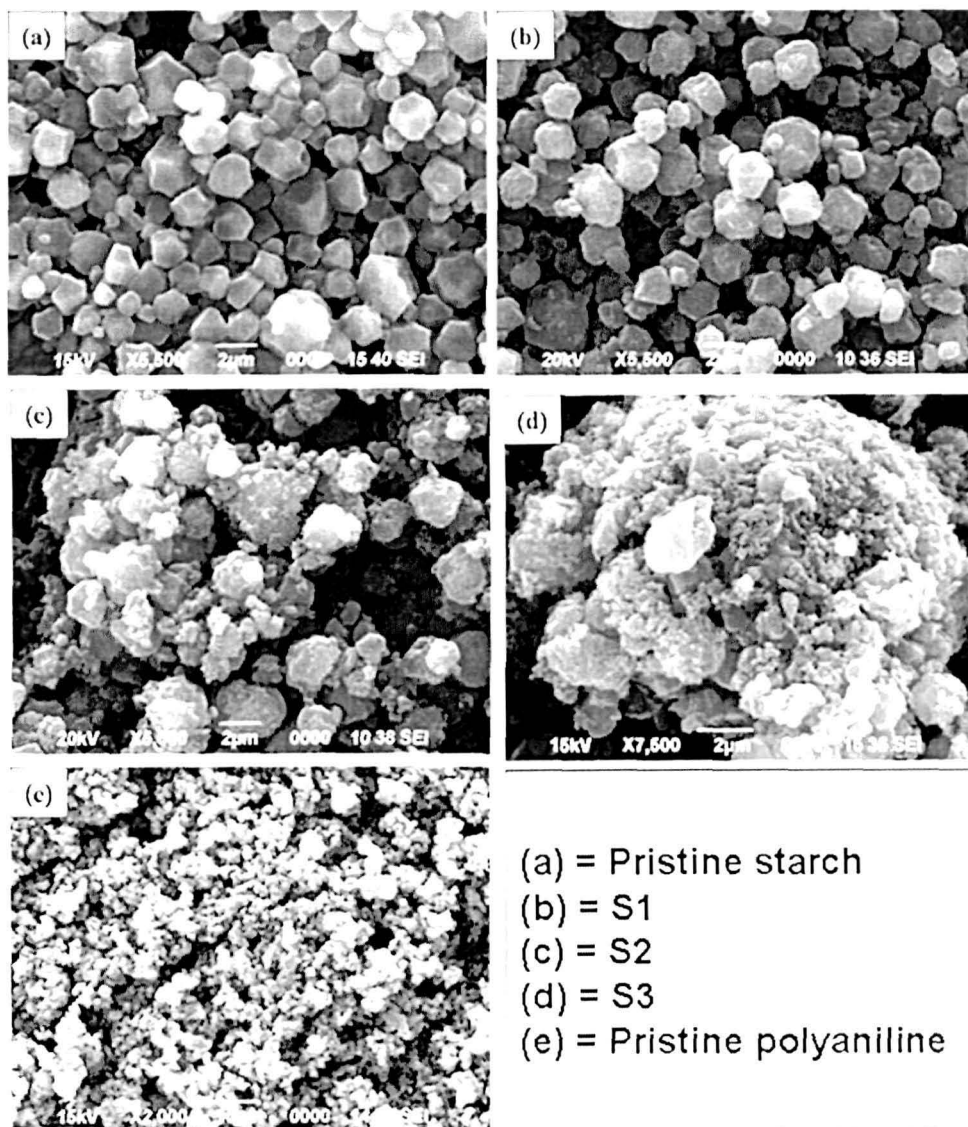


Figure 4.35. SEM of the composites and pristine polymers showing their morphology

The X-ray diffraction (XRD) patterns of the aroid starches are presented in Figure 4.36. The change in the crystallinity of the composites and the development of new characteristics is prominent from the figure.

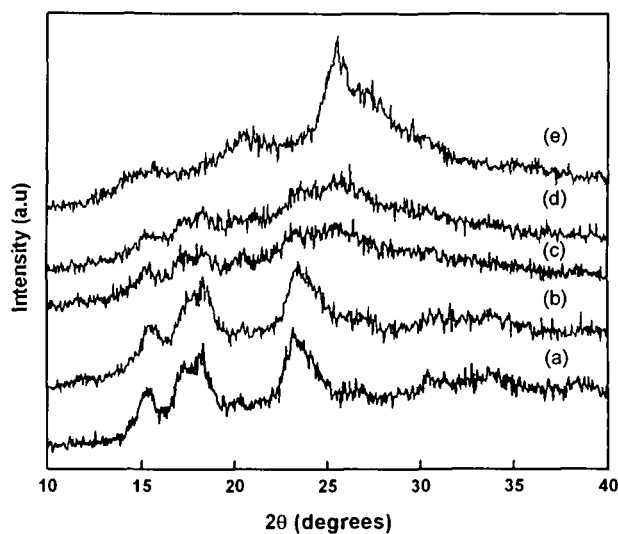


Figure 4.36. XRD pattern of (a) pure starch, (b) composite sample S1, (c) composite sample S2, (d) composite sample S3, and (e) pure polyaniline (PAni)

The FTIR spectroscopy of the composites and the pristine polymers are presented in Figure 4.37. There was the presence of new functional groups in the composites, but absent in the pristine polymers. The UV-Vis spectra of the dispersed composites and pure polymers are shown in Figure 4.38. The shift in the absorption maxima of the polyaniline in the composites could clearly be seen.

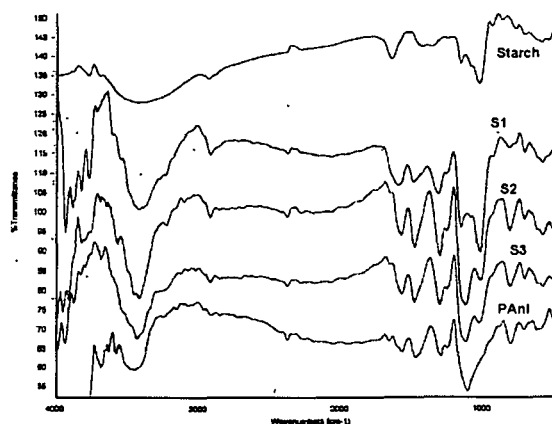


Figure 4.37. FT-IR spectra of the composites and pristine polymers (PAni=Polyaniline)

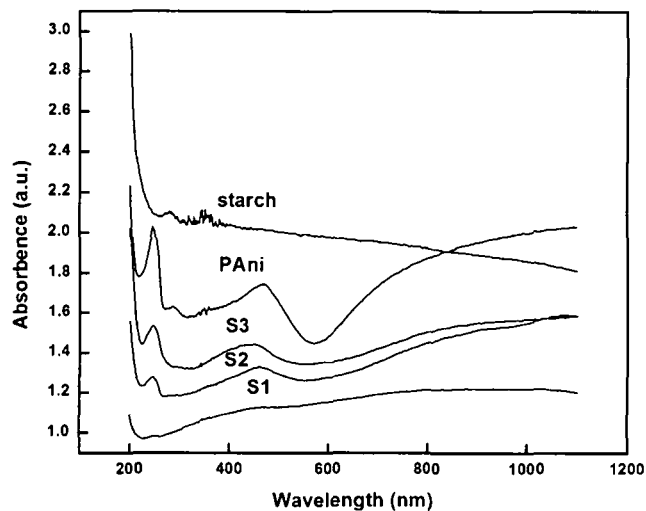


Figure 4.38. UV-Vis spectroscopy of the composites, starch and polyaniline (PANi=Polyaniline)

The DSC of the composites and pure polymers is presented in Figure 4.39. The figure depicts changes in the degradation pattern of the composites (S1, S2 and S3) as compared to the pristine polymer.

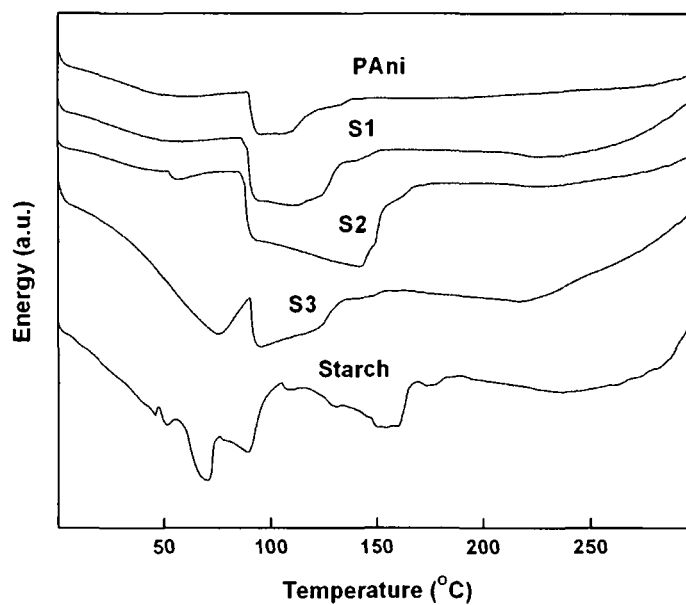


Figure 4.39. DSC of the composites with pristine polymer

The antioxidant activity of the pure polymer compounds and that of the synthesized composites are shown in Figure 4.40. A sample of 0.4 mg was applied to each of five materials. With increasing polyaniline concentration, there was an increase in the DPPH scavenging. The weight dependent antioxidant activity was performed using the composite S2 and data obtained are presented in Figure 4.41. The decrease in the peak at 517 nm due to DPPH indicated the enhancement in the antioxidant activity of the material as there was an increase in the weight of the material. The time dependent DPPH scavenging assay was performed using the composite S3 from 0-60 min and the data obtained are presented in Figure 4.42.

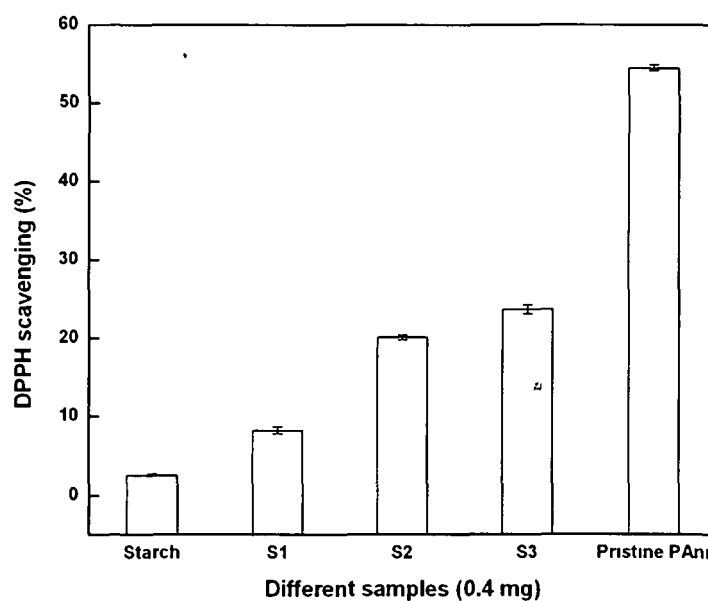


Figure 4.40. Comparative graph showing the antioxidant activity of the composite samples and pure components

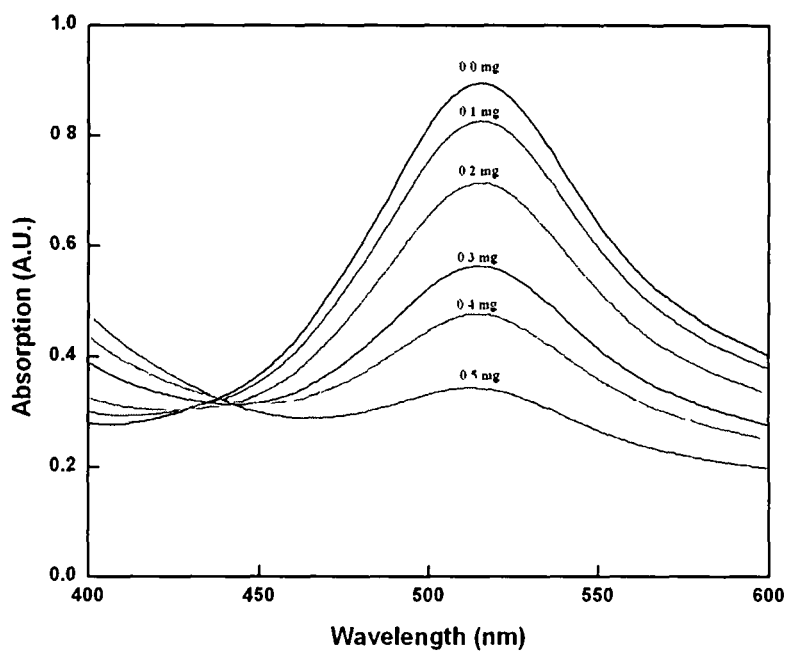


Figure 4.41. UV-Vis spectra showing the weight dependent DPPH activity of the composite sample S2 synthesized with 0.5M aniline

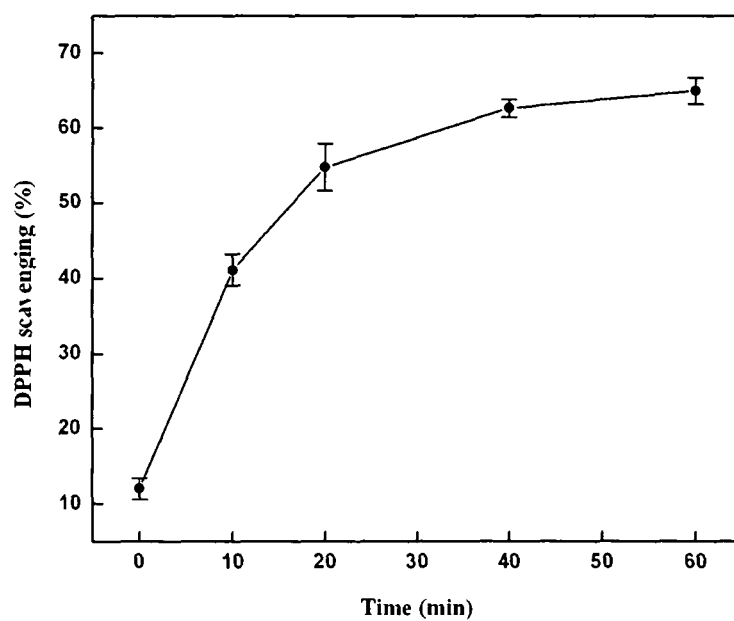


Figure 4.42. Time dependent DPPH scavenging activity of 0.4 mg of the composite sample S3 from t=0-60 min

The H_2O_2 mediated induced haemolysis prevention activity of the composites and pristine PANi is presented in Figure 4.43. The graph reveals the enhancement in the haemolysis prevention activity when the starch content was more. The assay was performed with an applied weight of 0.1-0.5 mg. The SEM of the goat RBC without any treatment, RBC treated with H_2O_2 , and RBC treated with H_2O_2 and S1 [applied weight 0.5 mg of Figure 4.43] are presented in Figure 4.44. From the figure, it could be confirmed that the composite S1 at the applied weight of 0.5 mg in 3 ml of RBC suspension in phosphate buffer saline could prevent haemolysis.

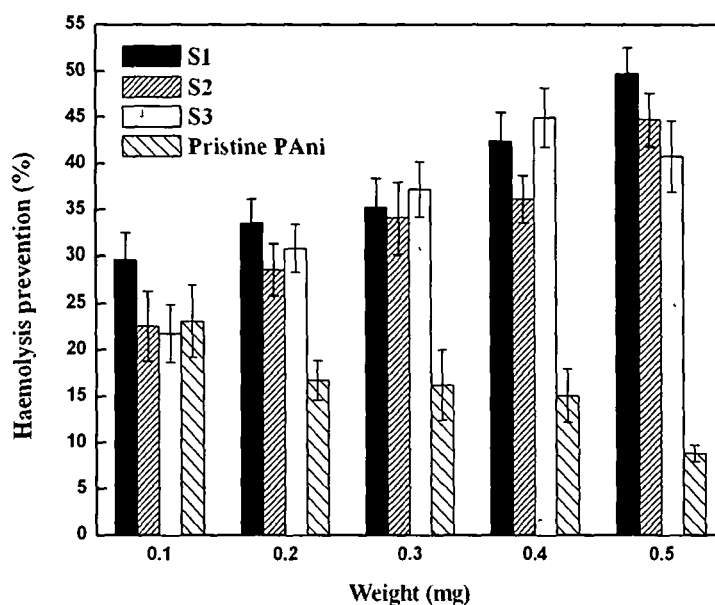


Figure 4.43. Comparative graphical representation of the haemolysis prevention activity of the different weights of the composite samples S1, S2, S3 and pure polyaniline

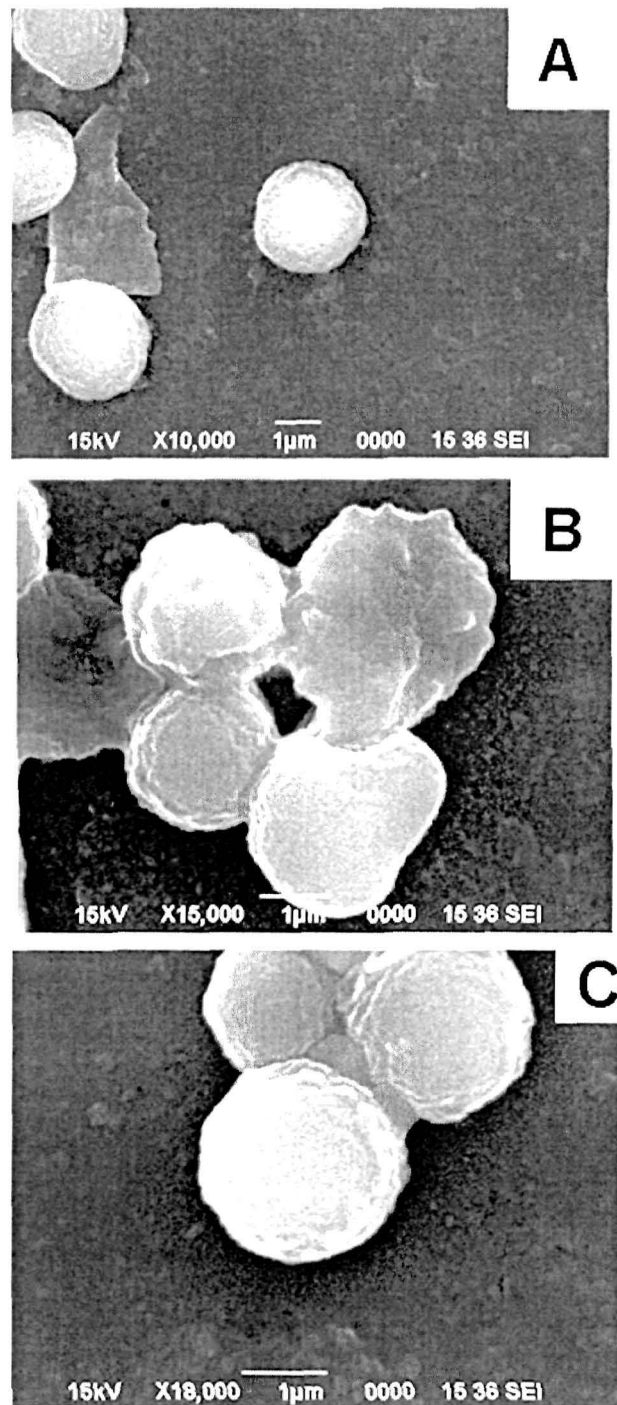


Figure 4.44. Scanning electron micrograph showing morphology of the normal RBC (A), damaged RBC due to H₂O₂ treatment (B) and (C) H₂O₂ and SI treated RBC

CHAPTER 5

DISCUSSION

5.1 Morphological study

Aroids are the most promising starch source in the tropical regions of the world. The energy entrapment done by the aroid plants was higher than that of rice and other starchy plants²²⁰. The morphology of the aroid is always confusing and most of the time the local name is taken into account to designate the cultivated varieties. This is also important for researchers dealing with starch of aroids and other root crops, as because the physico-chemical properties of starch get affected by the environmental factors like temperature, humidity, rain fall, soil type etc⁸⁹. On the basis of morphological characters (Table 4.1) and coloured photograph of the aroids (Figure 4.1 and 4.2), the stem of the species *C. esculenta* was found to be swollen. The outline of the leaf is broadly ovate, peltate, cordate, head pendate from the erect petiole, apex obtuse, basal lobe round; lateral veins prominent on the lower surface, distal side veinlet of primary lateral veins arching towards margin and forming parallel regular sieves. Petiole junction of both aroids was found to be not at the blade border. The *X. caracu* leaf showed a narrow 'V' shape depression as compared to *C. esculenta* along with a less triangular tendency. The height of *X. caracu* was also found to be lesser to *C. esculenta*. The corm of *C. esculenta* was unique in having multiple petiole origins or fusiform corms as described by Lakhanpaul *et al.*¹¹². Corm morphology of *X. caracu* was similar to *X. sagittifolium* but the lower part was tapering. *X. sagittifolium* and *X. caracu* possessed short and stout aerial stem that exude milky sap on being cut or injured. Leaf is rosulate, blade sagittate, deep green above, horizontal to slightly pendent (not vertically pendent). The petiole is connected to the leaf at the border i.e. at the bottom of the 'V' shaped depression. Two secondary veins are more prominent as compared to *Colocasia* species. The morphology of *A. paeonifolius* was quite different from the other three species; its single petiole rose up from the upper central depression of the corm. The petiole continued up to the leaf apex like other aroids but before that it trifurcated. Each trifurcation again bifurcated two-three times followed by the lamellae of leaf to give a false individual leaf appearance. Corms of all four species are the modified stem that stores starch.

They also act as organs of regeneration to tide over the unfavorable conditions. The morphology of *Xanthosoma* species was described by Castro *et al.*²²¹. They described the growth conditions of *X. violaceum*, height at maturity being 62.9-111.4 cm was found to be shorter than *X. caracu* (80.25 - 135.60 cm) and *X. sagittifolium* (84.43 - 116.60 cm). In the present study, plants of *Xanthosoma* species were found to be bigger. This could be due to the growing conditions as mentioned by soil type, availability of sunlight etc. The number of petiole or leaves in *X. violaceum* was reported to be 3.6-5.1 which was found to be 3.4-4.1 in the present *Xanthosoma* species. The leaf surface area of *X. violaceum* was found to be higher (674-1479 cm²) as compared to the observed value of 1213.1 - 1533.63 cm² in *X. caracu* and 956.23- 1936.75 cm² in *X. sagittifolium* (Table 4.1). The variation in leaf area of *X. violaceum* could be ascribed to the different strains as studied by Castro *et al.*²²¹. Boyce *et al.*²²² described the morphological features of *Araceae* with generic keys. Their description for the genus *Amorphophallus* matched with the observed results for the present study with special reference to conspicuous and snake-skin like markings of petiole and leaf lamina.

5.2 Biochemical characterization

The moisture content of the aroid corms were found to be in the order of *A. paeonifolius* > *X. caracu* > *X. sagittifolium* > *C. esculenta* (Table 4.2). In general, the moisture content was found to be higher as compared to reports by earlier authors. This could be attributable to the geographical location. High moisture content is a problem in post harvest storage of corms. The ash content was in the order of *X. sagittifolium* > *C. esculenta* > *A. paeonifolius* > *X. caracu*. The crude protein content was in the order of *C. esculenta* > *A. paeonifolius* > *X. sagittifolium* > *X. caracu* where as the crude lipid content *C. esculenta* > *A. paeonifolius* > *X. sagittifolium* > *X. caracu*; starch content *C. esculenta* > *X. caracu* > *X. sagittifolium* > *A. paeonifolius*; crude fiber content *X. caracu* > *A. paeonifolius* > *X. sagittifolium* > *C. esculenta*; and soluble sugar content *C. esculenta* > *X. sagittifolium* > *X. caracu* > *A. paeonifolius*. The species *C.*

esculenta was found to be promising. The starch and protein content of the aroid corms ranged from 11-20% and 1-3%, respectively. In the case of corms assayed, *Amorphophallus* species was found to contain lesser than the average starch and protein. The granule size of *C. esculenta* starch was observed to be smaller as compared to earlier reports indicating more suitability of its starch for the various nutritional applications²²³. Maximum variation in the starch granule size was observed in the case of *Xanthosoma* species as reported by several workers. As compared to other species, the starch was spherical in the case of *C. esculenta*.

In *A. paeoniifolius* moisture content was $81.64 \pm 3.49\%$, Na 33.91 ± 0.18 mg/100 gm (dry wt), K 40.91 ± 1.69 mg/100gm (dry wt), Ca 3.76 ± 0.17 mg/100 gm and the largest starch granule size of 4.86 - 7.20 μm . The highest content of ash was estimated in *X. sagittifolium* ($3.91 \pm 0.16\%$) and crude fiber ($1.98 \pm 0.05\%$) in *X. caracu*. In the case of *C. esculenta* contents of crude protein $2.89 \pm 0.04\%$, crude lipid $1.24 \pm 0.03\%$, starch content $14.81 \pm 0.60\%$, soluble sugar $1.80 \pm 0.06\%$, net energy 103.25 cal/100 gm (fresh weight) and Mg 1.44 ± 0.07 mg/100gm (dry weight) were the highest. The moisture content of *X. sagittifolium* corm was found to be $80.36 \pm 3.26\%$ against the earlier report of $69.81 \pm 0.11\%$ ²²⁴. There was variation in the other biochemical compositions of *X. sagittifolium*, the crude protein content also varied to $1.261 \pm 0.10\%$ against the reported value of $2.83 \pm 0.30\%$. The moisture content of the apical part of *X. sagittifolium* was reported to be 77.4% which was also found to be lower as compared to the moisture content estimated in the present study²²⁵. The high moisture content of the corm might be due to the environmental effects like growth condition, soil type, rainfall etc. The protein, lipid, ash and starch content of *X. sagittifolium* corms were also found to be lower as compared to the earlier reports⁸. The moisture content of *C. esculenta* was also found to be lower; where as the average crude lipid content of the species was higher $1.24 \pm 0.03\%$. The ash content of *C. esculenta* ($2.86 \pm 0.08\%$) was comparable to the reported value of 1.88% ²²⁵. The mineral content of *C. esculenta* and *X. sagittifolium* including K was found to be low, where as Na comparable. Huang

*et al.*²²⁶ reported moisture content of *C. esculenta* to be 63.6-72.4% as compared to the present value of $77.25 \pm 3.42\%$. The starch content was found to be $14.81 \pm 0.60\%$ against the reported value of 21.1-26.1%.

5.3 Karyotyping

The active cell division of *C. esculenta* was half an hour earlier to the other aroids. The maximum number of metaphase cells was observed for all four aroids during their maximum active cell division period (Figure 4.3). The number of chromosomes observed in the aroid species was $2n=28$ in *A. paeoniifolius* and *C. esculenta* whereas in *X. caracu* and *X. sagittifolium* $2n=26$. Parvin *et al.*²²⁷ described karyotype of seven varieties of *Colocasia esculenta* from Bangladesh. The somatic chromosome complement as arranged in the present study showed the basic number to be $x=7$, which was also supported by Parvin *et al.*²²⁷. It suggested that *C. esculenta* is a tetraploid ($2n=28$). In *A. paeoniifolius* the arrangement suggests that the species is diploid ($2n=28$) with basic chromosome number $x=14$ and is also supported by the earlier report of Chauhan and Brandham¹¹⁴. The basic chromosome number of *X. caracu* and *X. sagittifolium* was found to be $x=13$ and the same ($x=n=13$, $2n=26$) was also reported by Marchant¹²⁴.

5.4 Molecular biological study

Gel electrophoresis data of genomic DNA (Table 4.4 and Figure 4.5) of all four aroid species established the yield of quality DNA²⁰⁶. The yield of DNA of all four aroids was in the order of *X. sagittifolium* > *A. paeonifolius* > *C. esculenta* > *X. caracu*. The species *X. sagittifolium* showed the highest yield of quality DNA.

The genome size of the aroids was in the order of *C. esculenta* > *X. caracu* > *X. sagittifolium* > *A. paeoniifolius* (Table 4.5). The genome size of the species *C. esculenta* was found to be 14.1 pg and it would be between 2C-3C value as given by Bennett and Leitch²²⁸ for *C. antiquorum*. They also reported 1C value of *X. sagittifolium* to be 8.8 pg, which is 0.76 pg higher than that of

the present investigation (Table 4.5). Genome size of *A. paeoniifolius* (5.04 pg) recorded in the present investigation was higher as compared to the earlier report of 4.2 pg²²⁸. There are very few reports on the genome sizes of *Xanthosoma* species.

The primer OPW-15 possessed sequence complementation *C. esculenta* (Figure 4.7) genome, but absence of complementation of the primers OPW-15 and OPW-16 sequences with that of *A. paeoniifolius*. Amplification of genomic DNA using six primers yielded 25 reproducible RAPD loci for an average of 4.16 bands per primer; 21 (84%) of them were polymorphic and 4 (16%) were monomorphic. Among *Xanthosoma* species only four bands (16%) were polymorphic with the rest of polymorphism existing between *Colocasia* and *Amorphophallus* species (Figure 4.7, Table 4.6).

The primers were selected on the basis of their polymorphism in Indian *Colocasia* cultivars¹¹². The results showed that both *Xanthosoma* species are closely related to each other (66%) as compared to their similarity to others (Table 4.7). *Amorphophallus* species was found to be 50% similar to both *X. caracu* and *C. esculenta* but dissimilar to *X. sagittifolium*. Hence, it could be concluded that *X. caracu* and *C. esculenta* species are equally distant from *A. paeoniifolius* species. *C. esculenta* used in the study might be the same morphotype M-5 having ID no. TC5 used for RAPD analysis by Lakhanpaul *et al.*¹¹². The relation between the species was properly understood from the dendrogram prepared by feeding the data generated from the RAPD (Figure 4.8). In the dendrogram *X. caracu* and *X. sagittifolium* were found to be closer (100%) as compared to completely separate species of *C. esculenta*. *A. paeoniifolius* related to two *Xanthosoma* species by 64%.

In the study, an effort was made to estimate the genetic similarity and dissimilarity among the edible aroid species at the molecular level. The primers (OPW-04, OPW-05, OPW-08, OPW-10, OPW-15 and OPW-16) in the investigation were extensively used to characterize *C. esculenta*. The primers used provided reliable polymorphism in *A. paeoniifolius*. Primers selected for the study showed 88.9-100.0% polymorphism in the case of Indian *C. esculenta*

morphotypes, which was also reported by Lakhanpaul *et al.*¹¹². The genome diversity analyses of aroids with a limited number of genotypes were not enough to prepare a dendrogram. A number of morphotypes with more primers would be needed for the same.

The genome size of the edible species was determined using a comparatively easy and established method than prevalent expensive methods like fuelgen densitometry and flow cytometry. At present, flow cytometry is becoming a popular method in the determination of genome size. The method needs the establishment of the sophisticated costly equipment, flow cytometer. The cost is indeed prohibitive for most of the organizations and the handling of the equipment needs the expert manpower. On the other hand, discrepancies are observed in flow cytometry data of a single sample analysed in different laboratories. Hence, an effort was made by Konwar *et al.*¹³¹ to develop a novel but simple and less expensive method for the determination of genome size of plants without compromising the quality. With the collection of suitable tender leaves from the raised corms of the selected edible aroids, quality genomic DNA was isolated¹³¹. The protocol could yield quality DNA as evident from the UV-Vis spectrophotometric absorbance ratio at 260:280 nm being 1.735-1.916 (Table 4.7). Two critical points were taken into account in this method; firstly, the method for the isolation of genomic DNA was such that it could isolate almost all the DNA from the nuclei, and secondly the accurate determination of the intercellular space in the aroid species. The developing countries on one hand have vast resources of plant biodiversity while on the other hand face the problem of acquisition and maintenance of Flowcytometers²²⁹. Hence, the present method could be of great help for the researchers of developing countries having limited access to the facilities like Flowcytometer.

5.5 Compound purification

5.5.1 Total polyphenol content

The total polyphenol content (TPC) extracted from the aroid corms was estimated and data obtained are presented in Figure 4.9. The solvents were

100% and 80% MeOH and water. The TPC of aroids were in the order of *A. paeoniifolius* (0.303 ± 0.02 mg/100 g) > *C. esculenta* (0.21 ± 0.03 mg/100 g) > *X. caracu* (0.16 ± 0.06 mg/100 g dry corm) > *X. sagittifolium* (0.11 ± 0.02 mg/100 g) for gallic acid equivalent (in 80% MeOH extract); *A. paeoniifolius* (0.203 ± 0.04 mg BHT and 1.373 ± 0.12 mg tannic acid/100 gm dry corm) > *X. sagittifolium* (0.14 ± 0.08 mg and 0.59 ± 0.05 mg) > *C. esculenta* (0.14 ± 0.02 mg and 0.51 ± 0.08 mg) > *X. caracu* (0.10 ± 0.04 mg and 0.16 ± 0.06 mg) for BHT and tannic acid equivalent (in 80% MeOH extract); *A. paeoniifolius* (1.896 ± 0.10 mg/100 gm dry corm) > *X. caracu* (0.86 ± 0.05 mg/100 gm) > *X. sagittifolium* (0.82 ± 0.04 mg/100 gm) > *C. esculenta* (0.70 ± 0.07 mg/100 gm) for quercetin dihydrate equivalent (in 80% methanol extract). In the absolute methanol extract, gallic acid and BHT possessed the same trend like quercetin equivalent in 80% methanol extract; tannic acid and quercetin dihydrate equivalent in the absolute methanol extract were not detected. In the water extract, the total polyphenol equivalent was in the order of *A. paeoniifolius* > *X. caracu* > *X. sagittifolium* > *C. esculenta* for all four standards.

5.5.2 Total flavonoid estimation

In view of the significant polyphenol content in water and 80% methanol extracts (Figure 4.10), the absolute methanol extract was not considered for the total flavonoid estimation. The flavonoid content (quercetin equivalent) followed the order *A. paeoniifolius* (62.26 ± 3.51 mg/100gm dry corm) > *X. caracu* (9.65 ± 1.64 mg/100gm) > *X. sagittifolium* (5.89 ± 0.86 mg/100gm) > *C. esculenta* (not detected) in 80% methanol extract and *A. paeoniifolius* (178.71 ± 12.22 mg/100 gm) > *C. esculenta* (142.39 ± 11.94 mg/100 gm) > *X. caracu* (93.54 ± 7.85 mg/100 gm) > *X. sagittifolium* (86.02 ± 5.55 mg/100 gm) in the water extract. The flavonoid content in the water extract was significantly higher as compared to 80% methanol. Both solvent extracts were used for the blood clotting experiment.

5.5.3 The antioxidant capacity

The corm extracts were used for assaying antioxidants. The order of the antioxidant capacity was *X. caracu* > *A. paeonifolius* > *X. sagittifolium* > *C. esculenta* in the case of 80% methanol extract and *A. paeonifolius* > *X. caracu* > *C. esculenta* > *X. sagittifolium* in the case of water extract. The water extract of *C. esculenta* and *X. sagittifolium* were similar in their antioxidant activity (Figure 4.12).

5.5.4 Blood clotting

With the exception of *C. esculenta* in 80% methanol, other corm extracts were found to enhance the process of blood clotting, whereas, water extract of all aroid corms were found to be blood clotting inhibitor (Figure 4.13).

The total polyphenolic content (0.44 ± 0.09 mg galic acid equivalent/100 gm dry weight) and flavonoid content (178.71 ± 12.22 mg quercetin equivalent/100 gm dry weight) of water extract of *A. paeoniifolius* were recorded to be the highest. Blood coagulation enhancing property was the highest in *X. sagittifolium* 80% methanolic extract (18.1 sec.). The DPPH scavenging property was the highest in *X. caracu* ($19.00 \pm 1.54\%$). Non-detection of flavonoid content in 80% methanol extract of *C. esculenta* could be attributed to the high response of quercetine dihydrate to the estimation method and the occurrence below the detection level of flavonoid in the aroid.

Flavonoids are the molecules which are not only known for their antioxidant activity, but also provide health benefits against cancer and heart diseases. Blood clotting was tested to investigate the scientific ground for the traditional practice of applying aroid sap in wounds as done by the people of the North Eastern India. The positive results with 80% methanol extracts of *Amorphophallus* and *Xanthosoma* species opened the prospect for further study of activity *in vivo*. On the other hand, the tribal people use water for grinding corms to prepare the extract for applying to wounds. This suggests that there is a need to study their preparation process carefully as well as *in vivo* study for evaluating the exact wound healing property.

The polyphenol content in water extract followed the pattern of the antioxidant activity as described above (Figure 4.9 and 4.12). The water extract of four edible corms though showed the presence of maximum polyphenols and flavonoids, but possessed poor activity, except for *A. paeoniifolius*. In the case of *X. caracu*, 80% methanol extract showed $19.00 \pm 1.54\%$ scavenging of DPPH-stable free radical which was maximum among the corms and types of extracts with 1,479.48 mg in every 100 gm dry corm powder, as calculated from the standard curve of antioxidant activity of quercetine dihydrate. The observed antioxidant activity of the extracts might be due to the neutralization of free radical character of DPPH²³⁰.

5.5.5 Antimicrobial activity

5.5.5.1 Antibacterial activity

All extracts were used for the determination of the antibacterial activity against *E. coli* and *S. aureus*. In the case of extracts loaded with 80% methanolic extract showed small zones for both bacteria. The other two types of extracts i.e. water and methanol only extracts did not show any activity against these two tested bacteria (Figure 4.14).

5.5.5.2 Antifungal activity

Eighty percent methanolic extract and water extracts were used to test antifungal activity against *F. oxysporium* and *C. albicans*. The *X. sagittifolium* 80% methanol, water only extract showed activity against both the tested fungi. The water only extract of *C. esculenta* was found to be positive against both the tested fungi. *A. paeoniifolius* water only extract was found to be positive against both the tested fungi. All other extracts were found to be negative against the tested fungi (Figure 4.15).

5.5.6 Thin layer chromatography (TLC)

On the basis of high polyphenolic content of 80% methanol extract in water and its positive results in antibacterial and antifungal study, it was

concluded that the polyphenolic compounds might be responsible for the antimicrobial activity. Taking this into account the polyphenolic compounds were accessed in 80% methanolic extract; and as such the other two extracts were discarded. TLC of 80% methanol-water extract was done to separate the phenols (Figure 4.16).

5.5.7 Column chromatography

Column chromatography was done using the same solvent as used for developing TLC with a hope of partial purification of the crude extract. The fractions were profiled with respect to their polyphenol content. The highest polyphenol containing fractions were collected for further purification using HPLC (Figure 4.17). For *A. paeoniifolius*, fractions 9 (AC-I) and 31 (AC-II); *X. caracu*, fractions 10 (BC-I) and 31 (BC-II); *C. esculenta* fractions 15 (CC-I) and 29 (CC-II); and for *X. sagittifolium* fraction 19 (XC-I) were taken for further purification as they were found to contain the highest polyphenolic content.

5.5.8 High Performance Liquid Chromatography (HPLC)

The peak generated from HPLC purification was presented in Table 4.8. The HPLC profile of the AC-I (Figure 4.18) fraction showed 2 prominent peaks which were collected by repetitive injection and evaporated to dryness. The collected peaks were labelled as AC-I (1) and AC-I (2). From AC-II fraction also two prominent peaks were collected and labeled as AC-II (1) and AC-II (2). Similarly, from *X. caracu* the collected fractions were labelled as BC-I (1), BC-I (2) and BC-I (3); BC-II (1) and BC-II (2). *C. esculenta* fractions collected from HPLC were labeled as CC-I (1), CC-I (2), CC-I (3) and CC-I (4); CC-II (1), CC-II (2), CC-II (3), CC-II (4) and CC-II (5). The single peak collected from the single fraction of *X. sagittifolium* was labeled as XC-I (1).

Some of the above mentioned HPLC fractions were not collected as the amounts were not sufficient to trace, as such was not possible to proceed for further analysis. These fractions were AC-I (2), AC-II (2) and CC-II (5). The

other fractions were subjected to antimicrobial study, FT-IR and NMR (H^1 and C^{13}).

5.5.9 Fourier transform Infrared spectroscopy (FTIR)

The results obtain from FT-IR peak analysis was presented in Table 4.9. All fractionated compounds contained at least a benzene ring which was confirmed by the FTIR spectral pattern (Figure 4.20 and 4.21). The broad peaks left to $3,000\text{ cm}^{-1}$ might be attributed to the stretching vibration of the bonds between an aromatic ring and H atom. The peaks ranged from $1,400\text{-}1,500\text{ cm}^{-1}$ and $1,585\text{-}1,600\text{ cm}^{-1}$ might be ascribed to the C=C stretching of an aromatic ring. The peaks between $660\text{-}1,000\text{ cm}^{-1}$ might be due to the loop bending of R=C-H of an aromatic ring.

The peaks between $3,231\text{-}3,657\text{ cm}^{-1}$ of AC-I (1) and XC-I (1) might be due to the O-H bond stretching of -COOH group associated with the aromatic ring. The peaks might get broaden due to superimposition with the C-H stretching peaks of aromatic ring. The strong peak $1,673\text{ cm}^{-1}$ of the compounds might be due to the C=O stretching of -COOH group. The broadening near the base of the peak at $1,294\text{ cm}^{-1}$ might be due to stretching vibration of C-O of COOH group. The pattern of the aromatic C-H loop bending peaks near 693 cm^{-1} (lower intensity) and 761 cm^{-1} (higher intensity) might be due to the presence of mono-substituted benzene. From these observations it could be concluded that the above mentioned compound might be benzoic acid. Further confirmation was carried out with the use of NMR analysis.

In compounds AC-II (1), BC-I (1), BC-II (1), CC-I (2) and CC-II (2) the presence of COOH group was evident. The peaks near $696, 808$ and 896 cm^{-1} might be ascribed to the presence of meta-disubstituted benzene. A minute peak between the above mentioned peaks near 850 cm^{-1} might be due to para-disubstituted benzene. A small bulging due to merge with the base of the peak near 808 or the prominent peak at 774 [in BC-II (1)] might be due to the ortho-disubstituted benzene. The sharp peaks near $3,422\text{ cm}^{-1}$ might be due to the O-H stretch of -OH group. The strong peak near $1,213\text{ cm}^{-1}$ might be due to the C-O

stretch of OH group associated with a benzene ring. It was concluded that the structure could be a benzene ring substituted with three different functional groups in three different positions. These three functional groups are –OH and –COOH. One of them substituted the ring in two places²³¹. The compounds might be caffeic acid²³². Further analysis would be required for confirmation of the structure.

A similar trend of FT-IR spectra was observed for CC-II (4), BC-I (2) and CC-I (4), except the substitution pattern being prominent for a meta-di-substitution only. One of the groups was found to be OH and the other COOH. The structural elucidation would need further analysis.

The spectrum of BC-I (3) was almost similar with caffeic acid but there is a narrow and intensive band at 3430 cm^{-1} referring to the spectrum of ferulic acid²³².

The FT-IR spectra of BC-II (2), CC-II (3) and CC-I (3) were found to be similar with the data provided by Surowiec *et al.*²³³. The comparison suggested that the compound might be syringic acid. The band at 1462 cm^{-1} was assigned to CH stretching of methyl or methylene groups²³⁴.

5.5.10 Nuclear magnetic resonance

As seen in Table 4.10 and Figure 4.22, it could be observed that all the isolated compounds could be grouped in to five different compounds. These results also coincide with the results obtained from the FT-IR analysis of 14 different fractions. Five different compounds identified with the help of FT-IR and NMR spectra were benzoic acid, caffeic acid, coumaric acid, ferulic acid and syringic acid (Table 4.10).

5.6 Antimicrobial study

As documented in Figure 4.23, 4.24, 4.25 and 4.26 and Table 4.11, it could be seen that the compounds were not effective against the selected fungus species but most of them were well effective against bacterial species selected for the present study. The activity of AC-I (1) and XC-I (1) was found to be the

highest against *E. coli*; and BC-I (2), CC-I (4) and CC-II (4) against *S. aureus*. So, it could be deduced that the antimicrobial activity of 3,4-dihydroxy benzoic acid (as concluded from structure elucidation) was the highest against *E. coli*; and coumaric acid (trans-in-hydroxycinnamic acid) against *S. aureus*. In the overall depiction it was found that *S. aureus* (gram positive bacteria) was more sensitive to the isolated compounds as compared to *E. coli* (gram negative).

5.7 Compound identified

The polyphenolic compounds were purified with reference to the background that antimicrobial property might be due to their presence in the composition and was found to be true. Similar observations were reported by Agbor-Egbe and Rickard⁷⁴ in aroid corms. Along with the antimicrobial property, 3,4-dihydroxybenzoic acid (protocatechuic acid) was reported to have mixed effects on normal and cancerous cells in *in vitro* and *in vivo* studies²³⁵. Protocatechuic acid has been reported to induce apoptosis of human leukemia cells, as well as malignant HSG-1 cells taken from human oral cavities²³⁶. Protocatechuic acid was found to have mixed effects on 12-O-tetradecanoylphorbol-13-acetate (TPA) induced mouse skin tumours. Depending on the amount of protocatechuic acid and the time before the application, it could reduce or enhance tumor growth²³⁷. The antibacterial activity of protocatechuic acid extracted from the coffee plant was reported by Almeida *et al.*²³⁸. The antibacterial effect of protocatechuic acid isolated from *Alchornea cordifolia* leaf was reported to be positive against *E. coli* by Lamikanra *et al.*²³⁹. Similar activity was reported in the case of wines and many other sources^{240, 241, 242}. Many antibacterial and antioxidant activities of polyphenol compounds were reported by several other workers^{243, 244}.

5.8 Antioxidant activity of the pure compounds

The antioxidant activity of the pure compounds was tested using induced haemolysis by hydrogen peroxide (Figure 4.27). The haemolysis prevention was

found to be the highest in the caffeic acid and the lowest in the case of coumaric acid. The order of haemolysis was found to be coumaric acid>protocatechuic acid>syringic acid>ferulic acid>caffeic acid. The order of haemolysis prevention was found to be caffeic acid>ferulic acid>syringic acid>coumaric acid>protocatechuic acid. Out of the caffeic acids, CC-I (2) was found to have the highest haemolysis prevention, as well as to be responsible for the highest haemolysis among the group.

5.9 Starch isolation and physicochemical characterization

The starch granule size of *A. paeonifolius* (5-12 μm) (Table 4.12) was smaller as against the report of Hoover⁸⁸ (3-30 μm). Similarly, amylose content in *C. esculenta* $22.4 \pm 4.5\%$ was higher than 21.4% reported by Hoover⁸⁸; but, both values were lower than those reported ($30.62 \pm 0.16\%$)²⁴⁵. The total lipid content of *C. esculenta* was reported to be 0.39% against the previously reported value of 0.09 ± 0.02 (Table 4.12). The moisture content of the starch of *C. esculenta* and *X. sagittifolium* was 11.2 ± 0.74 and $12.2 \pm 1.2\%$ (Table 4.12) against the earlier reported value of 14.01 ± 0.05 and $13.43 \pm 0.01\%$, respectively²⁴⁵. The ash content of *C. esculenta* and *X. sagittifolium* starch were 1.3 ± 0.6 and $1.2 \pm 0.8\%$ against the earlier reports of 0.31 ± 0.01 and $0.20 \pm 0.04\%$, respectively²⁴⁵.

5.9.1 Starch granule morphology

In protein-starch separation, small starch granules are entrapped in the protein and the fine fiber sediments generated during centrifugation¹⁵⁶. These problems were encountered in the case of *C. esculenta* and *X. caracu*. After the centrifugation, a dark brown layer was observed on top of the white starch. The upper layer was scraped off, but it caused loss of some small granules²⁴⁶. In *X. sagittifolium* the size of starch granules ranged from 2.1-2.84 μm which are similar to the size of 2.0–12.5 μm reported by Perez *et al.*²⁴⁵. In the case of *C. esculenta*, the granule size of 0.5–5.0 μm as reported by Perez *et al.*²⁴⁵ was much bigger to 0.71-1.25 μm , observed in the present investigation²⁴⁵.

5.9.2 X-ray Pattern and Crystallinity of Starch Granules

Starch is broadly divided into two types A and B; both are based on parallel standard double helices. A-type starch helices are more closely packed and they could be determined by X-ray diffraction studies. A-type starch (mostly cereals) exhibits reflection at 15.3, 17.0, 18.0, 20.0 and 23.4° 2θ angles. They also differ (B>A) in the content of intra-helical water²⁴⁷. The double helices of A and B-type starches are packed in a pseudo hexagonal array. The lattice associated with B type starch has a large void (channel) which could accommodate 36 water molecules. However, in A-type starch, the lattice contains a helix in the center rather than a column of water. In both A and B-type starches, there is a spacing of double helix that corresponds to 1.10 nm distance between the axes of the two double helices²¹¹. All four aroid species exhibited A-type starch pattern except an extra peak at 31.9° (2θ) in the case of *C. esculenta* (Figure 4.29). The crystallinity of starch granules was found in the order of *A. paeonifolius*>*X. caracu*>*X. sagittifolium*> *C. esculenta* (Figure 4.30). The size of crystal and the strain of polymer chain of starches were found to be in the order of *X. caracu*>*A. paeoniifolius*>*X. sagittifolium*>*C. esculenta* (Table 4.14) and lattice strain refers to the slight, atomic-level displacement in the structure of a material (Figure 4.31).

5.9.3 Detection of functional groups using FT-IR Spectroscopy

The wide band observed at 3,331.91 cm⁻¹ could be attributed to O-H bond stretching of the starch and its width ascribed to the formation of inter and intra-molecular hydrogen bonds which were observed maximum in *A. paeonifolius*. Similar observation was reported by Dragunski and Pawlicka²⁴⁸. The characteristic peak between 1,019 and 1,156 cm⁻¹ attributed to C–O stretch in C-O-C bonding and the peaks near 1081 and 1,154 cm⁻¹ could be attributed to C–O stretch in C–O–H bonding²⁴⁹. The peak near 1,154 cm⁻¹ was not very prominent in *A. paeonifolius*. The peak near 2,930 cm⁻¹ might be attributed to the asymmetric stretching of C–H, while the band near 1,644 cm⁻¹ was ascribed to the adsorbed water and the bands near 1,420 and 1,368 cm⁻¹ to the angular

deformation of C–H; the later one was prominent in *A. paeonifolius*. The FTIR spectra not only revealed the purity of the starch isolated but also the functional groups present in the starch of the aroid species.

5.9.4 Gelatinization parameter

As seen in Table 4.13 the gelatinization parameters of the aroid satches found to vary from species to species. The order of ΔH was found to be in *A. paeonifolius* > *C. esculenta* > *X. sagittifolium* > *X. caracu* > Starch soluble. Similarly, the order of T_p was *C. esculenta* > *A. paeonifolius* > *X. caracu* > *X. sagittifolium* > Starch soluble. The ΔH generated due to the thermal decomposition of the starch granules suggested the complexity of the starch copolymer.

5.9.5 Recording of amylose leaching by colorimetric method

The small granule-starch tend to leach more amylose out of the intact granules at temperature 50°C and above than those of larger granules (Figure 4.33)⁸⁹. The pattern of leaching of amylose followed the normal prediction except in the use of *X. caracu* which might be attributed to less crystallized arrangement of the polysaccharide chains, a larger portion of amorphous zone leading to more accessibility to water. Larger specific surface area might also contribute to higher water absorption by B-type granules⁸⁹.

5.9.6 Acid hydrolysis

Starch granules from the aroid species were hydrolyzed for 15 days with 2.2 M HCl at 35°C and the reducing sugar was estimated as per the standard method. The amorphous region of the starch was degraded during initial days which were followed by slow degradation of the crystalline region (Figure 4.34). The difference in the extent of acid hydrolysis of starch might be attributed to granule size, interaction in relation to amorphous and crystalline regions, composition of starch in respect of phosphate content and amylose/amylopectin ratio²⁵⁰. In B-type starch, α -1,6 branch is located mainly

in the amorphous region making it very susceptible to acid hydrolysis; whereas, in A-type starch, α -1,6 branch is located in the crystalline region making it resistant to hydrolysis by H_3O^+ . Starch hydrolysis could be explained on the basis of granule surface area and composition. Low amylose content and large granule size starch in *A. paeonifolius* as compared to other three aroid species might be responsible for the reduced hydrolysis during the initial and later periods. In *X. sagittifolium*, a sharp exception was observed which could be due to the starch type. In *C. esculenta*, a slight depression in the rate of hydrolysis after the ninth day might be due to the presence of amylopectins. Several workers reported wide variation (9–25 days) in regard to the time period required for the degradation of the crystalline region by H_3O^+ depending on the source of starch^{251, 220}. Data suggested that during the hydrolysis, only amorphous regions were degraded by H_3O^+ . But, the aroids did not possess sharp difference in their crystallinity. Difference in the rate and extent of acid hydrolysis among starches could be attributed to granule size; interaction between starch chains; amylopectin chain length distribution; and phosphorus content^{252, 253, 220}. But, most of these factors were negated by the size of starch granule, which was prominently revealed in the present assay. Differences in hydrolysis among the aroid starches could be attributed to the interplay of granule size, phosphorus content, and total amylose content. The difference in the extent of hydrolysis among the aroids suggested the combined effect of these three factors. In *X. caracu* and *X. sagittifolium*, the difference was negated by the granule size; and the interaction of amylose-amylopectin might be responsible for the higher rate of hydrolysis in *X. caracu* starch. The extent of hydrolysis of aroid starch (Figure 4.34) was much lower than those reported in potato, cassava, yam and sweet potato, in which starch hydrolysis exceeded 70% after 12 days^{251, 214}.

5.9.7 Enzymatic hydrolysis

The susceptibility of aroid starch to α -amylase enzyme was analyzed (Table 4.12). The extent of enzymatic hydrolysis followed the order as *C.*

esculenta > *X. caracu* > *X. sagittifolium* > *A. paeonifolius*. The difference in *in vitro* digestibility of starch among the species could be attributed to the interplay of many factors such as starch source, granule size, amylose/amylopectin ratio, extent of molecular association between starch chains, degree of crystallinity and unit cell structure²¹¹.

Starch damage was found to be in the order of *A. paeonifolius* > *X. sagittifolium* > *C. esculenta* > *X. caracu*. The damage of *A. paeonifolius* was found to be two times more as compared to others in the present investigation. Normally, amylose leaching increases due to starch damage. The starch damage of 4.54% might be a very small factor in the case of granules having 5-12 μm size. This could play a vital role in amylose leaching.

The moisture content of the starch of *C. esculenta* and *X. sagittifolium* as reported by Perez *et al.*²⁴⁵ ($14.01 \pm 0.05\%$ and $13.43 \pm 0.01\%$) was slightly higher as compared to the present finding of $11.2 \pm 0.74\%$ and $12.2 \pm 1.20\%$, respectively. The results showed major difference in the composition and physicochemical properties among the aroid starches. However, variations were caused due to the interplay of factors like granule size, crystallinity and phosphorus content.

5.10 Starch and polyaniline composite

5.10.1 Morphology of the polyaniline loaded starch granules

SEM micrograph of starch (Figure 4.35) revealed hexagonal granules with the average size of 2.0 μm , the surface being quite smooth and well defined. In the case of the starch/polyaniline (Figure 4.35 and Table 4.15) composite with the lowest concentration of aniline, the surface of the starch granules was observed to be rough than that of the pure starch. This was indicative of polymerization of aniline over the surface of the starch granules forming a layer over it. In the case of low concentration of aniline, polymerization preferably occurred in the surface of the surface of the starch granule and then in the bulk which was evident from the micrographs (Figure 4.35). With the enhancement of aniline concentration, overgrowth of polyaniline is noticed.

5.10.2 X-ray diffraction studies

Two characteristic types of X-ray patterns of starch, A and B types are based on parallel standard double helices and the major difference between them is the packing of the helices (A-type being more closely packed); and differ in the content of intra-helical water ($B > A$)²⁴⁷. The starch extracted from *C. esculenta* was found to possess A-type X-ray pattern with characteristic peaks at $2\theta = 15.3^\circ$, 17.0° , 18.0° , 20.0° and 23.4° .

X-ray diffraction pattern for the pristine polyaniline (Figure 4.36) showed two major peaks at $2\theta = 20.95^\circ$ and 26.03° which could be ascribed to the parallel and perpendicular periodicity of polyaniline²⁵⁴. X-ray patterns for the polyaniline/starch composites showed the evolution of peaks corresponding to the polyaniline with the increase in polyaniline concentration. Composites containing 0.1 M and 0.5 M of aniline however did not provide prominent evidence of peaks ascribed to the polyaniline. There was a prominent change in the percentage of crystallinity as observed in S2 and S3.

5.10.3 UV-Visible spectroscopy

As observed in Figure 4.38, the peak in the visible region corresponding to polyaniline shifted towards UV region in the case of S3 where as in the case of S1 it became a valley. The UV region peak of the polyaniline lost its sharpness in the composites. The UV region peak broadened up in S3 and S2, but became a small valley in the case of S1. The presence of polyaniline increased the absorption intensity of the materials after about 600 nm. The UV-vis spectroscopy suggested the presence of characteristic changes in the material as far as the absorption of UV or visible light concerned but the composites showed the UV-vis absorption pattern of polyaniline.

5.10.4 FT-IR spectroscopy

As depicted in Figure 4.37, the characteristic peaks of polyaniline at $1,567$ and $1,483$ cm^{-1} could be assigned the vibration of quinoid and benzene rings, respectively. The bands at $1,300$ and $1,246$ cm^{-1} corresponded to C-H

stretching vibration with the aromatic conjugation. In the case of starch as shown in Figure 4.36, the characteristic peak between 1,019 and 1,156 cm^{-1} attributed C–O stretch in C–O–C bonding, and peaks near 1,081 and 1,154 cm^{-1} could be attributed to C–O stretch in C–O–H bonding. The band near 1,644 cm^{-1} was ascribed to the adsorbed water and the bands near 1,420 and 1,368 cm^{-1} to the angular deformation of C–H. As seen in Figure 4.36, the peak at 1,567 cm^{-1} of polyaniline and 1,644 cm^{-1} of starch fuses with each other and broaden the peak suggesting the presence of moisture absorption property of starch in the composite S1. The peak near 1,154 cm^{-1} attributed to the C–O stretch in C–O–H bonding was also prominent in S1 but absent in the S2, S3 and polyaniline. The absence of the peak in 1,644 cm^{-1} in S2 and S3 suggested the loss of moisture absorption capacity of the composites. The peak at 1,483 cm^{-1} representing the stretching vibration of the benzene ring became prominent from S1 to S3 suggesting increase of polyaniline property in the composites. The bands at 1,300 and 1,246 cm^{-1} corresponding to C–H stretching vibration with the aromatic conjugation were also prominent in the composites with the increasing concentration of polyaniline (S2 and S3).

5.10.5 Differential scanning calorimetry (DSC)

The gelatinization temperature of the aroid starch was found to be 75°C [Figure 4.39 (starch)]. The exothermic curve of starch was sharp as compared to polyaniline and ending of the former was the starting point of the second. The pattern of DSC curve obtained for polyaniline was the characteristic feature of the same. In the case of S1 and S2, the gelatinization temperature increased up to 150°C as compared to polyaniline and starch. In S3 two separate peaks of gelatinization were observed, one of which was similar to that of starch but the other one near 75°C. The appearance of the new peak suggested the formation of a different composite. The overall difference suggested that composites were not only different in their thermal properties from parent polymers but differences were also prominent among them.

5.10.6 Antioxidant activity

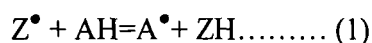
Reactions with the fixed amount of starch-polyaniline composite with the different amounts of polyaniline and the pure components viz. starch and polyaniline were carried out and the UV-Visible spectra of the solutions were recorded after 10 min. The results for the reaction of the free radical DPPH with the composite consisting of 0.5 M polyaniline (Figure 4.41) revealed a progressive decrease in the absorption band of DPPH at 517 nm with the increasing weight of the material. The antioxidant activity of a material depends on its capability to donate hydrogen for reducing DPPH and therefore, the structural conformation of the material plays a vital role in its antioxidant activity. A single unit of the emeraldine salt form of polyaniline donates one hydrogen atom and thereby eliminates DPPH free radicals which lead to the decrease in the peak intensity at 517 nm. More is the decrease in peak intensity better is the antioxidant activity. This is possible owing to the molecular structure of the emeraldine salt form of polyaniline.

Similar antioxidant activity was exhibited by the same amount (0.4 mg) of composites and pure samples. It was observed that the antioxidant property of the composites increases with the increase in the concentration of polyaniline. This could be attributed to the fact that polyaniline owing to its redox active nature is efficient in scavenging the free radical DPPH and as such with the increasing concentration of polyaniline there is a corresponding increase in the antioxidant activity of the material. Pure starch however shows a very little activity when it comes to scavenging free radicals but polyaniline in its bulk form seems to be exhibiting the best antioxidant activity. As a result the antioxidant activity of the composites is found to be better in the samples with more amount of polyaniline which is obvious because more the amounts of the polyaniline present more is the number of hydrogen atoms donated for eliminating the DPPH.

The time dependence of antioxidant activity of an antioxidant can give important information about the reaction mechanism. This was time dependence on the antioxidant activity of the composite synthesized with 1M aniline (Figure

4.42). The antioxidant activity increased linearly up to a certain time after which the rate of DPPH scavenging decreased indicating the fact that the material was used up and there was no more hydrogen atoms that could be donated for eliminating the DPPH free radical. All composites and bulk polyaniline exhibited similar behavior. However for the composites, the reaction saturation time decreased with the decrease in the concentration of the polyaniline.

A solution of DPPH on reacting with that of a substance capable of donating a hydrogen atom, gives rise to the reduced form with the loss of violet colour. Representing the DPPH radical by Z^\bullet and the donor molecule by AH, the primary reaction is:



Where, ZH is the reduced form and A^\bullet is a free radical produced in the first step. The free radical (A^\bullet) undergoes further reaction controlling the overall stoichiometry of the reaction. The reaction (1) is therefore intended to provide the link with the reactions taking place in an oxidizing system, such as auto-oxidation of a lipid or other unsaturated substances; the DPPH molecule Z^\bullet is thus intended to represent the free radicals formed in the system whose activity is to be suppressed by the molecule AH.

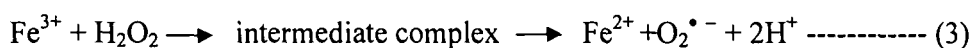
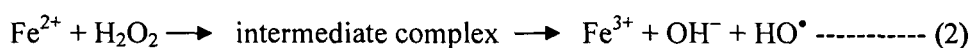
The mechanism of the reaction between aniline and DPPH was investigated by many researchers^{255,256}. After reacting with DPPH, the emeraldine salt-form gets converted into the fully oxidized pernigraniline of polyaniline which does not possess any hydrogen atom for reducing the DPPH. The saturation in the DPPH scavenging activity (Figure 4.42) could therefore be attributed to the formation of the fully oxidized pernigraniline from the emeraldine salt form leading to loss of its free radical scavenging activity.

5.10.7 Cytotoxicity by anti-haemolysis

Polyaniline inspite of its high antioxidant activity is accompanied with certain degree of cytotoxicity. The idea of synthesizing an all organic composite consisting of a biocompatible material with a redox active conjugated polymer is intended to reduce the cytotoxicity of the conjugated polymer in order to

realize its use in biomedical applications. With the view, the anti-cytotoxicity of pure and composite samples was investigated.

Hydrogen peroxide (H_2O_2), a well known pro-oxidant can harm the blood cells by causing haemolysis. The reaction of hydrogen peroxide with iron causes the formation of free radicals and other charged species (equation 2 and 3). So, RBC (erythrocytes) itself acts as a Fenton reagent and generates hydroxyl radicals (OH^\bullet) and super-oxide anions ($\text{O}_2^{\bullet -}$) which finally lead to the release of iron ions from the haemeprotein²⁵⁷. As a result, the blood cell gets deformed due to the formation of “splenic pitting” through proteases²⁵⁸.



The haemolysis prevention activity of the composites (Figure 4.43) was better than that of polyaniline in spite of its high antioxidant activity. Pure polyaniline shows a progressive decrease in the haemolysis prevention activity. This reveals the cytotoxic nature of polyaniline which in spite of being relatively low needs to be reduced. The sample S1 showed a gradual increase in the haemolysis prevention with the increase in the weight of the material. The effect of S1 in its highest dose could be estimated from the deformation of the RBC membranes as observed in H_2O_2 treated samples (Figure 4.44). A similar behavior was also observed in S2 but its activity was less than that of S1. However, in the case of S3, there was a decrease in the haemolysis prevention activity on the addition of 1.0 mg of the composite. H_2O_2 owing to its oxidizing nature has the tendency of oxidizing the emeraldine salt. As a result, the oxidizing power of H_2O_2 gets reduced and the molecule becomes less harmful to the blood cells. But the remaining polyaniline, due to whatever low cytotoxicity it possesses, harms the RBC and leads to haemolysis (Figure 4.44). As and when the weight of polyaniline was increased the haemolysis prevention activity decreased. The fact was further confirmed by the sudden drop in the haemolysis prevention activity when 1.0 mg of the composite S3 having the highest aspect ratio of polyaniline was applied to the blood in the presence of H_2O_2 . The haemolysis prevention activity was found to be the best in the

composite with the least amount of polyaniline (Figure 4.44). In the case of sample S1, the aspect ratio of polyaniline to starch was quite low and as such its haemolysis prevention activity increased with the weight of the material. When the amount of polyaniline in the composites increased, the activity of the composites got reduced. Thus, it is evident that the incorporation of starch which is non-toxic in nature reduces the cytotoxicity of polyaniline.

Investigation of organic materials for biomedical applications is not new but the conducting organic polymers having redox activity and enhanced biocompatibility could lead to the development of advanced functional materials for the biomedical applications. In the present work, starch/polyaniline composite was synthesized with a view to reduce the cytotoxicity of polyaniline. The biocompatibility of starch/polyaniline composites was found to increase with the increasing starch content and it exhibited dose dependence. Antioxidant activity alone is not enough for biocompatibility, and there is always a need of investigation in a biological media like RBC. The fact became clear when the contrast was obtained from the antioxidant activity and haemolysis prevention assay. It was observed that in spite of having very high antioxidant activity; pure polyaniline was much more cytotoxic than the composites. Looking into the bioactivity of starch/polyaniline composite, it might have the potential in the field of controlled drug release and scavenging of the oxidants generated through chemotherapeutic drugs. Subsequently, they could help in neutralizing the chemotherapeutic side effects of cancer treatment tremendously.

CHAPTER 6

CONCLUSION

The molecular and biochemical characterization of the four aroids leads to following conclusions:

1. Morphological characters of four aroids are distinctive enough to be recognized as separate species and fusiform corm of *C. esculenta* is a unique type of morphotype. The corm size of *A. paeoniifolius* is found to be biggest among aroids selected for present study.
2. Analysis of biochemical composition suggests that *C. esculenta* species is most promising as food except in case of crude fiber content for which the species was a poor source. Moisture content of *C. esculenta* was found to be lowest promising an increase in shelf life during post harvest storage.
3. Chromosome analysis suggests that *X. caracu* ($2n=2x=26$), *X. sagittifolium* ($2n=2x=26$) and *A. paeoniifolius* ($2n=2x=28$) species are diploid, whereas the *C. esculenta* ($2n=4x=28$) is tetraploid.
4. The genome size (C value=14.1 pg) of *C. esculenta* was found to be bigger among the selected aroids.
5. *A. paeoniifolius* has similarity percentage of 67 with *Xanthosoma* species cluster. *C. esculenta* has a similarity of 11% with *Xanthosoma* and *Amorphophallus* cluster.
6. Total phenolic and flavonoid content was found highest in *A. paeoniifolius* water extract.
7. The DPPH free radical scavenging property was found highest in *X. caracu* 80% methanol extract.
8. Blood coagulation enhancing property was found highest in *X. sagittifolium* 80% methanol extract.
9. The antibacterial and antifungal activities of 80% methanol extracts were found to be more pronounced as compared to other two types of extracts.

10. Based on HPLC, a total of 14 compounds were isolated from selected aroids and their characterization (NMR and FTIR) lead to identification of 5 different polyphenolic compounds viz 3,4-dihydroxy benzoic acid, 3,4-dihydroxycinnamic acid, trans-in-hydroxycinnamic acid, 4-hydroxy-3-methoxycinnamic acid and 4-hydroxy-3,5-dimethoxybenzoic acid.
11. All the isolated compounds showed antibacterial activity. Protocatechuic acid [AC-I (1) and XC-I (1)] showed highest activity against *E. coli* and coumaric acid [CC-I (4) and CC-II (4)] showed highest activity against *S. aureus*.
12. The antioxidant activity carried out by induced haemolysis prevention was found to be best in case of caffeic acid [CC-I (2)]. The lowest haemolysis prevention was observed in case of protocatechuic acid [XC-I (1) and AC-I (1)].
13. The amylose content of *C. esculenta* starch was found highest and granule size of the same was smallest. The biggest starch granule size and highest relative crystallinity were recorded in case of *A. paeoniifolius* starch.
14. Due to small granule size *C. esculenta* starch was found to be most suitable for composite preparation with polyaniline
15. The starch-polyaniline composites were prepared and characterized using parameters like SEM, XRD, DSC and UV-Vis indicating clear formation of three new types of composites having better antioxidant activity along with biocompatibility.
16. The small granule-sized starch of *C. esculenta* could be used in baby food, fine printing paper, plastic sheets as binder with orally active ingredients, and as carrier material in cosmetics. There is a potential of this starch in cosmetic, paper, textile and photographic industries.
17. *C. esculenta* starch could be used in the synthesis of edible films for food coating. The thrust in starch research could be estimated from the various research works carried out in the field of acid thinning, resistant

starch, starch extrudates, starch-gum, starch blend and thermal treatment of starch.

Starches analyzed in the present investigation were not reported earlier from this region of biodiversity as well as centre of origin of the aroid species *C. esculenta*.

Future research

The cytotoxic property of starch/polyaniline composites was found to be dependent on the composition of the sample. Although, the details of cytotoxic behaviour of the polyaniline was not clear, it could be assumed that owing to the redox activity, polyaniline reacts with the iron molecule of hemeprotein and damage blood cells by causing haemolysis. Further research in this field is essential to understand the cytotoxic nature of polyaniline.

REFERENCES

1. Meeuse, B.J.D. Thermogenic respiration in aroids. *Ann. Rev. Pl. Physiol.* **26**, 117-126 (1975).
2. Yocum, C.S.; Hackett, D.P. Participation of cytochromes in the respiration of the aroid spadix. *Plant Physiology*. **32**, 186-191 (1957).
3. Hackett, D.P. Respiratory Mechanisms in the Aroid Spadix. *J. Exp. Bot.* **8**, 157-171 (1957).
4. Godfray, H.C.J.; Clark, B.R.; Kitching, I. J.; Mayo, S. J.; Scoble, M. J. The Web and the Structure of Taxonomy. *Systematic Biology* **56**, 943-955 (2007).
5. Genua, J.M.; Hillson, C.J. The Occurrence, Type and Location of Calcium Oxalate Crystals in the Leaves of Fourteen Species of Araceae. *Annals of Botany* **56**, 351-361 (1985).
6. Mantovani, A.; Pereira, T.E.; Coelho, M.A.N. Leaf midrib outline as a diagnostic character for taxonomy in *Anthurium* section *Urospadix* subsection *Flavescentiviridia* (Araceae). *Hoehnea* **36**, 269-277 (2009).
7. Benzing, D.H. Vascular Epiphytism: Taxonomic Participation and Adaptive Diversity. *Annals of the Missouri Botanical Garden*, **74**, 183-204 (1987).
8. Tam, S. *et al.* Intergeneric and infrafamilial phylogeny of subfamily Monsteroideae (Araceae) revealed by chloroplast trnL-F sequences. *American Journal of Botany*. **91**, 490-498 (2004).
9. Schmid, P.C.; Holman, R.T.; Soukup, V.G. 13-Phenyltridecanoic acid in seed lipids of some aroids. *Phytochemistry* **45**, 1173-1175 (1997).
10. Barabé, D.; Bruneau, A.; Forest, F.; Lacroix, C. The correlation between development of atypical bisexual flowers and phylogeny in the Aroideae (Araceae). *Plant Systematics and Evolution* **232**, 1-19 (2002).
11. Cabrera, L.I. *et al.* Phylogenetic relationships of aroids and duckweeds (Araceae) inferred from coding and noncoding plastid DNA. *American Journal of Botany* **95**, 1153-1165 (2008).
12. Kuruvilla, K.M.; Singh, A. Karyotypic and electrophoretic studies on taro and its origin. *Euphytica* **30**, 405-413 (1981).

13. Yen, D.E.; Wheeler, J.M. Introduction of Taro into the Pacific: The Indications of the Chromosome Numbers. *Ethnology* **7**, 259-267 (1968).
14. Niew, Z.; Sun, H.; Lia, H.; Wen, J. Intercontinental biogeography of subfamily Orontioideae (Symplocarpus, Lysichiton, and Orontium) of Araceae in eastern Asia and North America. *Molecular Phylogenetics and Evolution* **40**, 155-165 (2006).
15. Plucknett, D.L.; Pena, de la R.S.; Obrero, F. Taro (*Colocasia esculenta*). *Field Crop Abstracts* **23**, 413-426 (1970).
16. Matthews, P.J. *The origins, dispersal and domestication of taro*. PhD Thesis. (Australian National University, Canberra, 1990).
17. Matthews, P.J. Genetic diversity of taro, and the preservation of culinary knowledge. *Ethnobotany Research & Applications* **2**, 55-71 (2004).
18. Golson, J. *Bulmer Phase II: early agriculture in the New Guinea Highlands*. In 'Man and a Half: Essays in Pacific Anthropology and Ethnobiology in Honour of Ralph Bulmer' (The Polynesian Society, Auckland, 1991).
19. Loy, T.H.; Spriggs, M.; Wickler, S. Direct evidence for human use of plants 28,000 years ago: starch residues on stone artifacts from the northern Solomons. *Antiquity* **66**, 898-912 (1992).
20. Léon, J. *Origin, evolution, and early dispersal of root and tuber crops*. In 'Proceedings of the 4th symposium of the International Society for Tropical Root Crops.' (Eds. J. Cook, R. MacIntyre, M. Graham) 20-36. (International Development Research Centre: Ottawa, Canada. 1977).
21. Yen, D.E. *The history of cultivated plants*. In 'Melanesia: Beyond diversity' (Australian University Presss, Canberra, 1982).
22. Coates, D.J.; Yen, D.E.; Gaffey, P.M. Chromosome variation in taro, *Colocasia esculenta*: implications for its origin in the Pacific. *Cytologia* **53**, 551-560 (1988).
23. Matthews, P.J. A possible tropical wildtype taro: *Colocasia esculenta* var. *aquatilis*. *Indo-Pacific Prehistory Association Bulletin* **11**, 69-81(1991).

24. Matthews, P.J. Aroids and the Austronesians. *Tropics* **4**, 105-126 (1995).
25. Jackson, G.V.H. *Regeneration guidelines: major aroids*. (CGIAR System-wide Genetic Resource Programme, Rome, Italy, 2008).
26. Yen, D.E.; Wheeler, J.M. Induction of taro into the Pacific: the indications of chromosome numbers. *Ethnology* **7**, 259-267(1968).
27. Crepet, W.L. Investigations of angiosperms from the Eocene of North America: An aroid inflorescence. *Review of Palaeobotany and Palynology* **25**, 241-252 (1978).
28. Andrade, I.M.; Mayo, S.J. Dynamic Shoot Morphology in *Monstera adansonii* Schott var. *klotzschiana* (Schott) Madison (Araceae). *Kew Bulletin* **53**, 399-417 (1998).
29. Fls, D.B.; Lacroix, C. The developmental floral morphology of *Montrichardia arborescens* (Araceae) revisited. *Botanical Journal of the Linnean Society* **135**, 413–420 (2001).
30. Daghljan, C.P. A review of the fossil record of monocotyledons. *The Botanical Review* **47**, 517-555 (2008).
31. Wilde, V.; Kvaček, Z.; Bogner, J. Fossil Leaves of the Araceae from the European Eocene and Notes on Other Aroid Fossils. *Int. J Plant Sci.* **166**, 157–183 (2005).
32. Hesse, M.; Zetter, R. The fossil pollen record of Araceae. *Plant Systematics and Evolution* **263**, 93-115 (2007).
33. Murata, J. Diversity in the Stem Morphology of *Arisaema* (Araceae). *Plant Species Biology* **2**, 57-66 (1987).
34. Ray, T.S. Leaf Types in the Araceae. *American Journal of Botany*, **74**, 1359-1372 (1987).
35. Cai, X.Z.; Long, C.L.; Liu, K.M. *Colocasia yunnanensis* (Araceae), a new species from Yunnan, China. *Ann. Bot. Fennici* **43**, 139-142 (2006).
36. Hather, J.G. *Tropical Archeobotany Applications and New Development*. (Routledge, New York, 1994).

37. Minorsky, P.V. The Hot and the Classic. *Plant Physiology*, **132**, 25–26 (2003).
38. Ervik, F.; Barfod, A. Thermogenesis in palm inflorescences and its ecogocial significance. *Acta. Bot. Venez.* **22**, 195–212 (1999).
39. Seymour, R.S.; Blaylock, A.J. Switching off the heater: influence of ambient temperature on thermorgulation by eastern skunk cabbage *Symplocarpus foetidus*. *J. Exp. Bot.* **50**, 1525–1532 (1999).
40. Gibernau, M.; Barabe, D.; Moisson, M.; Trombe, A. Physical Constraints on Temperature Difference in Some Thermogenic Aroid Inflorescences. *Annals of Botany* **96**, 117–125 (2005).
41. Ito-Inaba, Y.; Hida, Y.; Inaba, T. What is critical for plant thermogenesis? Differences in mitochondrial activity and protein expression between thermogenic and non-thermogenic skunk cabbages. *Planta*. **231**, 121-130. (2009).
42. Lebot, V.; Arhadya, K.M. Isozyme variation in taro (*Colocasia esculenta* (L.) Schott) from Asia and the Pacific. *Euphytica* **56**, 55-66 (1991).
43. Lebot, V. *et al.* Characterisation of taro (*Colocasia esculenta* (L.) Schott) genetic resources in Southeast Asia and Oceania. *Genetic Resources and Crop Evolution* **51**, 381–392 (2004).
44. Kreike, C.M.; Van-Eck, H.J.; Lebot, V. Genetc diversity of taro, *Colocasia esculenta* (L.) Schott, in Southeast Asia and the PACIFIC. *Theoretical and Applied Genetics* **109**, 761-768 (2004).
45. Irwin, S.V.; Kaufusi, P.; Banks, K.; de la Peña, R.; Cho, J.J. Molecular characterization of taro (*Colocasia esculenta*) using RAPD markers. *Euphytica* **99**, 183-189 (1998).
46. Lebot, V. Genetic vulnerability of Oceania's traditional crops. *Experimental Agricultural* **28**, 309-323 (1992).
47. Mace, E.S. *et al.* Rationalization of taro germplasm collections in the Pacific Island region using simple sequence repeat (SSR) markers. *Plant Genetic Resources* **4**, 210–220 (2006).

48. Hay, A. The genus *Alocasia* (Araceae-Colocasieae) in West Malesia and Sulawesi. *Gardeners' Bulletin Singapore* **50**, 221-334 (1998).
49. Hay, S.; Wise, R. The genus *Alocasia* (Araceae) in Australasia. *Blumea* **35**, 499-545 (1991).
50. Hay, A. The genus *Alocasia* (Araceae-Colocasieae) in the Philippines. *Gardeners' Bulletin Singapore* **51**, 1-41 (1999).
51. Paroda, R.S.; Arora, R.K. *Plant Genetic resources conservation and management concepts and approaches*. (International Board for Plant Genetic Resources, Regional Office for South and Southeast Asia, New Delhi, India, 1991).
52. Hettterscheid, W.; Ittenbach, S. Everything you always wanted to know about *Amorphophallus*, but were afraid to stick your nose into! *Aroideana* **19**, 7-131 (1996).
53. Hay, A. *Amorphophallus* (Araceae) in Australasia). *Aroideana* **11**, 14-19 (1988).
54. Sivan, P. (1984) *Edible Aroids* (Clarendon Press, Oxford, 1984).
55. Palaniswami, M.S.; Anil, S.R. *Regional technologies for tropical root and tuber crops in India*. (Technical Bulletin series No. 47, Central Tuber Crops Research Institute, Thiruvananthaouram, India, 2006).
56. Abraham, K. *et al. Tuber crop varieties released by the Central Tuber Crops research Institute* (Central Tuber Crops Research Institute, Thiruvananthapuram, India, 1998).
57. Clement, C.R. *Neglected Crops: 1492 from a Different Perspective* (FAO Plant Production and Protection Series, Rome, 1994).
58. Coursey, D.C. The edible aroids. *World Crops* **20**, 25-30 (1968).
59. Wilson, J.E. Cocoyam. *The Physiology of Tropical Field Crops* (John Wiley & Sons Ltd., Newyork, 1984).
60. Onwueme, I.C.; Charles, W.B. Cultivation of cocoyam. *Tropical root and tuber crops. Production, perspectives and future prospects*. (FAO Plant Production and Protection Paper, FOA press, 1994).

61. Onokpise, O.U.; Meboka, M.M.; Eyango, A.S. Germplasm collection of macabo cocoyams in Cameroon. *African Technology Forum* **6**, 28–31 (1993).
62. Tambong, J.T.; Sapra, V.T.; Garton, S. In vitro induction of tetraploids in colchicine treated cocoyam plantlets. *Euphytica* **104**, 191-197 (1998).
63. Schnell, R.J.; Goegnaga, R.; Olano, C.T. Genetic similarities among cocoyam cultivars based on random amplified polymorphic DNA (RAPD) analysis. *Scientia Horticulturae* **80**, 267-276 (1999).
64. Offei, S.K.; Asante, I.K.; Danquah, E.Y. Genetic structure of seventy cocoyam (*Xanthosoma sagittifolium*, Linn, Schott) accessions in Ghana based on RAPD. *Hereditas* **140**, 123–128 (2004).
65. Jube, S.; Borthakur, D. Recent advances in food biotechnology research. *Food Biochemistry and Food Processing* (Blackwell Publishing, Oxford, U.K., 2006).
66. Santacruz, S.; Koch, K.; Svensson, E.; Ruales, J.; Eliasson, A. C. Three under-utilised sources of starch from the Andean region in Ecuador, Part I. Physico-chemical characterisation. *Carbohydrate Polymers* **49**, 63–70 (2002).
67. FAO. *Quarterly Bulletin of Statistics* (Food and Agriculture Organization of the United Nations, Vol. 4, Roam, 1991).
68. Bradbury, J. H. The chemical composition of tropical root crops. *ASEAN Food Journal* **4**, 34–38 (1988).
69. Davidson, S.; Passmore, R.; Brock, J.F.; Truswell, A.S. *Human nutrition and dietetics* (Churchill Livingstone, Edinburg, 1979).
70. Bhandari, M.R.; Kasai, T.; Kawabata, J. Nutritional evaluation of wild yam (*Dioscorea* spp.) tubers of Nepal. *Food Chemistry* **82**, 619–623 (2003).
71. Englberger, L. *et al.* Further analyses on Micronesian banana, taro, breadfruit and other foods for provitamin A carotenoids and minerals. *Journal of Food Composition and Analysis* **16**, 219–236 (2003).

72. Huang, A.S.; Titchenal, C.A.; Meilleur, B.A. Nutrient composition of taro corms and breadfruit. *Journal of Food Composition and Analysis* **13**, 859–864 (2000).
73. Wills, R.B.H.; Lim, J.S.K.; Greenfield, H.; Bayliss-Smith, T. Nutrient composition of taro (*Colocasia esculenta*) cultivars from the Papua Guinea Highlands. *Journal of the Science of Food and Agriculture* **34**, 1137–1142 (1983).
74. Agbor-Egbe, T.; Rickard, J. Evaluation of the chemical composition of fresh and stored edible aroids. *Journal of the Science of Food and Agriculture* **53**, 487–495 (1990).
75. Shewry, P.R. Tuber Storage Proteins. *Ann. Bot.* **91**, 755-769 (2003).
76. Njintang, N.Y. *et al.* Effect of taro (*Colocasia esculenta*) flour addition on the functional and alveographic properties of wheat flour and dough. *Journal of the Science of Food and Agriculture* **88**, 273-279 (2008).
77. Sahoo, M.R.; Dasgupta, M.; Kole, P.C.; Mukherjee, A. Biochemical Changes in Leaf Tissues of Taro [*Colocasia esculenta* L. (Schott)] Infected with *Phytophthora colocasiae*. *Journal of Phytopathology* **158**, 154-159 (2009).
78. Martensson, L.; Savage, G.P. Composition and bioavailability of oxalates in baked taro (*Colocasia esculenta* var. Schott) leaves eaten with cows milk and cows milk and coconut milk. *International Journal of Food Science & Technology* **43**, 2213-2218 (2008).
79. Omokolo, N.D.; Boudjeko, T. Comparative analyses of alterations in carbohydrates, amino acids, phenols and lignin in roots of three cultivars of *Xanthosoma sagittifolium* infected by *Pythium myriotylum*. *South African Journal of Botany* **71**, 432–440 (2005).
80. Das, D. *et al.* Isolation and characterization of a heteropolysaccharide from the corm of *Amorphophallus campanulatus*. *Carbohydrate Research* **344**, 2581-2585 (2009).
81. Mandal, P.; Misra, T.K.; Singh, I.D. Antioxidant activity in the extracts of two edible aroids. *Indian J. Pharm. Sci.* **72**, 105-108 (2010).

82. Dring, J.V.; Kite, G.C.; Nash, R.J.; Reynolds, T. Chemicals in aroids: a survey, including new results for polyhydroxy alkaloids and alkylresorcinols. *Botanical Journal of the Linnean Society* **117**, 1-12 (1995).
83. Smith, A.M. Prospects for increasing starch and sucrose yields for bioethanol production. *Plant J.* **54**, 546-558 (2008).
84. Buleon, A.; Colonna, P.; Planchot, V.; Ball, S. Starch granules: structure and biosynthesis. *Int. J. Biol. Macromol.* **23**, 85-112 (1998).
85. Hizukuri, S. Polymodal distribution of the chain lengths of amylopectins, and its significance. *Carbohydr. Res.* **147**, 342-347 (1986).
86. Jenkins, P.J.; Cameron, R.E.; Donald, A.M. A universal feature in the structure of starch granules from different botanical sources. *Starch* **45**, 417-20 (1993).
87. Zeeman, S.C. *et al.* Starch synthesis in Arabidopsis: granule synthesis, composition and structure. *Plant Physiol.* **129**, 516-529 (2002).
88. Hoover, R. Composition, molecular structure, and physicochemical properties of tuber and root starches, a review, *Carbohydrate Polymers* **45**, 253-267 (2001).
89. Lindeboom, N.; Chang, P.R.; Tyler, R.T. Analytical, Biochemical and Physicochemical Aspects of Starch Granule Size, with Emphasis on Small Granule Starches, A Review. *Starch* **56**, 89 -99 (2004).
90. Tester, R.F.; Karkalas, J.; Qi, X. Starch composition, fine structure and architecture. *Journal Cereal Sciences* **39**, 151-165 (1997).
91. Langeveld, S.M.J.; van Wijk, R.; Stuurman, N.; Kijne, J.W.; de Pater, S. B-type granule containing protusions and interconnections between amyloplasts in developing wheat endosperm revealed by transmission electron and GFP expression. *Journal of Experimental Botany* **51**, 1357-1361 (2000).
92. Nair, L.S.; Laurencin, C.T. Biodegradable polymers as biomaterials. *Polym. Sci.* **32**, 762-798 (2007).

93. Gultekin, G. *et al.* Fatty acid-based polyurethane films for wound dressing applications. *Journal of Materials Science: Materials in Medicine* **20**, 421-431 (2009).
94. Usuki, A. *et al.* Mechanical properties of nylon6-clay hybrid. *J. Mater. Res.* **8**, 1179-1184 (1993).
95. Yurekli, K.; Karim, A.; Amis, E.J. Krishnamoorti R. Influence of layered silicates on the phase separated morphology of PS-PVME blends. *Macromolecules* **36**, 7256–7267 (2003).
96. Billotey, C. *et al.* Cell internalization of anionic maghemite nanoparticles: Quantitative effect on magnetic resonance imaging. *Magnetic Resonance in Medicine* **49**, 646–654 (2003).
97. Wilhelm, C.; Gazeau, F.; Bacri, J.C. Magnetophoresis and ferromagnetic resonance of magnetically labeled cells. *European Biophysics Journal* **31**, 118–125 (2002).
98. Wu, T.H. *et al.* Preparation, physicochemical characterization, and antioxidant effects of quercetin nanoparticles. *International Journal of Pharmaceutics* **346**, 160–168 (2008).
99. Komarek, K. *et al.* Extraction of Alkylphenols and Nonylphenol Mono- and Diethoxylates from Water Using Magnetically Modified Adsorbents. *Chromatographia* **69**, 133–137 (2009).
100. Safarikova, M.; Lunackova, P.; Komarek, K.; Hubka, T.; Safarik, I. Preconcentration of middle oxyethylated nonylphenols from water samples on magnetic solid phase. *Journal of Magnetism and Magnetic Materials* **311**, 405-408 (2007).
101. Halliwell, B. Antioxidants in Human Health and Disease. *Annual Review of Nutrition* **16**, 33-50 (1996).
102. Aruoma, O.I.; Halliwell, B.; Gajewski, E.; Dizdaroglu, M. Damage to the bases in DNA induced by hydrogen peroxide and ferric ion chelates. *J. Biol. Chem.* **264** 20509-20512 (1989).

103. Banerjee, S.; Saikia, J. P.; Kumar, A.; Konwar, B. K. Antioxidant activity and haemolysis prevention efficiency of polyaniline nanofibers. *Nanotechnology* **21** 45101-45108 (2010).
104. Deka, D.; Sarmah, G.C. Ethno medicinal aroids of Goalpara district, Assam. *Advances in Plant Sciences* **18**, 121-125 (2005).
105. Denk, T.; Oh, I.C. Phylogeny of Schisandraceae based on morphological data, evidence from modern plants and the fossil record. *Plant Systematics and Evolution* **256**, 113-145 (2005).
106. Singh, D. *et al.* Assessment and rationalization of genetic diversity of Papua New Guinea taro (*Colocasia esculenta*) using SSR DNA fingerprinting. *Genetic Resources and Crop Evolution* **55**, 811-822 (2007).
107. Reyescastro, G.; Nyman, M.; Ronnberg, W.A. Agronomic performance of three cocoyam (*xanthosoma violaceum* schott) genotypes grown in nicaragua. *Euphytica* **142**, 265-272 (2005).
108. Gow, J.E. Observations on the Morphology of the Aroids. *Botanical Gazette* **56**, 127-142 (1913).
109. Quero-Garcia, N.J.; Perrier, J.L.; Marchand, X.; Lebot, J.L. A germplasm stratification of taro (*Colocasia esculenta*) based on agromorphological descriptors, validation by AFLP markers. *Euphytica* **137**, 387-395 (2005).
110. Wang, J. Taro, A Review of *Colocasia esculenta* and its Potentials (University of Hawaii Press, 1983).
111. Kawasaki, M.; Matsuda, T.; Miyake, H.; Taniguchi, M.; Nitta, Y. Morphological studies on the mobilization of reserves in Japanese yam (*Dioscorea japonica* Thunb.) seed tuber and eddo (*Colocasia esculenta* Schott var. *antiquorum* Hubbard & Rehder) seed corm on and after sprouting. *Plant Prod. Science* **4**, 304-310 (2001).
112. Lakhanpaul, S.; Velayudhan, K.C.; Bhat, K.V. Analysis of genetic diversity in Indian taro [*Colocasia esculenta* (L.) Schott] using random

- amplified polymorphic DNA (RAPD) markers. *Genetic Resources and Crop Evolution* **50**, 603-609 (2003).
113. Strauss, M.S. Anatomy and morphology of taro: *Colocasia esculenta* (L.) Schott. In: Wang J. K. *Taro: a review of Colocasia esculenta and its potential* (University of Hawaii Press, Honolulu, 1983)
 114. Chauhan, K. P. S.; Brandham, P. E. Chromosome and DNA Variation in *Amorphophallus* (Araceae). *Kew Bulletin* **40**, 745-758 (1985).
 115. Petersen, G. New Chromosome Numbers in Araceae. *Willdenowia* **23**, 239-244 (1993).
 116. Camp W.H. Notes on the physiology and morphology of *Amorphophallus titanum*. *J. New York Bot. Gard.* **38**, 190-197 (1937).
 117. Li, H.; Long, C.L. New taxa of *Amorphophallus* from China. *Aroideana* **11**, 4-9 (1988).
 118. Bogner, J.; Hetterschëid, W.L.A. Notes on the genus *Amorphophallus* (Araceae). I: Three new species from tropical Asia. *Blumea* **36**, 467-475 (1992).
 119. Leimberk, R.M.; Balslev, H. Species richness and abundance of epiphytic Araceae on adjacent flood plain and upland forest in Amazonian Ecuador. *Biodiversity and Conservation* **10**, 1579-1593 (2001).
 120. Croat, T.B. Species Diversity of Araceae in Colombia: A Preliminary Survey. *Annals of the Missouri Botanical Garden* **79**, 17-28 (1992).
 121. Wolf, J.H.D.; Flamenco, A. Patterns in species richness and distribution of vascular epiphytes in Chiapas, Mexico. *Journal of Biogeography* **30**, 1689-1707 (2003).
 122. Amsing, J.J.; Schrama, P.M.M.; Stapel, L.H.M. Population dynamics and damage potential of the burrowing nematode, *Radopholus similis*, on *Anthurium andreanum* grown in soil-less medium. *Nematology* **4**, 421-427 (2002).

123. Zhenhua, Z.G.Y. Studies on chromosome number of main cultivars of *Colocasia esculenta* in China. *Acta Horticulturae Sinica* DOI: CNKI:SUN:YYXB.0.1984-03-008 (1984).
124. Marchant, C.J. Chromosome Variation in Araceae: II: Richardieae to Colocasieae. *Kew Bulletin* **25**, 47-56 (1971).
125. Ekanem, A.M.; Osuji, J.O. Mitotic index studies on edible cocoyams (*Xanthosoma* and *Colocasia* spp.). *African Journal of Biotechnology* **5**, 846-849 (2009).
126. Chunlin, L.; Heng, L. *Amorphophallus zengianus* (Araceae), a new Chinese species from Yunnan. *JSTOR* **10**, 125-127 (2000).
127. Li, H.; Gui, Z.J.; Long, C.L.; Yang, Y.P. Reports on the karyotypes of amorphophallus from China. *Guihaia* DOI: cnki-1000-3142.0.1990-01-003 (1990).
128. Bennett, M.D.; Leitch, I.J. Nuclear DNA amount in angiosperms, Progress, Problems and Prospects. *Annals of Botany* **95**, 45-90 (2005).
129. Hinegardner, R. The cellular DNA content of sharks, rays and some other fishes, Comparative Biochemistry and Physiology Part B. *Comparative Biochemistry* **55**, 367-370 (1976).
130. Dolezel, J.; Barto, J. Plant DNA Flow Cytometry and Estimation of Nuclear Genome Size. *Annals of Botany* **95**, 99-110 (2005).
131. Konwar, B.K.; Chowdhury, D.; Buragohain, J.; Kandali, R. A new less expensive method for genome size determination of plants. *Asian Journal of Plant Sciences* **6**, 565-567 (2007).
132. Ochiai, T.; Nguyen, V.X.; Tahara, M.; Yoshino, H. Geographical differentiation of Asian taro, *Colocasia esculenta* (L.) Schott, detected by RAPD and isozyme analyses. *Euphytica* **122**, 219-234 (2001).
133. Wenbing, C.; Chunlin, L.; Jianfu, Z. Study on Genetic Diversity of RAPD Markers in *Amorphophallus*. *Journal of Agricultural* DOI: cnki:1006-1304.0.2001-04-024 (2001).

134. Zhen, R.; Jia-yi, T. Study on the Genetic Diversity of the Konjac Soft Rot in Yunnan Province. *Journal of Yunnan Agricultural University* DOI: cnki:SUN:YNDX.0.2005-06-007 (2005).
135. Pérez, E.E.; Gutiérrez, M.E.; De-Delahaye, E.P.; Tovar, J.; Lares M. Production and characterization of *Xanthosoma sagittifolium* and *Colocasia esculenta* flours. *J Food Sci.* **72**, S367-72 (2007).
136. Meija, J.; Soukup, V.G. Phenyl-terminated fatty acids in seeds of various aroids. *Phytochemistry.* **65**, 2229-37 (2004).
137. Huang, C.C.; Chen, Y.F.; Wang C.C. Effects of micronization on the physico-chemical properties of peels of three root and tuber crops. *J Sci Food Agric.* **90**, 759-63 (2010).
138. Radek, M.; Savage G.P. Oxalates in some Indian green leafy vegetables. *Int J Food Sci Nutr.* **59**, 246-60 (2008).
139. Lako, J.; Sotheeswaran, S.; Aalbersberg, W.; Sreekumar, K.P. The glycemic index (GI) and glycemic load (GL) of five commonly consumed foods of the South Pacific. *Pac. Health Dialog.* **11**, 47-54 (2004).
140. Bahado-Singh, P.S.; Wheatley, A.O.; Ahmad, M.H.; Morrison, E.Y.; Asemota H.N. Food processing methods influence the glycaemic indices of some commonly eaten West Indian carbohydrate-rich foods. *Br J Nutr.* **96**, 476-481(2006).
141. Essumang, D.K.; Doodoo, D.K.; Obiri, S.; Yaney, J.Y. Arsenic, cadmium, and mercury in cocoyam (*Xanthosoma sagittifolium*) and watercocoyam (*Colocasia esculenta*) in Tarkwa a mining community. *Bull Environ Contam Toxicol.* **79**, 377-379 (2007).
142. Dilworth, L.L.; Omoruyi, F.O.; Asemota, H.N. In vitro availability of some essential minerals in commonly eaten processed and unprocessed Caribbean tuber crops. *Biometals.* **20**, 37-42 (2007).
143. Schmourlo, G.; Mendonça-Filho, R.R.; Alviano, C.S.; Costa, S.S. Screening of antifungal agents using ethanol precipitation and

- bioautography of medicinal and food plants. *J. Ethnopharmacol.* **96**, 563-568 (2005).
144. Uhegbu, F.O. Dietary secondary amines and liver hepatoma in Port Harcourt, Nigeria. *Plant Foods Hum Nutr.* **51**, 257-263 (1997).
145. Onwuka, N.D.; Eneh, C.O. The cocoyam, *Xanthosoma sagittifolium*, as a potential raw material source for beer brewing. *Plant Foods Hum Nutr.* **49**, 283-293 (1996).
146. Ohazurike, N.C.; Arinze, A.E. Changes in phenol oxidase and peroxidase levels in cocoyam tubers of different post-harvest ages infected by *Sclerotium rolfsii* sacc. *Nahrung.* **40**, 25-27 (1996).
147. Rashid, M.M.; Daunicht, H.J. Chemical composition of nine edible aroid cultivars of Bangladesh. *Scientia Horticulturae* **10**, 127-134 (1979).
148. Hussain, M.; Norton, G.; Neale, R. J. Composition and nutritive value of cormels of *Colocasia esculenta* (L.) Schott. *Journal of the Science of Food and Agriculture* **35**, 1112-1119 (2006).
149. Huang, A.S.; Titchenal, C.A.; Meilleur, B.A. Nutrient composition of taro corms and breadfruit. *Journal of Food Composition and Analysis* **13**, 859-864 (2000).
150. Njintang, N.Y. *et al.* Rheology and microstructure of achu, a food based on taro *Colocasia esculenta* L. Schott, as affected by method of preparation. *Journal of the Science of Food and Agriculture* **86**, 902-907 (2006).
151. Barminas, J.T.; Charles, M.; Emmanuel, D. Mineral composition of non-conventional leafy vegetables. *Plant Foods for Human Nutrition* **53**, 29-36 (1998).
152. Chattopadhyay, A.; Saha, B.; Pal, S.; Bhattacharya, A.; Sen, H. Quantitative and Qualitative Aspects of Elephant Foot Yam. *International Journal of Vegetable Science*, **16**, 73-84 (2010).
153. Raeker, M.O.; Gaines, C.S.; Finney, P.L.; Donelson, T. Granule size distribution and chemical composition of starches from 12 soft wheat cultivars. *Cereal Chemistry* **75**, 721-728 (1998).

154. Ratto, J.A.; Stenhouse, P.J.; Auerbach, M.; Mitchell, J.; Farrell, R. Processing, performance and biodegradability of a thermoplastic aliphatic polyester/starch system. *Polymer*. **40**, 6777-6788 (1999).
155. Zhou, G.; Willett, J.L.; Carriere, C.J.; Wu, Y.V. Effect of Starch Granule Size on Viscosity of Starchfilled Poly (hydroxy ester ether) Composites. *Journal of Polymers and the Environment* **8**, 145-150 (2000).
156. Lim, S.T.; Lee, J.H.; Shin, D.H.; Lim, H.S. Comparison of protein extraction solutions for rice starch isolation and effects on residual protein content on starch pasting properties. *Starch/Stärke* **51**, 120-125 (1999).
157. Ahamed, N.T.; Singhal, R.S.; Kulkarni, P.R.; Kale, D.D.; Pal, M. Studies on chenopodium quinoa and amaranthus paniculatas starch as biodegradable fillers in LDPE films. *Carbohydr. Polym.* **31**, 157-160 (1996).
158. Debon, S.J.J.; Tester, R.F. "In vivo" and "in vitro" annealing of starches. *Gums and stabilizers for the food industry*. (The Royals Society of Chemistry, Cambridge University Press, 2002).
159. Saikia, J.P.; Konwar, B. K., Physicochemical properties of starch from Aroids of north east India. *International Journal of Food Properties* DOI: 10.1080/10942912.2010.491929 (2011).
160. Shilpi, J.A.; Ray, P.K.; Sarder, M.M.; Uddin, S.J. Analgesic activity of *Amorphophallus campanulatus* tuber. *Fitoterapia* **76**, 367-369 (2005).
161. Varandani, B.P. Indigenous Therapy for Piles. *The Indian Practitioner* **XXII**, 545 (1969).
162. Sakano, Y. *et al.* Inhibition of human lanosterol synthase by the constituents of *Colocasia esculenta* (taro). *Biological & Pharmaceutical Bulletin* **28**, 299-304 (2005).
163. Leong, A.C. *et al.* Flavonoid glycosides in the shoot system of Okinawa Taumu (*Colocasia esculenta* S.). *Food Chemistry* **119**, 630-635 (2010).
164. Kim, K.H.; Moon, E.; Kim, S.Y.; Lee, K.R. Lignans from the tuber-barks of *Colocasia antiquorum* var. *esculenta* and their antimelanogenic

- Activity. *J. Agric. Food Chem.* **58**, 4779-4785 (2010).
165. Lewu, M.N.; Adebola, P.O.; Afolayan, A.J. Effect of cooking on the mineral and antinutrient contents of the leaves of seven accessions of *Colocasia esculenta* (L.) Schott growing in South Africa. *Journal of Food, Agriculture & Environment* **7**, 359-363 (2009).
 166. Fokou, E.; Domnangang, F. In vivo assessment of the nutritive value of proteins “in situ” in the leaves of *Solanum nigrum* L., *Xanthosoma* sp. and *Gnetum africanum* L. *Indian. J. Nutr. Diet.* **26**, 366-373 (1989).
 167. Rong-zhen, L.I.U. *et al.* Study on the effect of Moyu capsule on weight control in rat. *China Tropical Medicine* DOI: cnki 1009-9727.0.2006-01-012 (2006).
 168. Chua, M.; Baldwin, T.C.; Hocking, T.J.; Chan, K. Traditional uses and potential health benefits of *Amorphophallus konjac* K. Koch ex N.E.Br. *Journal of Ethnopharmacology* **128**, 268-278 (2010).
 169. Yeh, S.L.; Lin, M.S.; Chen, H.L. Partial hydrolysis enhances the inhibitory effects of konjac glucomannan from *amorphophallus konjac* c. koch on dna damage induced by fecal water in caco-2 cells. *Food Chemistry* **119**, 614-618 (2009).
 170. Tarwadi, K.; Agte, V. Potential of commonly consumed green leafy vegetables for their antioxidant capacity and its linkage with the micronutrient profile. *International Journal of Food Science and Nutrition* **54**, 417-425 (2003).
 171. Fawole, O.A. *et al.* Anti-inflammatory, anticholinesterase, antioxidant and phytochemical properties of medicinal plants used for pain-related ailments in South Africa. *J Ethnopharmacology* **127**, 235-241 (2010).
 172. Mollik, M.A.H. *et al.* A Comparative Analysis of Medicinal Plants Used by Folk Medicinal Healers in Three Districts of Bangladesh and Inquiry as to Mode of Selection of Medicinal Plants. *Ethnobotany Research & Applications* **8**, 195-218 (2010).
 173. Volpato, C.G.; Godínez, D.; Beyra, A.; Barreto, A. Uses of medicinal plants by Haitian immigrants and their descendants in the Province of

- Camagiüey. *Journal of Ethnobiology and Ethnomedicine* **5**, 16-22 (2009).
174. Khan, A.; Rahman, M.; Islam, M.S. Antibacterial, antifungal and cytotoxic activities of amblyone isolated from *Amorphophallus campanulatus*. *Indian Journal of Pharmacology* **40**, 41-44 (2008).
175. Freedman, B.M. Topical polyphenolic antioxidants reduce the adverse effects of intense pulsed light therapy. *Journal of Cosmetic and Laser Therapy*, **11**,142-145 (2009).
176. Yang, C.S.; Wang, X.; Lu G.; Picinich, S.C. Cancer prevention by tea: animal studies, molecular mechanisms and human relevance. *Nature Reviews Cancer* **9**, 429-439 (2009).
177. Rushworth, S.A.; Micheau, O. Molecular crosstalk between TRAIL and natural antioxidants in the treatment of cancer. *British Journal of Pharmacology* **157**, 1186-1188 (2009).
178. Strube, M.; Dragsted, L.O.; Larsen, J.C. Naturally occurring antitumorigens. I. *Plant phenols*. (Nordiske Seminar- og Arbejdsrapporter 605. Copenhagen, Denmark: Nordic Council of Ministers, 1993).
179. Harborne, J.B. *The Flavonoids: Advances in Research Since 1986* (Chapman & Hall, London, UK, 1994).
180. Haddock, E.A. *et al.* The metabolism of gallic acid and hexahydroxydiphenic acid in plants: biogenetic and molecular taxonomic considerations. *Phytochem* **21**, 1049–1062 (1982).
181. Harborne, J.B. *The flavonoids: recent advances. Plant Pigments* (Academic Press, London, England, 1988)
182. Macheix, J.J.; Fleuriet, A.; Billot, J. *Fruit Phenolics* (CRC Press, Boca Raton, USA, 1990).
183. Hakkinen, S. *Flavonols and Phenolic Acids in Berries and Berry Products* (Kuopio University Library, Finland, 2000).

184. Wu, Y.; Qi, Q.; Liang, G.; Zhang, L. A strategy to prepare high performance starch/rubber composites: In situ modification during latex compounding process. *Carbohydr. Polym.* **65**, 109-113 (2006).
185. Elvira, C.; Mano, J.F.; San, R.J.; Reis, R.L. Starch-based biodegradable hydrogels with potential biomedical applications as drug delivery systems. *Biomaterials* **23**, 1955-1966 (2002).
186. Doane, W.M. Opportunities and challenges for new industrial uses of starch. *Cereal Foods World* **39**, 556-557 (1994).
187. Davis, G.; Song, J.H., Biodegradable packaging based on raw materials from crops and their impact on waste management. *Ind. Crop Product* **23**, 147-161 (2006).
188. Webery, C.J.; Haugaard, V.; Festersen, R.; Bertelsen, G. Production and Applications of Biobased Packaging Materials for the Food Industry. *Food Addit. Contam.* **19**, 172-177 (2002).
189. Santander-Ortega, M.J. *et al.* Nanoparticles made from novel starch derivatives for transdermal drug delivery. *Journal of Controlled Release* **141**, 85-92 (2010).
190. Freireira, C.; Podczeka, F.; Veigab, F.; Sousab, J. Starch-based coatings for colon-specific delivery. Part II: Physicochemical properties and in vitro drug release from high amylose maize starch films. *European Journal of Pharmaceutics and Biopharmaceutics* **72**, 587-594 (2009).
191. Sun, D. *et al.* A Novel Nanoparticle Drug Delivery System: The Anti-inflammatory Activity of Curcumin Is Enhanced When Encapsulated in Exosomes. *Molecular Therapy* **18**, 1606-1614 (2010).
192. Singh, R.; Lillard Jr., J.W. Nanoparticle-based targeted drug delivery. *Experimental and Molecular Pathology* **86**, 215-223 (2009).
193. Lee, J.E. *et al.* Uniform Mesoporous Dye-Doped Silica Nanoparticles Decorated with Multiple Magnetite Nanocrystals for Simultaneous Enhanced Magnetic Resonance Imaging, Fluorescence Imaging, and Drug Delivery. *J. Am. Chem. Soc.* **132**, 552-557 (2010).

194. Victor, M.; Esplugues, J.V.; Hernandez-Mijares, A.; Rocha, M. Oxidative Stress and Mitochondrial Dysfunction in Sepsis: A Potential Therapy with Mitochondria-Targeted Antioxidants. *Drug Targets* **9**, 376-389 (2009).
195. Egashira, K.; Fukuoka, J.P. DRUG-CONTAINING NANOPARTICLES (United States Patent Application 20100331373, 2010).
196. Acevedo-Rodriguez P.; Strong M.T. *Monocotyledons and Gymnosperms of Puerto Rico and the Virgin Islands* (United States National Herbarium, 2005).
197. Llamas, K.A. *Tropical Flowering Plants: A Guide to Identification and Cultivation* (Pub. Tibmer Press. Inc., 2003).
198. Santosa, E.; Sugiyama, N.; Hikosaka, S.; Takano, T. Classification of *Amorphophallus variabilis* in West Java, Indonesia, Based on Morphological Characteristics of Inflorescences. *Japanese Journal of Tropical Agriculture* **48**, 25-34 (2004).
199. Boyce, P.C.; Sulaiman, B.; Lintong, J. *Araceae of the crocker range national park sabah: a preliminary survey, checklist and generic key* (ASEAN Review of Biodiversity and Environmental Conservation, ARBEC press, 2002).
200. Cameiro, M.; Rodrigues, C.A.; De Castro, L.A.B.; da Silva M.C.; Coutinho, M.V. Isolation characterization of the major albumin from *Colocasia esculenta* corms. *Plant Sci.* **67**, 39-46 (1990).
201. Lowry, O.H.; Rosebrough, N.H.; Farr, A.L.; Randall, R.J. Protein measurement with the Folin phenol reagent. *J. Biol. Chem.* **193**, 265-75 (1951).
202. Rose, R. *et al.* Starch determination by perchloric acid. *J. agr. Food Chem.* **39**, 2-11 (1991).
203. Toth, S.J.; Prince, A.L.; Wallace, A.; Mikkelsen, D.S. Rapid quantitative determination of eight mineral elements in plant tissues by a systematic procedure involving use of a flame photometer. *Soil Sci.* **66**, 459-466 (1948).

204. Ringbom, A.; Pensar, G.; Wanninen, E.A. compleximetric titration method for determining calcium in the presence of magnesium. *Anal Chimica Acta* **19**, 525–553 (1958).
205. Ronning, C.M.; Schnell, R.J.; Gazit, S. Using randomly amplified polymorphic DNA (RAPD) markers to identify *Annona* cultivars, *American Society For Horticultural Science* **120**, 726-729 (1995).
206. Gallagher S.R. *Short protocol in Molecular Biology* (Wiley, USA, 1999).
207. Cordenunsi, B.R. *et al.* Chemical composition and glycemic index of Brazilian pine (*Araucaria angustifolia*) seeds. *J. Agric. Food Chem.* **52**, 3412- 3416 (2004).
208. Chang, Y.H.; Yang, C.C.; Wang, R.C. Physicochemical properties of taro and their effects on the texture profile. *Food Sci. (Taiwan)* **26**, 371-383 (2002).
209. Chen, C.; Ho, C. Antioxidant properties of polyphenols extracted from green and black teas. *J. of Food Lip.* **2**, 35-46 (1994).
210. Miki, M.; Tamai, H.; Mino, M.; Yamamoto, Y.; Niki E. Free-radical chain oxidation of rat red blood cells by molecular oxygen and its inhibition by α -tocopherol. *Arch. Biochem. Biophys.* **258**, 373-380 (1987).
211. Jayakody, L.; Hoover, R.; Liu, Q.; Donner, E. Studies on tuber starches. II. Molecular structure, composition and physicochemical properties of yam (*Dioscorea sp.*) starches grown in Sri Lanka. *Carbohydrate Polymers* **69**, 148-163 (2007).
212. St. Paul, M.N. *Official Methods of the AACC* (American Association of Cereal Chemists Press, 1984).
213. Morrison, W.R. A fast simple and reliable method for the micro determination of phosphorus in biological materials. *Analytical biochemistry* **7**, 218-224 (1964).

214. Gunaratne, A.; Hoover, R. Effect of heat-moisture treatment on the structure and physicochemical properties of tuber and root starches. *Carbohydrate Polymers* **49**, 425-437 (2002).
215. de-Keijser, T.H.; Langford, J.I.; Mittemeijer, E.J.; Vogels, A.B.P. Use of the Voigt function in a single-line method for the analysis of X-ray diffraction line broadening. *J. Appl. Cryst.* **15**, 308-314 (1982).
216. Medcalf, D.G.; Gilles, K.A. Determination of Starch Damage by Rate of Iodine Absorption. *Cereal Chem.* **42**, 546-557 (1965).
217. Sugimoto, Y.; Nishihara, K.; Fuwa, H. Some properties of Taro and Yam starch. *J. Jpn. Soc. Starch Sci.* **33**, 169-176 (1986).
218. Somogyi, M. Notes on sugar determination. *J. Biol. Chem.* **195**, 19-23 (1952).
219. Serpen, A.; Capuano, E.; Fogliano, V.; Gökmen, V. A New Procedure to Measure the Antioxidant Activity of Insoluble Food Components. *J. Agric. Food Chem.*, **55**, 7676–7681 (2007).
220. Opara L.U. *EDIBLE AROIDS: Post-Harvest Operation* (Massey University Press, New Zealand, 2007).
221. Castro, R.G.; Maradiaga, A. M. Reproduccion acelerada de semilla de quequisque (*Xanthosoma* sp.) y malanga (*Colocasia* sp.). *Guia tecnica* **8**, 11-15 (2005).
222. Boyce, C.K.; Knoll, A.H. Evolution of developmental potential and the multiple independent origins of leaves in Paleozoic vascular plants. *Paleobiology* **28**, 70-100 (2002).
223. Lu, T.; Chen, J.; Lin, C.; Chang, Y. Properties of starches from cocoyam (*X. sagittifolium*) tubers planted in different seasons. *Food Chem.* **91**, 69-77 (2005).
224. Akpan, E.J.; Usuh, I.F. Phytochemical screening and effect of aqueous root extract of *Raphia hookeri* (raffia palm) on metabolic clearance rate of ethanol in rabbits. *Biokemistri* **16**, 37-42 (2004).

225. Sefa-Dedeh S.; Agyir-Sackey E.K. Chemical composition and the effect of processing on oxalate content of cocoyam *Xanthosoma sagittifolium* and *Colocasia esculenta* cormels. *Food Chemistry* **85**, 479-487 (2004).
226. Huang, J.; Schols, H.A.; Jin, Z.; Sulmann, E.; Voragen, A.G.J. Characterization of differently sized granule fractions of yellow pea, cowpea and chickpea starches after modification with acetic anhydride and vinyl acetate. *Carbohydrate Polymers* **67**, 11-20 (2007).
227. Parvin, S.; Kabir, G.; Ud-Deen, M.M.; Sarker, J.K. Karyotype Analysis of Seven Varieties of Taro *Colocasia esculenta* (L.) Schott. from Bangladesh. *J. bio-sci.* **16**, 15-18 (2008).
228. Bennett, M.D.; Leitch, I.J. Plant Genome Size Research: A Field In Focus. *Annals of Botany* **95**, 1-6 (2005).
229. Temsch, E.M.; Greilhuber, J. Genome size in *Arachis duranensis*: a critical study. *Genome* **44**, 826-830 (2001).
230. Naik, G.H. *et al.* Comparative antioxidant activity of individual herbal components used in Ayurvedic medicine. *Phytochem.* **63**, 97-104 (2003).
231. Elegir, G.; Kindl, A.; Sadocco, P.; Orlandi, M. Development of antimicrobial cellulose packaging through laccase-mediated grafting of phenolic compounds. *Enzyme and Microbial Technology* **43**, 84-92 (2008).
232. Markovi, D.Z. Photolysis of incorporated benzophenone derivatives inside compressed lipid monolayers. *J.Serb.Chem.Soc.* **66**, 309-322 (2001).
233. Surowiec, I. *et al.* Flow-through microdispenser for interfacing μ -HPLC to Raman and mid-IR spectroscopic detection. *Journal of Chromatography A* **1080**, 132-139 (2005).
234. Ibrahim, U.I.; Mbaya, A.W.; Mahmud, H.; Mohammed, A. Prevalence of cryptosporidiosis among captive wild animals and birds in the arid region of north-eastern Nigeria. *Veterinarski Arhiv* **77**, 337-344 (2007).

235. Dawson, R.M.C.; Elliott, D.C.; Elliott, W.H.; Jones, K.M. *Data for Biochemical Research* (Oxford University Press, UK, 1989).
236. Babich, H.; Sedletcaia, A.; Kenigsberg, B. In vitro cytotoxicity of protocatechuic acid to cultured human cells from oral tissue: involvement in oxidative stress. *Pharmacol Toxicol.* **91**,245-253 (2002).
237. Nakamura Y. *et al.* A simple phenolic antioxidant protocatechuic acid enhances tumor promotion and oxidative stress in female ICR mouse skin: dose- and timing-dependent enhancement and involvement of bioactivation by tyrosinase. *Carcinogenesis* **21**, 1899-1907 (2000).
238. Almeida, A.A.P.; Farah, A.; Silva, D.A.M.; Nunan, E.A.; Glória, M.B.A. Antibacterial Activity of Coffee Extracts and Selected Coffee Chemical Compounds against Enterobacteria. *J. Agric. Food Chem.* **54**, 8738–8743 (2006).
239. Lamikanra, A.; Ogundaini, A.O.; Ogungbamila, F.O. Antibacterial constituents of *Alchornea cordifolia* leaves. *Phytotherapy Research.* **4**,198-200, (1990).
240. Vaquero M.J.R.; Alberto M.R.; de Nadra M.C.M. Antibacterial effect of phenolic compounds from different wines. *Food Control* **18**, 93-101 (2007).
241. Aziz, N.H.; Farag, S.E.; Mousa, L.A.A.; Abo-Zaid, M.A. Comparative antibacterial and antifungal effects of some phenolic compounds. *Microbios* **93**, 43-54 (1998).
242. Fernandez, M.A.; Garcia, M.D.; Saenz, M.T. Antibacterial activity of the phenolic acids fractions of *Scrophularia frutescens* and *Scrophularia sambucifolia*. *Journal of Ethnopharmacology* **53**, 11-14 (1996).
243. Qiu-Ling, S.; Ping-Hua, S.; Wei-Min, C. Exploring 3D-QSAR for Ketolide Derivatives as Antibacterial Agents Using CoMFA and CoMSIA. *Letters in Drug Design & Discovery* **7**, 149-159 (2010).
244. Lim, N. *et al.* Comparison of Polyhexamethylene Biguanide and Chlorhexidine as Monotherapy Agents in the Treatment of

- Acanthamoeba Keratitis. *American Journal of Ophthalmology* **145**, 130-135 (2008).
245. Perez, E.; Schultz, F.S.; de Delahaye, E.P. Characterization of some properties of starches isolated from *Xanthosoma sagittifolium* (tannia) and *Colocassia esculenta* (taro). *Carbohydrate Polymers*. **60**, 139-145 (2005).
246. Andersson, A.A.M.; Andersson, R.; Aman, P. Starch and byproducts from a laboratory-scale barley starch isolation procedure. *Cereal Chem.* **78**, 507–513 (2001).
247. Imberty, A.A Revisit to the three dimensional structure of B-type starch. *Biopolymers* **27**, 1205- 1221 (1988).
248. Dragunski, D.C.; Pawlicka, A. Preparation and Characterization of Starch Grafted with Toluene Poly (propylene oxide) Diisocyanate. *Materials Research* **4**, 77-81 (2001).
249. Fang, J.M.; Fowler, P.A.; Tomkinson, J.; Hill, C.A.S. The preparation and characterization of a series of chemically modified potato starches. *Carbohydrate Polymers* **47**, 245–252 (2002).
250. Rasper, V.; Coursey, D.G. Properties of starches of some West African yams. *Journal of the Science of Food and Agriculture* **18**, 240–244 (1996).
251. McPherson, A.E.; Jane, J.L. Comparison of waxy potato with other root and tuber starches. *Carbohydrate Polymers* **40**, 57-70 (1999).
252. Srichuwong, S.; Sunarti, T.C.; Mishima, T.; Isono, N.; Hisamatsu, M. Starches from different botanical sources. II. Contribution of starch structure to swelling and pasting properties. *Carbohydrate Polymers* **62**, 25-34 (2005).
253. Hoover, R.; Manuel, H.A. comparative study of the physicochemical properties of starches from two lentil cultivars. *Food Chemistry* **53**, 275-284 (1995).
254. Zhang, Z.; Wei, Z.; Wan, M. Nanostructures of Polyaniline Doped with Inorganic Acids. *Macromolecules* **35**, 5937-5942 (2002).

255. Singh, S.; Bhaskar, K.R.; Rao, C.N.R. Kinetics of hydrogen abstraction from proton donors by DPPH. *Can. J. Chem.* **44**, 2657-2662 (1966).
256. Hazell, J.E.; Russell, K.E. The reaction of 2, 2-diphenyl-1-picrylhydrazyl with secondary amines. *Can. J. Chem.* **36**, 1729-1734 (1958).
257. Gutteridge, J.M.C. Aspects to Consider When Detecting and Measuring Lipid Peroxidation. *Free Radical Research* **1**, 173-184 (1986).
258. Clark, M.R. Senescence of red blood cells: problems and progress. *Physiol. Rev.* **68**, 503-511 (1988).

List of publication

Journal Publications (peer reviewed national/ international journals)

1. Jyoti Prasad Saikia, Bolin Kumar Konwar and Susmita Singh. Genome size determination and RAPD analysis of four edible aroids of north east India. *IIOAB Journal* **1**, 25-30 (2010).
2. Jyoti Prasad Saikia and Bolin Kumar Konwar. Biochemical composition and bioactivity of four edible aroids. *Journal of Root Crops* (online 2011).
3. Rocktotpal Konwarh, Jyoti Prasad Saikia, Niranjana Karak and Bolin Kumar Konwar. 'Poly (ethylene glycol) – magnetic nanoparticles-curcumin' trio: directed morphogenesis and synergistic free radical scavenging. *Colloids and Surfaces B: Biointerfaces* **81**, 578-586 (2010).
4. Jyoti Prasad Saikia, Somik Banerjee, Bolin Kumar Konwar, Ashok Kumar. Biocompatible novel starch/polyaniline composites: characterization, anti-cytotoxicity and antioxidant activity. *Colloids and Surfaces B: Biointerfaces* **81**, 158-164 (2010).
5. Jyoti Prasad Saikia, Bolin Kumar Konwar. Physicochemical properties of starch from aroids of north east India. *International Journal of Food Properties* (DOI: 10.1080/10942912.2010.491929).
6. Jyoti Prasad Saikia, Samrat Paul, Bolin Kumar Konwar, Sanjoy Kumar Samdarshi. Ultrasonication: enhances the antioxidant activity of metal oxide nanoparticles. *Colloids and Surfaces B: Biointerfaces* **79**, 521–523 (2010).
7. A. Kumar, S. Banerjee, J. P. saikia, B. K. Konwar, Swift heavy ion irradiation induced enhancement in the antioxidant activity and biocompatibility of polyaniline nanofibers. *Nanotechnology* **21** (2010)175102(8pp) (Cited BY NATURE INDIA).
8. Jyoti Prasad Saikia, Samrat Paul, Bolin Kumar Konwar, Sanjoy Kumar Samdarshi. Nickel oxide nanoparticles: A novel antioxidant. *Colloids and Surfaces B: Biointerfaces* **78**, 146–148 (2010).
9. Suvangshu Dutta, Niranjana Karak, Jyoti Prasad Saikia and Bolin Kumar

- Konwar. Biodegradation of Epoxy / MF Modified Polyurethane Films Derived From a Sustainable Resource. *Journal of Polymer and environment* (DOI 10.1007/s10924-010-0161-8).
10. Somik Banerjee, Jyoti P Saikia, A Kumar, B K Konwar, Antioxidant activity and haemolysis prevention efficiency of polyaniline nanofibers, *Nanotechnology* **21** (2010) 045101 (8pp).
 11. Suvangshu Dutta, Niranjana Karak, Jyoti Prasad Saikia, Bolin Kumar Konwar. Biocompatible epoxy modified bio-based polyurethane nanocomposites: Mechanical property, cytotoxicity and biodegradation, *Bioresource Technology* **100**, 6391-6397 (2009).
 12. S. Paul, J. P. Saikia, S. K. Samdarshi, B.K. Konwar. Investigation of antioxidant property of iron oxide particles by 1'-1'diphenylpicryl-hydrazyle (DPPH) method, *Journal of Magnetism and Magnetic Materials*, **321**, 3621-3623 (2009).

Conference publications (national and international)

1. J. P. Saikia and B. K. Konwar. Bioactivity of four edible aroids of north east India, Indian National Science Academy (INSA), NCL, Pune, November 21-23, 2009.
2. S. Banerjee, A. Kumar, J. P. Saikia and B. K. Konwar. Polyaniline nanofiber: Potential antioxidant for biomedical and Industrial application. International Conference on Advanced Nanomaterials and Nanotechnology, IIT Guwahati, December 9-11, 2009.
3. B. K. Konwar, S. Banerjee, J. P. Saikia and A. Kumar. Investigation of antioxidant property of zinc oxide particles by 1'-1'diphenylpicryl-hydrazyle (DPPH) method, 4th Global Summit on Medicinal and Aromatic Plants, Sarawak, Malaysia (Borneo Island), December 1 – 5, 2009.
4. Jyoti Prasad Saikia and Bolin Kumar Konwar. Biochemical and Morphological study of four edible aroids of Assam, 96th Indian Science Congress, NEHU,

Shillong, January 3-7, 2009.

5. Jyoti Prasad Saikia, Subhansu Dutta, Bolin Kumar Konwar and Nirranjan Karak. Microbial degradation of *Mesua ferrera* Lin. seed oil based polyurethane films”, 49th Annual international symposium of Association of Microbiologist (India), University of Delhi, November, 2008.
6. Jyoti Prasad Saikia and B. K. Konwar. Comparative digestibility of some edible aroids of North East India, 76th Annual meeting of Society of Biochemist (India), Tirupati, 2007.